



United States
Department of
Agriculture

Forest Service

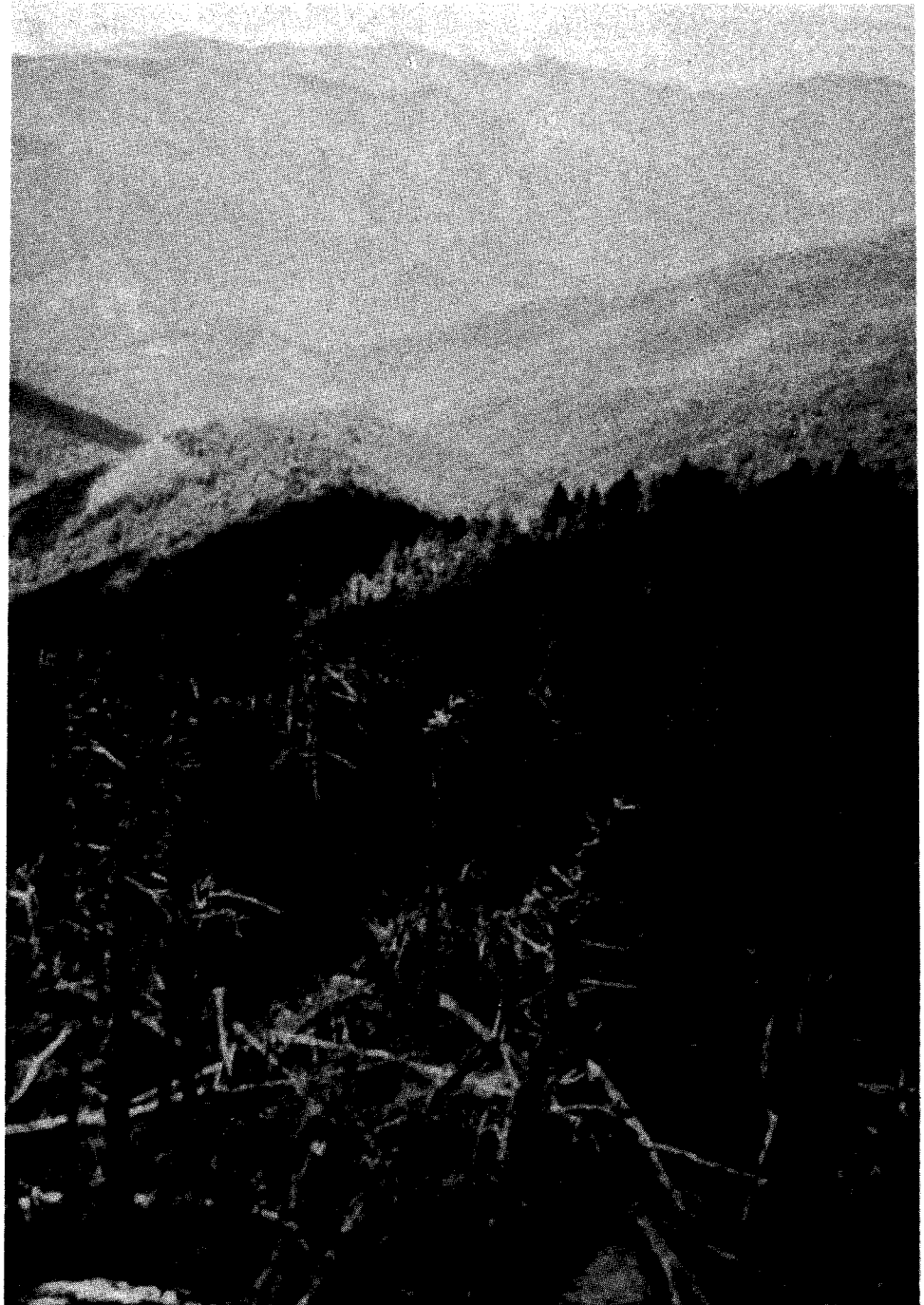
**Southern Forest
Experiment Station**

New Orleans,
Louisiana

General Technical Report
SO-69



Analyses of Great Smoky Mountain Red Spruce Tree Ring Data



SUMMARY

Both mortality rate and radial growth of high elevation (>900 m) red spruce-Fraser fir forests of the southern Appalachians have experienced change since approximately 1960. Scientific interest in a study of these forests have increased because atmospheric pollution is a possible cause of the change. Scientists with statistical and biological expertise independently analyzed a tree ring data set collected by the Tennessee Valley Authority and the National Park Service. The objective of the analysis was to develop new or improved techniques for extracting information from such data; tree rings represent a natural data storage system that is one of the few sources of long-term information for these forests.

Although no definite statements are made about the role of atmospheric deposition in observed forest decline, the results should contribute to the success of future research. The four techniques employed in the study involved: (1) a dendrochronological approach employing spline detrending and multiple regression to study the effects of climate on ring width, (2) an application of fractals to study the dependence of variance on mean ring width over time, (3) an approach that combined Box-Jenkins methods and spatial analysis, and (4) a method of studying time dependence of ring width on climate using the Kalman filter.

Analyses of Great Smoky Mountain Red Spruce Tree Ring Data

Paul C. Van Deusen

Editor



Contents

INTRODUCTION	1
Southern Appalachian Red Spruce--Fraser Fir Forests--Elizabeth Groton and Christopher Eagar.....	2
A Tree Ring Analysis of Red Spruce in the Southern Appalachian Mountains--Edward R. Cook.....	6
Utilizing Time Series Models and Spatial Analysis of Forecast Residuals for Tree Ring Analysis of Red Spruce--J. Keith Ord and Janice A. Derr	21
A Fractal Approach to Analysis of Tree Ring Increments--R. A. J. Taylor	40
Red Spruce Tree Ring Analysis Using a Kalman Filter--Paul C. Van Deusen	57



INTRODUCTION

The Institute for Quantitative Studies at the USDA Forest Service, Southern Forest Experiment Station, has been engaged in a study of statistical methods used in researching Atmospheric Deposition Influences on Forests (ADIF). The study was funded by the National Vegetation Survey, which is under the National Acid Precipitation Assessment Program (NAPAP). The study began with a distributed seminar; for 10 weeks articles about ADIF were sent to a number of participants who returned comments each week. A final report was produced (Kiestler and others 1985) consisting of critiques of past ADIF studies, suggestions for additional reading, and philosophy about the type and quality of research needed in the ADIF area.

The study indicated that tree ring analyses held promise for the study of ADIF, but further development of appropriate statistical methods would be useful. Therefore the idea of "replicated-statisticians" was employed. Because there are several ways to approach a tree ring analysis, it was probable that allowing a number of individuals to work independently would yield some interesting new dendrochronological techniques. Red spruce (*Picea rubens* Sarg.) was chosen for this study because claims were previously made that spruce forests were experiencing unexplained growth declines in both the Northeast and the South (Hornbeck and Smith 1985; Adams and others 1985). Although the study was intended to develop statistical methods and not explanations of growth declines, using this data allowed for that possibility.

This study was a joint endeavor by the USDA Forest Service, the National Park Service (NPS), and the Tennessee Valley Authority (TVA). Funding came from the Forest Service and the TVA, data from the TVA and NPS, and statistical analyses were conducted by the Forest Service. Agreements were made with the following scientists to perform analyses and provide individual reports:

- (1) Edward R. Cook, Ph.D.
Tree-Ring Laboratory
Lamont-Doherty Geological Observatory
of Columbia University
Palisades, New York 10964
- (2) Keith Ord, Ph.D. and Janice Derr, Ph.D.
Department of Management Science
Pennsylvania State University
University Park, PA 16802
- (3) Robin A. J. Taylor, Ph.D.
Department of Entomology
106 Patterson Building
Pennsylvania State University
University Park, PA 16802
- (4) Paul C. Van Deusen, Ph.D.
Institute for Quantitative Studies
Southern Forest Experiment Station
701 Loyola Avenue
New Orleans, LA 70113

Dr. Cook is considered to be one of the leaders in the field of dendrochronology, and his analysis therefore includes the most currently accepted techniques. He concluded that there is

evidence of anomalous behavior in the red spruce forests of the Great Smoky Mountains and suggests that this is partly due to warmer summer temperatures in recent years. He also states that the situation in southern red spruce is not similar to that in northern red spruce.

Drs. Ord and Derr performed a spatial analysis on the data. They concluded that there was a tendency for ring widths to diminish in recent years and that there is a strong spatial dependence in forecast residuals that cannot be explained by geographic or biotic factors alone. They did not consider climate, which they mention could explain some of the remaining spatial dependence. The analysis performed here is novel for the field of dendrochronology and may lead to useful results in the future.

To study the dependence of variance on the mean of the data, Dr. Taylor investigated the use of "fractals," a term coined to denote fractional dependence. He concluded that the change in fractional dimension over time may be due to successional, climatic, or anthropogenic influences. This technique has not been applied previously to tree ring data and may show promise after further development.

Dr. Van Deusen analyzed the data using the Kalman filter technique, which is commonly used in engineering applications. At the time of this study, the method had not been used in dendrochronology, although scientists in the Netherlands (Visser 1986) have recently published a paper on independent applications of the method to tree rings. The Kalman Filter allowed the climatic data to be modeled dynamically so that its effect over time could be studied. He concluded that these trees have become progressively more sensitive to climate since the late 1950's. This increased sensitivity may coincide with insect-caused thinning in the stands.

All the studies concluded that the growth patterns in these stands have changed in the last 20 years. The causes of these changes are uncertain, but the sensitivity of the stand to climate appears to be increasing. To enhance the reader's ability to interpret the various analyses, the individual reports are prefaced by a review by Elizabeth Groton and Christopher Eagar of the geographical and biological background of the Southern Appalachian Spruce Fir Forest.

References cited in this section are: Adams, H.S.; Stephenson, S.L.; Blasing, T.J.; Duvick, D.N. 1985. Growth-trend declines of spruce and fir in mid-Appalachian subalpine forest. *Environmental and Experimental Botany*. 25(4): 315-325. Hornbeck, J.W.; Smith, R.B. 1985. Documentation of red spruce growth decline. *Canadian Journal of Forest Research*. 15: 1199-1201. Kiestler, A.R.; Van Deusen, P.C.; Dell, T.R. 1985. Status of the concepts and methodologies used in the study of the effects of atmospheric deposition on forests. Internal report for the National Vegetation Survey of NAPAP. Visser, H. 1986. Analysis of tree ring data using the Kalman Filter techniques. *IAWA Bulletin n.s.*, Vol. 7(4) 289-297. Published at the Rijksherbarium, Netherlands.

Southern Appalachian Red Spruce--Fraser Fir Forests

Elizabeth Groton and Christopher Eagar

GEOGRAPHICAL AND BIOLOGICAL BACKGROUND

The southern Appalachian red spruce-Fraser fir[†] forests are found in southwestern Virginia, western North Carolina, and eastern Tennessee (fig. 1). Total area of these southern Appalachian spruce-fir forests is estimated at 26,577 hectares, with 19,755 hectares occurring within the Great Smoky Mountains National Park (GSMNP). Extensive logging and other disturbances early in the 20th century have reduced the extent of the southern Appalachian spruce-fir forests. Today this forest type occurs on high-elevation peaks (above 1,370 m) in islandlike patches.

Species' composition in the southern Appalachian forests changes with the elevational gradient. At lower elevations (1,370-1,580 m) in undisturbed forests such as those of the Great Smoky Mountains, red spruce (*Picea rubens* Sarg.) is found in combination with northern hardwood type species: maple (*Acer* spp.), American beech (*Fagus grandifolia* Ehrh.), yellow birch (*Betula alleghaniensis* Britton), eastern hemlock (*Tsuga canadensis* (L.) Carr.), northern red oak (*Quercus rubra* L.), Carolina silverbell (*Halesia carolina* L.), and yellow buckeye (*Aesculus octandra* Marsh.). As elevation increases, the fir component gains importance, and forest composition changes to predominantly red spruce-Fraser fir. Red spruce occurs less frequently at the highest end of the gradient (above 1,890 m), giving way to essentially pure Fraser fir (*Abies fraseri* (Pursh) Poir.) stands on mountain tops (Whittaker 1956). Mountains that were logged during the early part of this century and did not experience postlogging slash fires are dominated by Fraser fir. This includes most of the Black Mountains, Balsam Mountains, Roan Mountain, and Mount Rogers.

Red spruce grows larger and lives longer than Fraser fir, but Fraser fir grows more rapidly and produces more prolific seed crops than red spruce. Red spruce can live for over 350 years, grow to 40 meters in height, and have diameters at breast height (d.b.h.) in excess of 1 meter. Fraser fir seldom lives longer than 150 years and attains a maximum height of 25 meters and d.b.h. of 50 centimeters. Oosting and Billings (1951) found five times more Fraser fir than red spruce seedlings in old-growth stands in the Great Smoky Mountains. Both species are extremely shade tolerant and are capable of resuming normal growth after 50 years of suppression.

[†]Red spruce-Fraser fir forests will generally be referred to as simply spruce-fir forests.

THE BALSAM WOOLLY ADELGID

Most spruce-fir forests of the southern Appalachians have been recently disturbed by the extensive mortality of Fraser fir caused by an introduced insect, the balsam woolly adelgid (*Adelges piceae*). This pest, a native of Europe, is a tiny insect that feeds on the bark of true firs (*Abies* spp.). Fraser fir is quickly killed by the balsam woolly adelgid. Mortality occurs between 3 and 9 years from the time of initial infestation, depending on the size and vigor of the tree (Amman and Speers 1965). Tree death is caused by the diffusion of compounds secreted by the adelgid into the xylem during feeding, which causes formation of premature heartwood. Translocation of water and minerals to the crown are greatly reduced, causing water stress and eventual death of the tree (Puritch 1971, 1973, 1977, Puritch and Johnson 1971, Puritch and Petty 1971).

The balsam woolly adelgid was first identified in North America in 1908 on balsam fir (*Abies balsamea*) in Maine (Kotinsky 1916). The adelgid has caused extensive mortality to balsam fir throughout eastern Canada; however, infestations have not progressed more than 80 kilometers inland from the coast because of extreme inland winter conditions (Balch 1952, Schooley and Bryant 1978). The balsam woolly adelgid is not present in the northern Appalachian spruce-fir forest.

The balsam woolly adelgid was detected in the southern Appalachians on Mount Mitchell, North Carolina, in 1957 (Speers 1958). Subsequent surveys revealed that the adelgid had spread throughout the entire 3,035 hectares of Fraser fir type in the Black Mountains (Nagel 1959). High mortality of Fraser fir and widespread adelgid distribution indicated establishment prior to 1957, perhaps as early as 1940. Balsam woolly adelgids were detected in 1962 on Roan Mountain (Ciesla and Buchanan 1962), and in 1963 infestations were located on Grandfather Mountain and on Mount Sterling in the GSMNP.

The adelgid arrived in the Clingman's Dome area of the GSMNP in the early 1970's, and tree mortality began there in the late 1970's. Surveys found the adelgid in the Balsam Mountains and the nearby Plott Balsams of North Carolina in 1968 (Rauschenberger and Lambert 1970). The balsam woolly adelgid was not found on Mount Rogers, Virginia, until 1979; however, subsequent stem analysis of several trees within the infested areas revealed adelgid-caused red wood beginning in 1962 (Lambert and others 1980) in the annual rings.

By 1984 and 1985, the balsam woolly adelgid had caused extensive damage throughout the Black Mountains, Balsam Mountains, Plott Balsams,

Elizabeth Groton is forest biometrician for the Tennessee Valley Authority, Norris, TN. Christopher Eagar is ecologist for the National Park Service, Gatlinburg, TN.

Grandfather Mountain, and most of the Great Smoky Mountains. Limited use of insecticides at Roan Mountain reduced fir mortality in accessible areas, although nontreated areas experienced heavy damage. In the Clingman's Dome area of the GSMNP, adelgid infestations had caused significant fir mortality at elevations below 1,830 meters and minimal damage above this elevation. Mount Rogers had suffered the least Fraser fir mortality of the southern Appalachian spruce-fir forests. There were isolated, dead Fraser fir in areas known to have been infested for 23 years, but even within these areas the impact of the adelgid was surprisingly low. Possible explanations for this anomalous condition on Mount Rogers include: a genetic based difference in defense mechanism to adelgid infestation of this fir population, a reduction in the toxicity of the secretions of the Mount Rogers adelgid population, or a combination of both possibilities.

RESEARCH AND STUDY ENDEAVORS

National Park Service and Tennessee Valley Authority

Increased mortality (Siccama and others 1982, Scott and others 1984, Vogelmann and others 1985) and apparent reductions in radial increment (Adams and others 1985, Bruck 1986, McLaughlin and others 1983) in the high-elevation spruce-fir forests of the Eastern United States prompted two studies in the southern Appalachians. The studies were designed to assess the current condition of these forests, relate observed decline symptoms to site characteristics, and provide baseline data to monitor future changes in the forest condition.

The first study, conducted by the National Park Service (NPS), began in the summer of 1984 in the

spruce-fir forests of the GSMNP. The second study, conducted by the Tennessee Valley Authority (TVA) in the autumn of 1984, established plots throughout the range of the southern Appalachian spruce-fir type, excluding the GSMNP. Intending to combine data sets for future analyses, both agencies collaborated on sampling design in order to ensure that similar data were collected.

Problems of assessing change in forest productivity prompted the TVA and NPS to establish permanent vegetation plots in the southern range of the spruce-fir type. Plot establishment was also influenced by the need for additional information on stand dynamics in the spruce-fir forests. This led to a collaborative study between the TVA, NPS, and the Forest Service. Data collected by the TVA and NPS included tree increment core data and detailed plot information. The tree core data and plot data were summarized and made available to a number of individual researchers for independent analysis. Plot information included elevation, latitude and longitude, live and dead basal area, and stand density. Regional climatic data (monthly averages of precipitation and temperature since 1933) were also included in the data.

Sampling procedures utilized by the NPS and TVA were basically the same (table 1). Both agencies used stratified random sampling, locating plots on aerial photographs and topographic maps. Data that were collected from the plots included site characteristic data such as slope, aspect, topographic location, and descriptions of understory vegetation. Individual trees were mapped, measured, and evaluated for decline symptomology. Quantitative assessments were made of mortality and regeneration. Increment cores were collected from five dominant or codominant trees at each site. Two cores per tree were taken at d.b.h.

Table 1.—Comparison of Tennessee Valley Authority (TVA) and National Park Service (NPS) spruce-fir sampling procedures

Variable	TVA	NPS
Plot Location	Stratified random (Strata: Elevation and dry/wet)	Stratified random (Strata: Elevation, topo position, macro-aspect)
Elevation	Variable within strata	Held constant at a set strata
Plot Size	Circular, 0.08 ha	Square, 0.04 ha
Overstory stand data [†]	---	---
Site character- istic data [†]	---	---
Increment cores	Cores taken from five dominant or codominant trees from outside the plot and extended to tree center.	Cores taken from five dominant trees from within plot, cores not extended to tree center.

[†]Overstory stand data and site characteristic data were basically identical for both TVA and NPS.

The results of the analyses of tree core data may provide insight into the question of whether or not the southern Appalachian red spruce and Fraser fir are experiencing a decline that cannot be attributed to natural stresses. The plots established by the NPS and TVA will continue to be remeasured in order to monitor future changes in stand productivity.

Other Studies

Several studies have used annual radial increments from tree cores to evaluate changes in the growth rate of red spruce and Fraser fir from several sites in the southern Appalachians. These studies indicated an abrupt shift to narrow growth rings beginning in the late 1960's to early 1970's (Adams and others 1985, Bruck 1986, McLaughlin and others 1983) for red spruce and, to a lesser extent, for Fraser fir. This tendency was more drastic at high elevations (Adams and others 1985). The annual growth declines are very similar in timing to studies done in the Northeast, but they are not as geographically widespread and are less consistent within a given sample. Additionally, the analysis of tree ring data is extremely complicated because of the effects of tree age, stand competition, climate, and physiological responses to stress that may persist for several years. Therefore the interpretation of these data has been the subject of considerable controversy.

Vast differences exist in species' composition, structure, and stand productivity within the limited extent of the southern spruce-fir. These differences are a result of climatic disparities associated with elevational gradients, past management histories, and other site-specific variables. These environmental factors, and the lack of historical data in the South, preclude any analysis designed to discover either the causes of observed declines or even if the observed declines are abnormal in these forests.

LITERATURE CITED

- Adams, H.S.; Stephenson, S.L.; Blasing, T.J.; Duvick, D.N. 1985. Growth-trend declines of spruce and fir in mid-Appalachian subalpine forests. *Environmental and Experimental Botany*. 25(4): 315-325.
- Amman, G.D. 1962. Seasonal biology of the balsam woolly aphid on Mt. Mitchell, North Carolina. *Journal of Economic Entomology*. 55(1): 96-98.
- Amman, G.D. 1966. Some new infestations of balsam woolly aphid in North America with possible modes of dispersal. *Journal of Economic Entomology*. 59(3): 508-511.
- Amman, G.D.; Speers, C.F. 1965. Balsam woolly aphid in the Southern Appalachians. *Journal of Forestry*. 63(1): 18-20.
- Balch, R.E. 1952. Studies of the balsam woolly aphid. *Adelges piceae* (Ratz.) and its effects on balsam fir, *Abies balsamea* (L.) Mill. Canadian Department of Agriculture. Publication No. 867. 76 p.
- Bruck, R.I. 1986. Boreal montane ecosystem decline in the Southern Appalachian Mountains: potential role of anthropogenic pollution. In: Proceedings, Air pollutants effects on forest ecosystems; 1985 May 8-9; St. Paul, MN. St. Paul, MN: The Acid Rain Foundation, Inc.: 137-155.
- Ciesla, W.M.; Buchanan, W.D., 1962. Biological evaluation of balsam woolly aphid, Roan Mountain, Gardens, Toecane District, Pisgah National Forest, North Carolina. (Forest Pest Management Report 62-93 U.S. Department of Agriculture, Forest Service, Southern Area, State and Private Forestry p. 1-3. [unpublished].
- Kotinsky, J. 1960. The European fir louse, *Chermes (Dreyfusia) piceae* (Ratz.). Entomological Proceedings Society Washington. 18: 14-16.
- Lambert, H.L.; Morgan, S.W.; Johnson, K.D. 1980. Detection and evaluation of the balsam woolly adelgid infestations on Mount Rogers, Virginia-1979. Asheville, NC: U.S. Department of Agriculture, Forest Service. Southeastern Area State and Private Forestry Report No. 80-1-7. 23 p.
- McLaughlin, S.B.; Blasing, T.J.; Mann, L.K.; Duvick, D.N. 1983. Effects of acid rain and gaseous pollutants on forest productivity: a regional scale approach. *Journal of the Air Pollution Control Association*. 33(11): 1042-1049.
- Nagel, W.P. 1959. Forest insect conditions in the Southeast during 1958. Southeastern Station Paper No. 100. Asheville, NC: U.S. Department of Agriculture, Forest Service. 10 p.
- Oosting, H.J.; Billings, D.W. 1951. A comparison of virgin spruce-fir forest in the northern and southern Appalachian system. *Ecology*. 32(1): 84-103.
- Puritch, G.S. 1971. Water permeability of the wood of grand fir (*Abies grandis* (Doug.) Lindl.) in relation to infestation by the balsam woolly aphid. *Adelges piceae* (Ratz.). *Journal of Experimental Botany*. 22(73): 936-945.
- Puritch, G.S. 1973. Effect of water stress on photosynthesis, respiration and transpiration of four *Abies* species. *Canadian Journal of Forest Research*. 3(2): 293-298.
- Puritch, G.S. 1977. Distribution and phenolic composition of sapwood and heartwood in *Abies grandis* (Doug.) Lindl. and effects of the balsam woolly aphid. *Canadian Journal of Forest Research*. 7(1): 54-62.
- Puritch, G.S.; Johnson, R.P.C. 1971. Effects of infestation by the balsam woolly aphid, *Adelges piceae* (Ratz.), on the ultrastructure of bordered-pit membranes of grand fir, *Abies grandis* (Day.) Lindl. *Journal of Experimental Botany*. 22(73): 953-958.
- Puritch, G.S.; Petty, J.A. 1971. Effect of balsam woolly aphid. *Adelges piceae* (Ratz.), infestation on the xylem of *Abies grandis* (Doug.) Lindl. *Journal of Experimental Botany*. 22(73): 946-952.
- Rauschenberger, J.L.; Lambert, H.L. 1970. Status of the balsam woolly aphid in the southern Appalachians--1969. Southeastern Area, State and Private Forestry Report No. 70-1-44. Asheville, NC: U.S. Department of Agriculture, Forest Service. 20 p.

Schooley, H.O.; Bryant, D.G. 1978. The balsam woolly aphid in Newfoundland. Canadian Forest Service Information Report N-X-160. 72 p.

Scott, J.T.; Siccama, T.G.; Johnson, A.H.; Breisch, A.R. 1984. Decline of the red spruce in the Adirondacks, New York. Bulletin of Torrey Botanical Club. 111(4).

Siccama, T.G.; Bliss, M.; Vogelmann, H.W. 1982. Decline of red spruce in the Green Mountains of Vermont. Bulletin of the Torrey Botanical Club. 109(2): 162-168.

Speers, C.F. 1958. The balsam woolly aphid in the Southeast. Journal of Forestry. 56(7): 515-516.

Vogelmann, H.W.; Badger, G.J.; Bliss, M.; Klein, R.M. 1985. Forest decline on Camels Hump, Vermont. Bulletin of the Torrey Botanical Club. 112: 274-287.

Whittaker, R.H. 1956. The vegetation of the Great Smoky Mountains. Ecological Monographs. 26(1): 1-80.

A Tree Ring Analysis of Red Spruce in the Southern Appalachian Mountains

Edward R. Cook

INTRODUCTION

A recent analysis of red spruce (*Picea rubens* Sarg.) tree ring widths in southern Appalachian stands has caused concern that the red spruce forests of the southern Appalachian mountains may be in an early stage of decline (Adams and others 1985). Although many hypotheses have been generated regarding the cause of the red spruce decline, no definite answer has yet been found (McLaughlin 1985). If the decline in red spruce ring width can be explained by natural effects, then costly and needless pollution controls may be avoided.

The Tennessee Valley Authority (TVA) and the National Park Service (NPS) conducted studies on permanent plots established throughout forests of the southern Appalachians. Long-term changes in the composition and health of the forest were monitored. Using the data provided by the NPS and TVA, the objective of my analysis was to determine if the recent patterns in the ring widths indicate an anomalous decline and if this decline can be explained by natural environmental factors related to climate. The analyses were performed on annual tree ring chronologies (Fritts 1976, Cook 1985) developed from the ring width series of each plot.

TREE RING DATA QUALITY CHECK AND STANDARDIZATION

The quality of the data provided by the NPS and TVA was checked using the COFECHA program of Holmes (1983). The program checked for cross-dating errors, measurement errors, and other ring width irregularities that might limit the usability of ring width time series for tree ring analysis. Because the actual increment cores were not available for this quality check, the program output was used to verify cross-dating, make corrections of dating when possible, and eliminate ring width series for which no obvious corrections could be made. Approximately 15 percent of the ring width series were either

corrected or removed from the data set. Therefore the number of ring width series for some plots were reduced to as few as three.

After the quality check, the remaining ring width series of each plot were standardized (Fritts 1976, Cook 1985) to remove long-term trends in growth associated with tree age, size, and stand dynamics. The need for standardization prior to creating a stand-average tree ring chronology is discussed in detail in Fritts (1976) and Cook (1987). Because the ring width series were rarely more than 100 years long, negative exponential or linear regression curves were used to detrend the series.

However, it was unlikely that this conservative detrending method would remove any anomalous decline signal during standardization. After the growth curve was estimated for each series, the tree ring indices were computed as:

$$I_t = R_t / G_t$$

where I_t equaled the tree ring index, R_t was the ring width, and G_t equaled the growth curve value, all for year t . Therefore a tree ring index can be defined as the ratio of the actual ring width to the expected value as estimated by G_t . Tree ring indices have a long-term mean of 1.0 and a variance that is reasonably time stable. Thus tree ring indices are stationary processes that can be averaged into a stand-average series. After each ring width series was reduced to index form, the tree ring index series of each plot were averaged into a final tree ring chronology using the biweight robust mean (Mosteller and Tukey 1977) to reduce the influence of outliers on the computation of the mean-value function.

STRATIFICATION AND SCREENING OF PLOTS

The TVA and NPS plots were stratified by elevation into three groups: below 5,400 feet, 5,400 to 6,000 feet, and above 6,000 feet. These strata reflected a vegetational gradient in the

Edward R. Cook is a research scientist at Lamont-Doherty Geological Observatory in Palisades, New York.

mountains. The lowest red spruce stratum was predominantly a mixed conifer-hardwoods forest zone, while the strata above 5,400 feet were within the spruce-fir zone (White 1984). The highest elevational stratum contained the highest proportion of Fraser fir (*Abies fraseri* [Pursh] Poir.) relative to red spruce and was the zone most heavily impacted by the balsam woolly adelgid (Eagar 1984).

The elevational strata also reflected a climatic gradient of increasing precipitation and decreasing temperature with increasing elevation. Thus the below-5,400-foot stratum was the warmest and driest area and the above-6,000-foot stratum the coolest and wettest. Additionally, the highest stratum was enveloped in clouds most often and the lowest stratum was enveloped in clouds least often.

The climatic response of red spruce in the southern Appalachian Mountains has not been studied as thoroughly as it has in the northern Appalachians (Conkey 1979, McLaughlin and others 1987, Cook and others 1987). However, based on ecological principles, it is probable that the role of temperature will increase as a limiting factor in red spruce growth at the elevational extremes of the species' range. Precipitation will also be more important as a limiting factor at the below-5,400-foot plots. Therefore a gradient in the response of red spruce to climate should be found that will correlate well with some aspect of the known climatic gradient.

The stratification by elevation produced 11 TVA and 8 NPS plots in the above-6,000-foot stratum, 13 TVA and 6 NPS plots in the 5,400- to 6,000-foot stratum, and 24 TVA and 7 NPS plots in the below-5,400-foot stratum. At this stage, some of the plots were eliminated because of the shortness of the tree ring chronologies. Because 1930 was chosen as an initial criterion for the inclusion of tree ring series in the analyses, any series beginning after 1930 was eliminated. The year 1930 allowed for the inclusion of the large majority of plots and simultaneously provided an adequate time base for the dendroclimatic analyses. A longer time base would have been better, but it also would have eliminated too many sites. Furthermore, the best available climatic data began in 1931.

After the elimination of short series, the sample depth of the 1930 decade was examined for each remaining chronology. If the sample depth was largely based on only one increment core in that decade, then that chronology was eliminated. The reason for this step in the preliminary screening was to insure that the 1930 decade would not be unduly affected by poor replication at some sites.

The final result of the screening was the selection of 13 plots above 6,000 feet, 15 plots between 5,400 and 6,000 feet, and 29 plots below 5,400 feet. Eight above-6,000-foot series were from NPS plots, four were from TVA Mt. Mitchell, and one was from TVA Roan Mountain. Thus the above-6,000-foot series comprised 68 percent of the available plots. The geographic coverage of this stratum was obviously limited by the maximum elevations of the mountains. The 5,400- to 6,000-foot stratum was composed of six NPS plots and nine TVA plots; these represented 78 percent of the available plots. The geographic coverage

was much better. Only Roan Mountain and Grandfather Mountain were not represented. The below-5,400-foot stratum was composed of 7 NPS and 22 TVA plots, representing 93 percent of the available plots. The geographic coverage was complete, with all mountains represented.

AUTOREGRESSIVE TIME SERIES MODELING

Tree ring series invariably possess some degree of serial persistence or autocorrelation that is principally due to physiological preconditioning within the tree. Therefore the information contained in a given ring width is somewhat determined by past tree growth and vigor. Typically, the autocorrelation structure of tree ring indices can be adequately modeled as an autoregressive process (Cook 1985). The general autoregressive (AR) process of order p has the form (Box and Jenkins 1970):

$$Z_t = e_t + \sum_{i=1}^p \Phi_i Z_{t-i}$$

where Z_t is the observed process for year t , e_t equals an unobserved input or random shock that does not contain any autocorrelation, and Φ_i the autoregressive coefficients of the AR(p) process.

In the context of this tree ring analysis, the Z_t were the tree ring indices for a plot. Each tree ring series was modeled as an AR(2) for the common interval 1930-83. The choice of an AR(2) model was based on previous experience modeling longer red spruce chronologies as AR processes. The common AR persistence structure among all plots within each stratum was also estimated using a pooling procedure described in Cook (1985). Differences between the common AR model and those for the individual series were useful tools for measuring the level of autocorrelated noise in the individual series, which may have been caused by different stand histories and disturbance regimes.

For the above-6,000-foot stratum, the common or pooled AR coefficients and the percent variance explained by autoregression (R^2) were: $\Phi_1 = 0.461$, $\Phi_2 = 0.284$, and $R^2 = 46.1$ percent. For the 13 individual series, the average statistics were: $\Phi_1 = 0.566$, $\Phi_2 = 0.138$, and $R^2 = 47.9$ percent. Although the R^2 's were similar, the AR coefficients were noticeably different, probably because of residual trend or trendline lack-of-fit in the individual series. However, the similarity of the R^2 's suggested that the differences between the tree ring chronologies were largely random through time. Thus the long-term disturbance histories of these plots may have been similar since 1930.

For the 5,400- to 6,000-foot stratum, the pooled statistics were: $\Phi_1 = 0.324$, $\Phi_2 = 0.177$, and $R^2 = 18.1$ percent. For the 15 individual series, the average statistics are: $\Phi_1 = 0.484$, $\Phi_2 = 0.168$, and $R^2 = 39.1$ percent. The pooled AR(1) coefficient and R^2 were considerably smaller than the average values for the individual series. The latter indicated a high level of autocorrelated noise or out-of-phase behavior between series. Therefore the disturbance histories of these plots were probably more variable than those in the higher stratum.

For the below-5,400-foot stratum, the pooled

statistics were: $\Phi_1 = 0.422$, $\Phi_2 = 0.124$, and $R^2 = 24.4$ percent. For the 29 individual series, the average statistics were: $\Phi_1 = 0.530$, $\Phi_2 = 0.094$, and $R^2 = 39.3$ percent. These statistics were close to those from the intermediate elevation plots and indicated a similar degree of nonhomogeneity from plot to plot.

The lower levels of plot homogeneity in the strata below 6,000 feet suggested that these plots have more varied disturbance histories. An examination of the individual time series from these plots confirmed this inference. Some of the plots showed release patterns early in this century that were consistent with logging activity. Given the much reduced spatial coverage of the above-6,000-foot plots, the higher level of homogeneity among these plots was probably related to the lack of interference by man.

PRINCIPAL COMPONENTS ANALYSIS (PCA)

Because each chronology was based on a small sample of trees, the dendroclimatic modeling of each plot chronology was not considered a viable approach. The results would have been somewhat chaotic because of the very high level of noise in each chronology. Therefore the common variance among all series within each stratum was pooled using principal components analysis (PCA) (Cooley and Lohnes 1971). In PCA, the structure in the correlation matrix of variables is transformed into a new set of uncorrelated or orthogonal modes of behavior called eigenvectors. Each eigenvector accounts for a unique proportion of the total variance in the original data. The first eigenvector associated with the largest eigenvalue accounts for the greatest percentage of common variance among all variables in the correlation matrix.

Each eigenvector is composed of a number of loadings or coefficients equal to the number of original variables in the correlation matrix. These loadings, which may be positive or negative, reflect the relationships between variables for a specific eigenvector. Frequently the loadings of the first eigenvector are all positive or negative, which indicates that the variables being analyzed all behave similarly. Therefore, in this study, the tree ring series at each elevational stratum could exhibit a common signal due to climate, disturbance, or pollution.

The loadings of the first eigenvector can also be used to create a time series of scores that reveal how this most common component among all series behaves through time. This series of scores is similar to a weighted mean, because each series is weighted by its eigenvector loading and then summed with the other weighted series for each year. The weighting scheme is optimal in the sense that no other component can account for more of the common variance between series than the first eigenvector. Consequently, the scores for each elevational stratum should have a strong common signal for dendroclimatic analysis.

The PCA analyses were done twice for each stratum: once on the original tree ring indices and again on the indices after removing AR(2) persistence from each series. Indices are referred to as prewhitened after removal of AR(2) persistence. For the above-6,000-foot stratum of

13 plots, the first eigenvector of the original tree ring indices accounted for 50.7 percent of the total variance, while that of the prewhitened indices accounted for 53.6 percent of the variance. Common variance increased after prewhitening because of a reduction of noise variance resultant from autoregressive modeling. In figure 1, the loadings for this eigenvector are all positive, indicating an existing common signal among all series. The loadings for the prewhitened indices were more uniformly positive than those of the original indices. This uniformity indicated that some of the differences between the original indices were amplified by the autoregression within those series.

For the 5,400- to 6,000-foot stratum of 15 plots, the first eigenvector of the original tree ring indices accounted for 34.1 percent of the variance, while the prewhitened indices accounted for 45.9 percent. The larger increase in common variance after prewhitening indicated that these chronologies were less homogeneous than those in the higher stratum. Greater variability in site characteristics and stand histories in this intermediate stratum may have caused the difference. Comparing the single series and pooled autoregression models also indicated the lack of homogeneity between the chronologies. However, the more restricted geographic coverage of the high stratum may be a biasing agent in this comparison. As before, the eigenvector loadings (fig. 1) were also more uniform after prewhitening.

For the below-5,400-foot stratum of 29 plots, the first eigenvector of the original tree ring indices accounted for 32.6 percent of the variance, while that of the prewhitened indices accounted for 40.7 percent. The magnitude of the difference was similar to that of the intermediate stratum. Therefore the level of homogeneity between plots was similar, an inference also supported by the earlier autoregressive modeling results. The eigenvector loadings (fig. 1) of the prewhitened indices were also more uniform than the loadings of the original indices.

Generally the strength of the common signal within each stratum was directly correlated with the elevational gradient. The tree ring patterns of high plots were more similar among themselves than those of the lower plots. Although it may appear that this result reflected more limiting growth conditions towards the upper elevational limit, the bias in the geographic coverage of that stratum limits the strength of this interpretation.

The eigenvector amplitudes or scores of each stratum are shown in figure 2. The solid line plots were derived from the original tree ring indices, and the dashed line plots were derived from the AR(2) prewhitened indices.

The scores derived from the original indices indicate an overall pattern of below-average growth at all plots since about 1966. The largest departure was for the above-6,000-foot plots. The average score since 1966 was -2.65 with a standard error of ± 0.495 . For the 5,400- to 6,000-foot stratum, the average score was -1.54 ± 0.522 . And, for the below-5,400-foot stratum, the average score was -1.73 ± 0.638 . These long-term departures appeared to exceed the 95-percent significance level using a simple t-test. However, the use of a t-test on

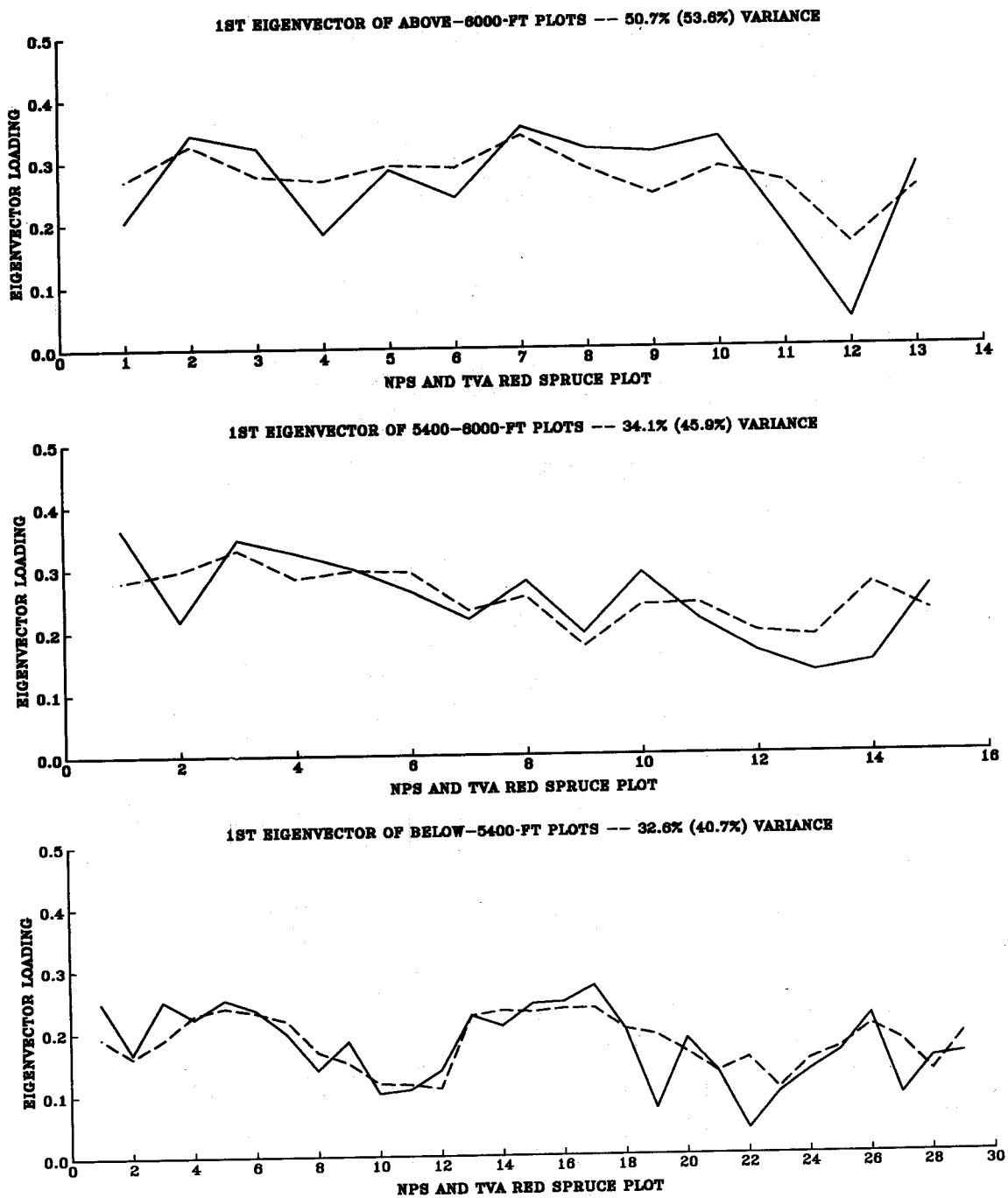


Figure 1.--The eigenvector loadings of the first principal component of each red spruce elevation stratum. The solid line plots correspond to the loadings of the original tree ring index chronologies. The dashed line plots correspond to the loadings of the same series after second-order autoregression has been removed from each one. The eigenvectors were extracted from the correlation matrix. The percent variance accounted for by each eigenvector, original (prewhitened), is indicated.

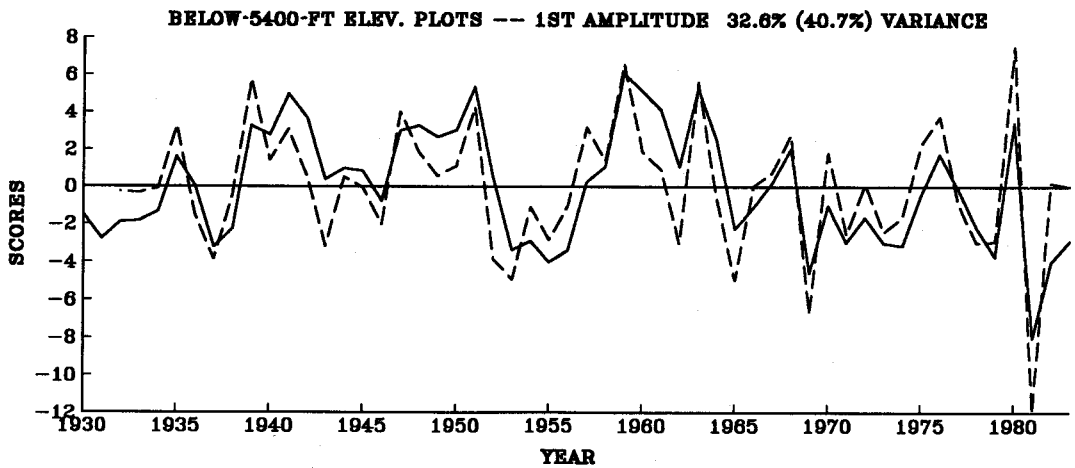
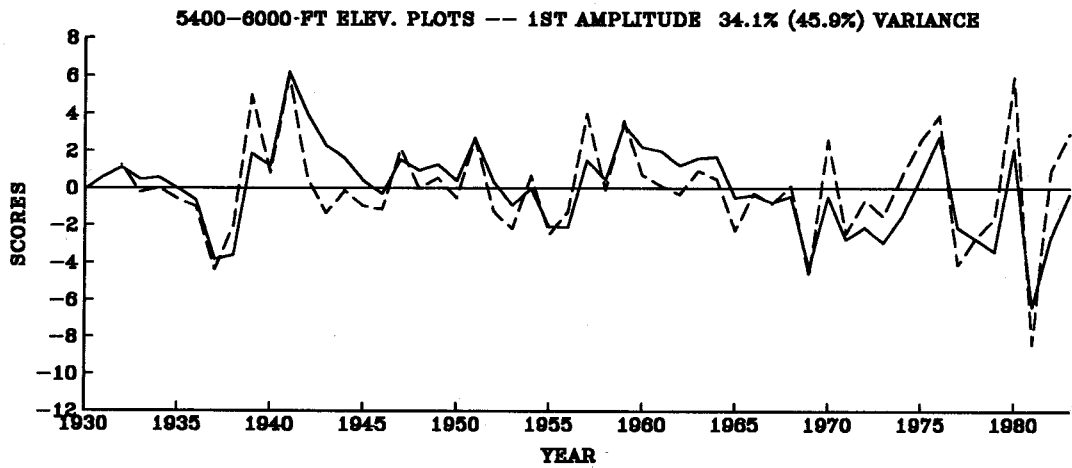
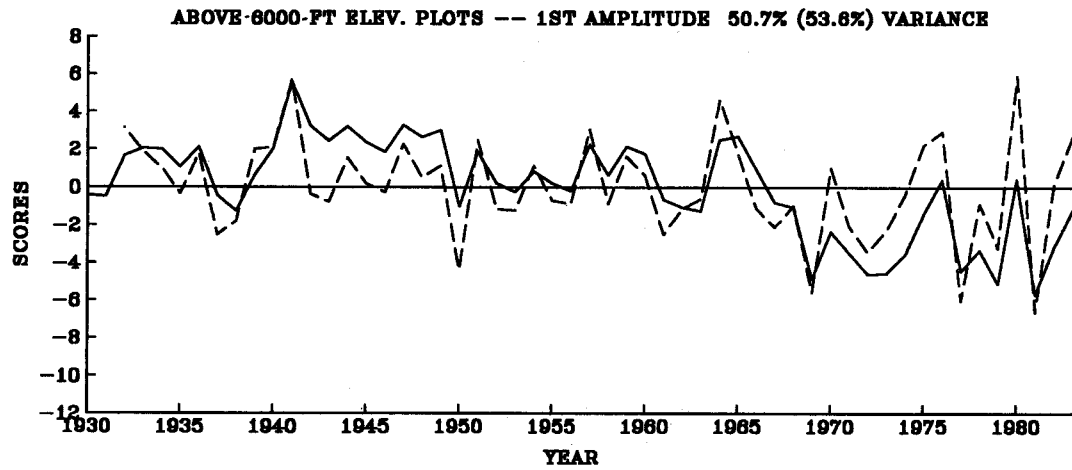


Figure 2.--The principal component amplitudes or scores corresponding to the eigenvectors in figure 1. The solid line plots are for the original series. The dashed line plots are for the prewhitened series.

autocorrelated time series such as these can be extremely misleading. The number of independent observations and the degrees-of-freedom may be much less than the number indicated by the available observations.

One way of avoiding the negative effect of autocorrelation on the degrees-of-freedom is to use the scores of the AR(2) prewhitened indices. By definition, these scores do not have any significant autocorrelation related to that level of autoregression. In figure 2, the prewhitened scores indicate a smaller reduction in growth since 1966 in all series. The post-1965 means confirmed this. For the above-6,000-foot, 5,400- to 6,000-foot, and below-5,400-foot strata, the 1966 to 1983 means were -1.09 ± 0.779 , -0.42 ± 0.807 , and -0.71 ± 0.992 , respectively. None of these means passed a t-test at the 95-percent significance level. Therefore there may have not been any reduction in growth since 1966. The decline in the original tree ring indices may be largely explained by the endogenous autoregressive persistence of the tree ring data and the way in which it amplifies the behavior of the random shocks, e_t , which are largely exogenous to the plots.

The above conclusion was conservative because the AR coefficients used for prewhitening were based on information in both the pre-1966 and post-1966 time periods. The method employed minimized the probability of a type I error because it assumed that the AR coefficients had not changed through time despite an intervention in the e_t that may have occurred in 1966. Since an intervention in the e_t could have a strong impact on the estimation of the AR coefficients, the prewhitening may have removed part of the response to an intervention had it occurred. In order to reduce the probability of a type II error in these analyses, an alternate method of intervention analysis (Box and Tiao 1975) testing for the occurrence of an intervention in autocorrelated time series was used.

INTERVENTION ANALYSIS

Intervention analysis specifically allows for autocorrelation when testing for the occurrence of an intervention in time series. A simple form of intervention analysis was used in this study to test for the occurrence of a decline in the scores since 1966. The form of the intervention chosen was a step-function, which is expressed as [0 0 0 ...] from 1930 to 1965 and [1 1 1 ...] from 1966 to 1983. This step-function served as one of the predictor variables in the analysis. To account for autocorrelation in each time series, the scores for years $t-1$ and $t-2$ were also used as predictors. The model used allowed for both the occurrence of a step reduction in growth and AR(2) persistence. The intervention model was set up as a multiple regression analysis problem. In each case, only the step-function and the lag-1 variable proved to be statistically significant at the 90-percent level or higher.

In contrast, the lag-2 variable never exceeded the 60-percent significance level. For this reason, lag-2 was not used in the final models. Although one might infer that the previous AR(2) models were reasonable only because an

intervention around 1966 changed the system, the timing of the intervention was hypothesized only after an examination of the data. Thus any inferences concerning a change in persistence structure because of an intervention must take into account the a posteriori nature of these analyses. This issue will be addressed later, as it affects significance tests.

The results of the intervention analysis were as follows:

Stratum	AR(1)	Step	R ²
Above 6,000 ft	0.260**	-0.566***	58.9%
5,400-6,000 ft	0.234*	-0.369**	27.6%
Below 5,400 ft	0.360***	-0.275**	28.8%

*p < 0.10, **p < 0.05, *** p < 0.01

The strength of the step intervention was directly correlated with elevation. The above-6,000-foot scores showed the strongest indication of an intervention in 1966, which resulted in a steplike reduction in growth. This result was consistent with the original examination of the 1966 to 1983 means for these scores. However, the step-elevation relationship was new. The high level of persistence in the above-6,000-foot scores was greatly reduced by the step. In contrast, the persistence in the lower strata was reduced less. The reduction in persistence from the earlier AR(2) modeling appears to be proportional to the strength of the step.

The probability levels of the intervention analysis were based on an a priori significance test in each case. Acceptance of these results would effectively minimize type II error at the expense of type I error, in contrast to the earlier prewhitening results that minimized type I error. Therefore these sets of results served as useful limits. As noted earlier, there was a problem in applying a priori significance tests to a statistical analysis problem that was principally based on an a posteriori examination of the data. Furthermore, the a posteriori examination of the scores for an intervention allowed for 50 possible intervention dates for a step-function.

Based on probability theory, the probability of finding a statistically significant step-function under such conditions is related to the a priori significance level as:

$$P = 1 - (1 - p)^m$$

where P is the a posteriori probability level, p is the a priori probability level of the test being applied, and m is the number of times the test could be applied to the data. If this correction is applied to the probability levels for the step interventions shown above, only the above-6000-foot step intervention remains statistically significant (P < 0.01). The other steps do not even pass the P < 0.50 level. This correction is probably overly severe since the a priori information about the probable timing of red spruce decline in the northern Appalachians (Johnson and Siccama 1983).

All available evidence indicated that the decline in the northern Appalachians started in the late 1950's to early 1960's. There is no

evidence to suggest that any decline in the southern Appalachians began before the northern decline. Thus no intervention should be found prior to 1960. If this information is used to limit the intervention time window to 1960-81, the results of the lower two strata still remain well outside the $P < 0.10$ level of significance, which is still unacceptable. For an a posteriori probability level of $P = 0.10$ to be achieved, an a priori probability of $p = 0.01$ and an intervention time window of 10 years are needed. Unless additional constraints based on a priori

information can be found to reduce the time window of the hypothesized intervention, the null hypothesis of no intervention for the lower strata cannot be rejected on statistical grounds.

Figure 3 shows each series of scores with its fitted intervention model. As the statistics indicate, the above-6,000-foot model revealed a much more pronounced step change than the other models.

All strata showed signs of decreasing growth after 1966. However, growth reduction in the lower strata diminished with decreasing

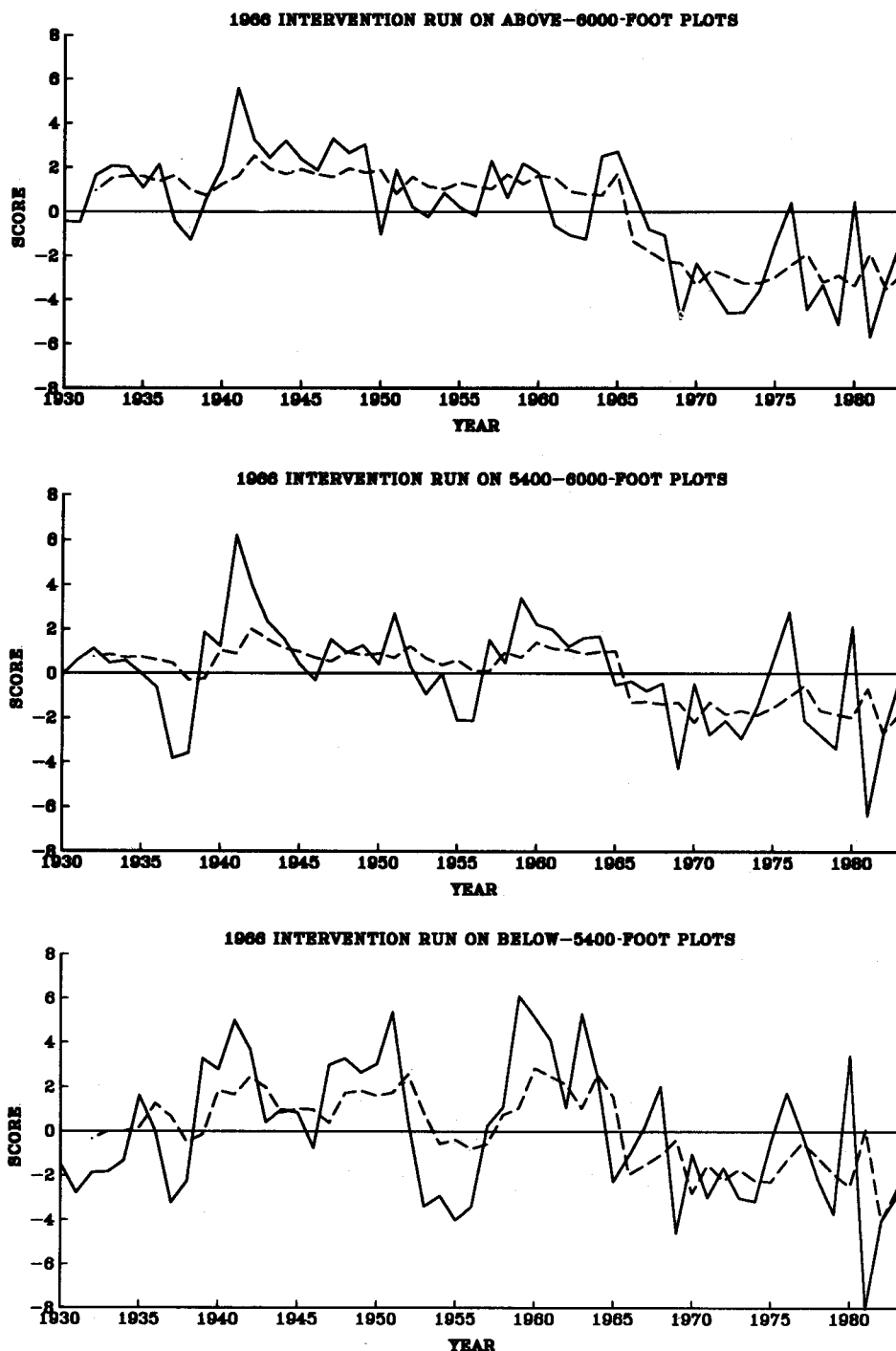


Figure 3.--The actual (solid) and estimated (dash) tree ring scores based on fitting a step intervention model to each series. The date of the intervention is 1966.

elevation. The cause of the growth reduction is still undetermined. Climate or other changes in natural influences are as probable a cause as are anthropogenic pollutants.

The reality of the elevational gradient in step size may be questioned. However, the existence of known environmental-climatic gradients in the mountains suggests that the step-size gradient is a reality. The step-size gradient may be due to a temperature-related phenomenon. This hypothesis is consistent with what is now known about the relationship between temperature stress and red spruce declines in the northern Appalachian Mountains (Cook and others 1987).

DENDROCLIMATOLOGY OF RED SPRUCE BY ELEVATIONAL STRATUM

As noted earlier, the three strata used in this study follow both vegetational and climatic gradients, which are directly correlated with elevation. To illustrate the reflection of this gradient in the tree rings, figure 4 shows the three series of original tree ring index scores superimposed on each other. Various time periods in figure 4 (1932-34, 1935-57, 1959-63) indicate striking gradients across scores correlated with elevation. The presence of these gradients across scores suggests that an elevational gradient in the climatic response of red spruce operates at times.

At other times in the scores (1940-42, 1958, 1969), the gradient breaks down, and the scores of all strata are similar. This similarity suggests that the relationship between climatic response and elevation is nonstationary through

time. The degree to which the gradient exists probably depends on which climatic variables are limiting to red spruce growth in a given year and how those climatic variables are influenced by elevation. For example, based on the physics of precipitation formation and its interaction with orography, the influence of drought on red spruce growth should diminish with increasing elevation. However, once the available moisture supply is no longer limiting to growth, this drought response gradient would probably disappear from the tree rings.

In this study, dendroclimatic modeling is limited by the lengths of the series being modeled and the unavailability of long climatic time series. Ideally, the modeling should proceed as described by Cook 1987; the dendroclimatic signal should be modeled for a long preintervention time period of perhaps 50 to 60 years. A model should then be used to forecast or predict tree rings through a period to the present that includes both another preintervention time block and the post-intervention period. The time stability of the dendroclimatic model must be tested; therefore another preintervention time period is needed. If the model is verified as time stable, then it can be used to test for an intervention that changes the tree ring response to the model. This method has been successively used in analyzing the red spruce decline in the Appalachian Mountains (McLaughlin and others 1987, Cook and others 1987).

Because of the insufficient tree ring time base, a weaker method of modeling was implemented that provided a basis for inference regarding the climatic response gradient hypothesized earlier.

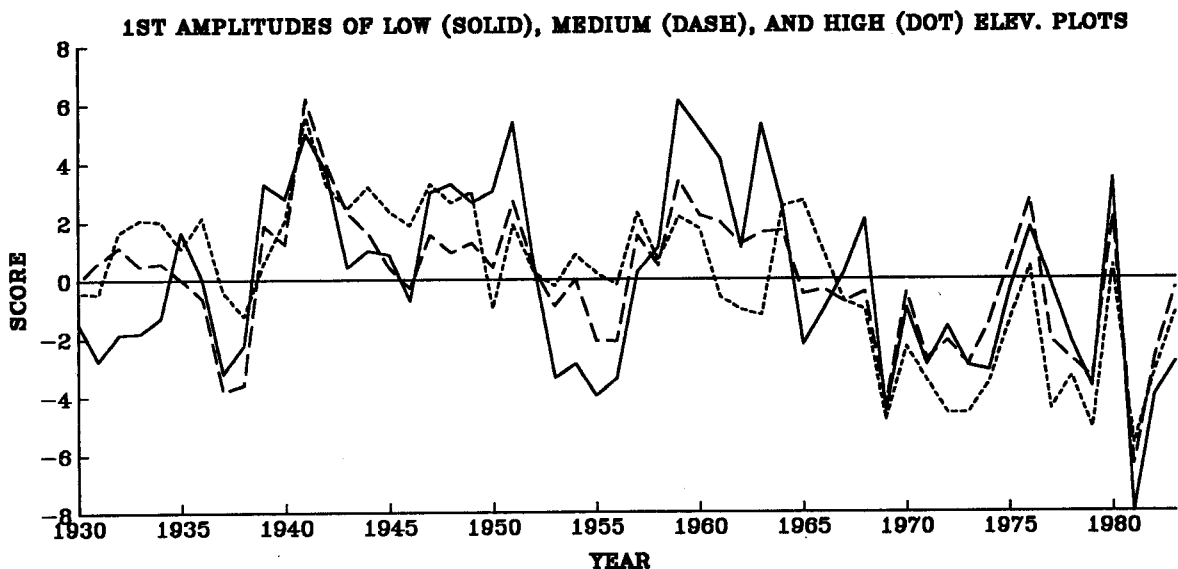


Figure 4.--The amplitudes of the original tree ring indices superimposed on each other. The purpose of this plot is to highlight certain time periods when elevation-related gradients in climate response are likely to be occurring.

This method was based on simple correlations between the tree ring scores and monthly climatic data for the period 1931-83.

Prior to the correlation analyses, the tree ring scores for each elevational stratum were prewhitened to remove autocorrelation. In each case, significant AR(1) or AR(2) persistence was removed. The monthly temperature and precipitation data, averaged over the northern and southern mountain climatic divisions of North Carolina and the southwestern mountain division of Virginia, were similarly modeled for autocorrelation. In this case, the climatic data showed very weak or nonexistent autocorrelation out to lag 3. Therefore, the climatic data were not prewhitened.

The dendroclimatic modeling was then treated as a multiple input-single output transfer function (Box and Jenkins 1970) in which ring width was a function of climate. Given the lack of autocorrelation in either the input or output series, the principal aim of the transfer function model was to identify those climatic variables that correlated significantly with tree rings and identify any delay or lag-response between the inputs and the output. The analysis assumed that the climatic variables were orthogonal, an assumption that was violated for almost all variables. This violation may have increased the number of significant climatic variables in the model. However, since the aim of these analyses is strictly correlative and not predictive, this should not have any serious impact on the results.

The tree ring scores were lagged up to 3 years in the transfer function analyses, meaning that each monthly climatic variable was correlated with each series of scores for years t , $t+1$, $t+2$, and $t+3$. A plot of the correlations by lag produced a normalized form of the impulse response function for 1932-62 and 1966-80 time periods of the system being modeled (Box and Jenkins 1970). For each period, 48 precipitation and 48 temperature correlation coefficients were computed. While the a posteriori nature of these analyses makes the use of a priori significance tests very questionable, these results should be viewed as more exploratory than confirmatory. Therefore the a priori confidence limits will be used to assess the significance of the correlation coefficients.

The results of this modeling were somewhat complex to explain. In each time period, some indications of climatic gradients were found. For example, in the 1932-62 period, the correlation between tree rings and March precipitation at lag $t+2$ were:

Above 6,000 feet: -0.102
 5400 to 6,000 feet: -0.604
 Below 5,400 feet: -0.636

The correlations of the lower two strata were significant ($p < 0.001$) in a statistical sense. However, the $t+2$ lags were very difficult to explain physiologically. More disconcerting, these correlations completely lost statistical significance (maximum $|r| < 0.15$) in the 1966-80 period. Therefore these significant correlations were either spurious or the climatic signal in the red spruce was highly nonstationary. The

latter problem may also indicate a loss of climatic signal comparable to what has apparently happened to the declining red spruce in the northern Appalachian Mountains (Cook 1987, McLaughlin and others 1987, Cook and others, 1987).

In the suite of 96 total correlations, only three monthly temperature variables showed any consistency through both time periods; July, August, and September temperatures correlated with $t+1$ lagged tree rings as follows:

Stratum		1932-62	1966-80
Above 6,000 feet	July	-0.343*	-0.273
	August	-0.268	-0.134
	Sept.	-0.223	-0.132
5,400-6,000 feet	July	-0.388**	-0.395*
	August	-0.334*	-0.361
	Sept.	-0.403**	-0.326
Below 5,400 feet	July	-0.351*	-0.547**
	August	-0.247	-0.576**
	Sept.	-0.365**	-0.453*

* $p < 0.10$ **, $p < 0.05$, *** $p < 0.01$

There is an indication, especially in the 1966-80 period, of an elevational gradient in the response to the temperature variables. The high-elevation stands seem to be less sensitive to summer temperatures than the lower stands. There is also an indication that the below-5,400-foot spruce have been more sensitive to summertime temperature since 1966.

On the basis of these monthly temperature correlations, the July, August, and September temperatures were averaged into a summer season temperature series (fig. 5). Of particular interest is the summer of 1980, the warmest summer in the southern Appalachians since 1931. According to figure 4, the poorest growth year for red spruce at all elevations was 1981. Given the $t+1$ lag response of red spruce to summer temperatures indicated above, the poor 1981 growth year was probably related to excessively warm summer temperatures in 1980, which extended to the highest elevations in the mountains.

Linear regression analyses of the summer temperature series versus prewhitened red spruce scores indicated that the below-5,400- and 5,400 to 6,000-foot strata were equally sensitive to previous summer temperatures over the period 1932-83. The regression R^2 's were, respectively, 0.199 and 0.182. In contrast, the above-6,000-foot regression R^2 was 0.137. The prewhitened scores and their temperature estimates are shown in figure 6. Interestingly, all strata follow the pattern of summer temperature almost perfectly since 1978. This corresponds to the warmer than average temperatures since 1977.

It was previously suggested that the lower elevation plots should be more stressed by precipitation deficiency than the higher elevation plots. In order to determine the degree of drought sensitivity in the prewhitened red spruce scores, the monthly Palmer Drought Severity Indices (PDSI) (Palmer 1965) were computed from the divisional average temperature and precipitation data. Simple correlations were

JULY-AUGUST-SEPTEMBER AVERAGE TEMPERATURES

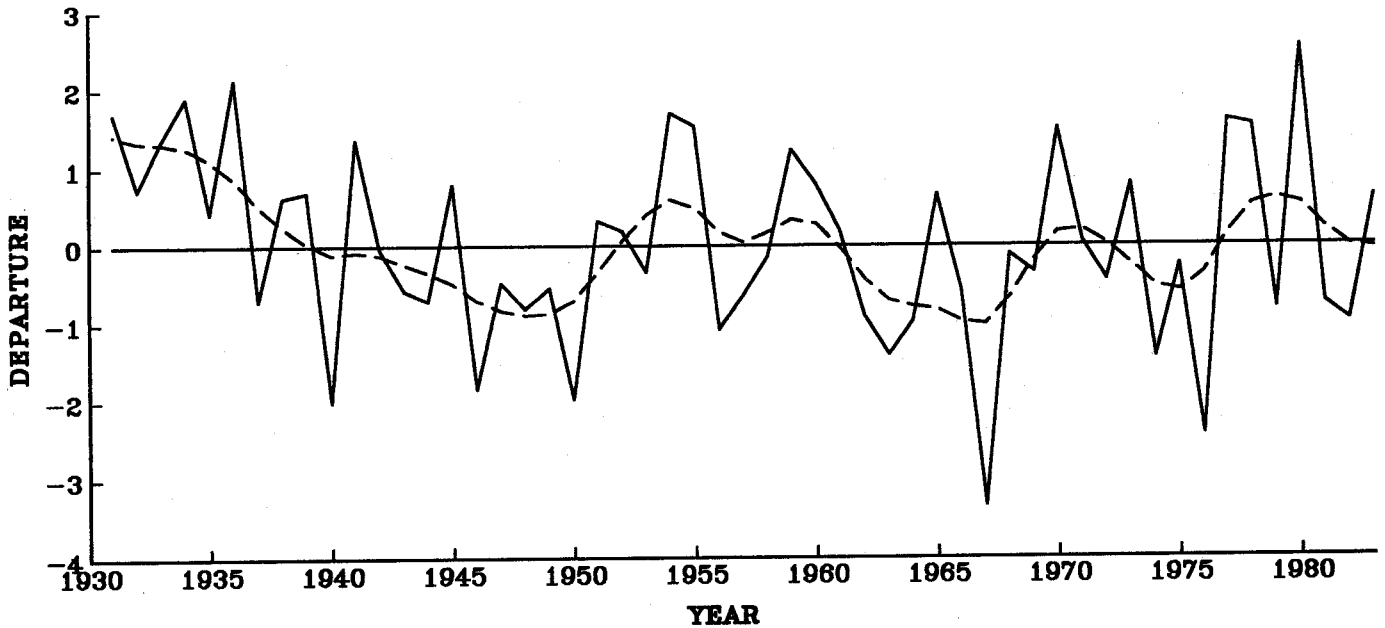


Figure 5.--July, August, and September average temperatures for the southern Appalachian Mountains since 1931. The dashed line highlights variance at frequencies of 1/10 year or less.

again computed between monthly PDSI and tree ring scores at lags t through $t + 3$ for the time periods 1932-62 and 1966-80. The results of these simple correlation analyses were very similar to the analyses reported earlier; the correlations were generally not time stable. However, as before, summertime drought and $t + 1$ lagged scores showed some time stability and statistical significance.

These correlations were as follows:

Stratum	Month	1932-62	1966-80
Above 6,000 feet	July	0.066	0.521**
	August	-0.004	0.640**
	Sept.	-0.281	0.728***
5,400-6,000 feet	July	0.442**	0.521**
	August	0.427**	0.666**
	Sept.	0.079	0.761***
Below 5,400 feet	July	0.457***	0.458*
	August	0.402**	0.641**
	Sept.	0.244	0.771***

* $p < 0.10$, ** $p < 0.05$, *** $p < 0.01$

In the 1932-62 period, there was a clear indication of an elevational gradient. The highest stratum showed no summertime drought signal in contrast to the lower strata. However, all strata showed a very pronounced summertime drought response in the 1966-80 period. This apparent increase in sensitivity to PDSI was stronger than that indicated by summertime temperature alone.

As before, the monthly PDSI's were averaged into a summertime season estimate of drought since 1931 (fig. 7). Of particular interest is

the time period of 1952-55, which contained the worst drought in the southern Appalachians since 1931. The very strong elevation-related gradient in the tree ring scores for this period was almost definitely caused by severity of this drought and the way in which it diminished with increasing elevation. It is difficult to explain why red spruce at all elevations showed approximately the same level of response to PDSI since 1966. Given the shortness of this time period, it is possible that these results are questionable, even with the high significance levels of the correlation coefficients. However, this apparent increase in sensitivity to summertime moisture availability should be investigated more fully, as better statistical methods and tree ring data become available.

Linear regression analyses of the prewhitened scores versus summer PDSI for the period 1932-83 indicated a weaker relationship overall than for summer temperature alone. The R^2 's for the below-5,400-, 5,400- to 6,000-, and above-6,000-foot strata were 0.151, 0.114, and 0.035, respectively. The actual and predicted scores

from these models are shown in figure 8. There generally appears to be less time stability in PDSI-spruce relationships.

Summer temperatures and PDSI were correlated ($r = -0.38$) because the temperature data were partially used to estimate the PDSI's. However, the level of correlation was not high enough to indicate that the PDSI correlations were completely confounded by the temperature effects. In fact, when the PDSI and temperature variables were used in a stepwise multiple regression analysis to predict red spruce scores, each variable entered the model according to the strength and sign of its original correlation

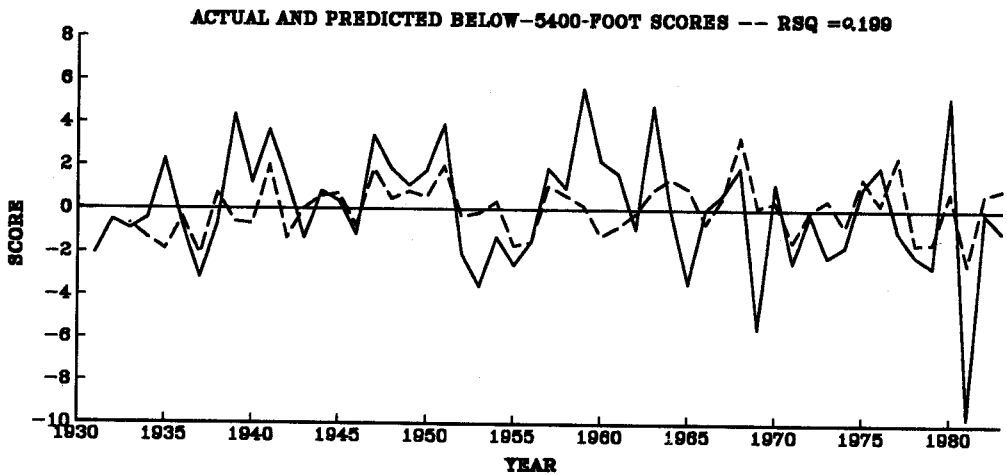
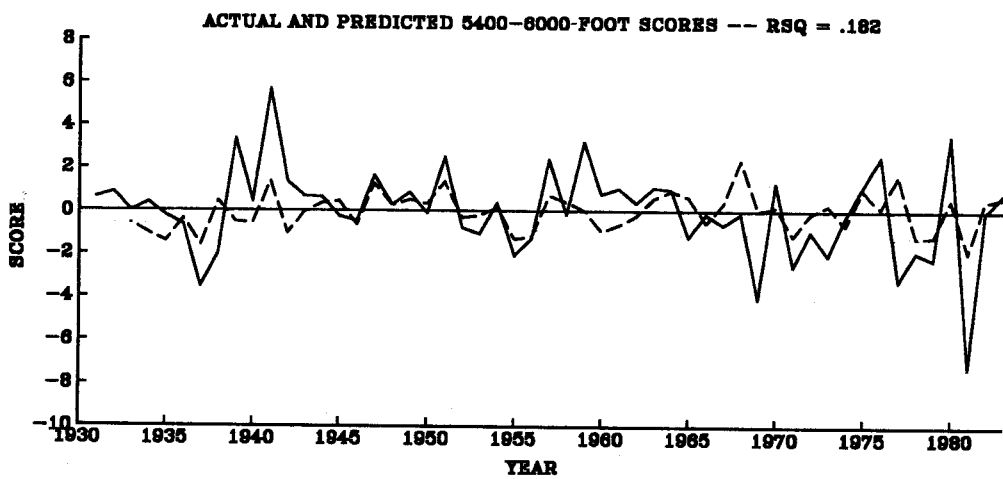
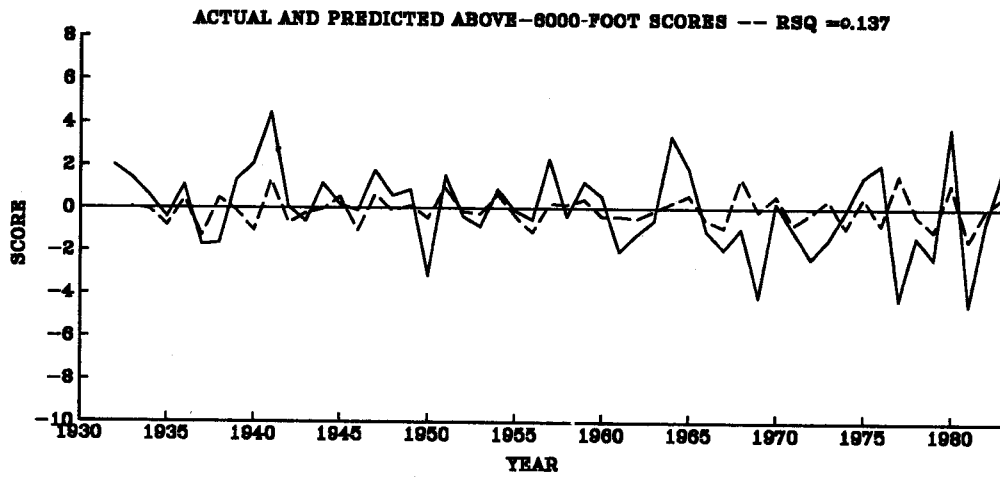


Figure 6.--Actual (solid) and predicted (dash) prewhitened tree ring scores. The summer temperature series (fig. 5) was used as the predictor of tree rings. The R^2 of each model is indicated by the RSQ value.

JULY-AUGUST-SEPTEMBER PALMER DROUGHT INDEX

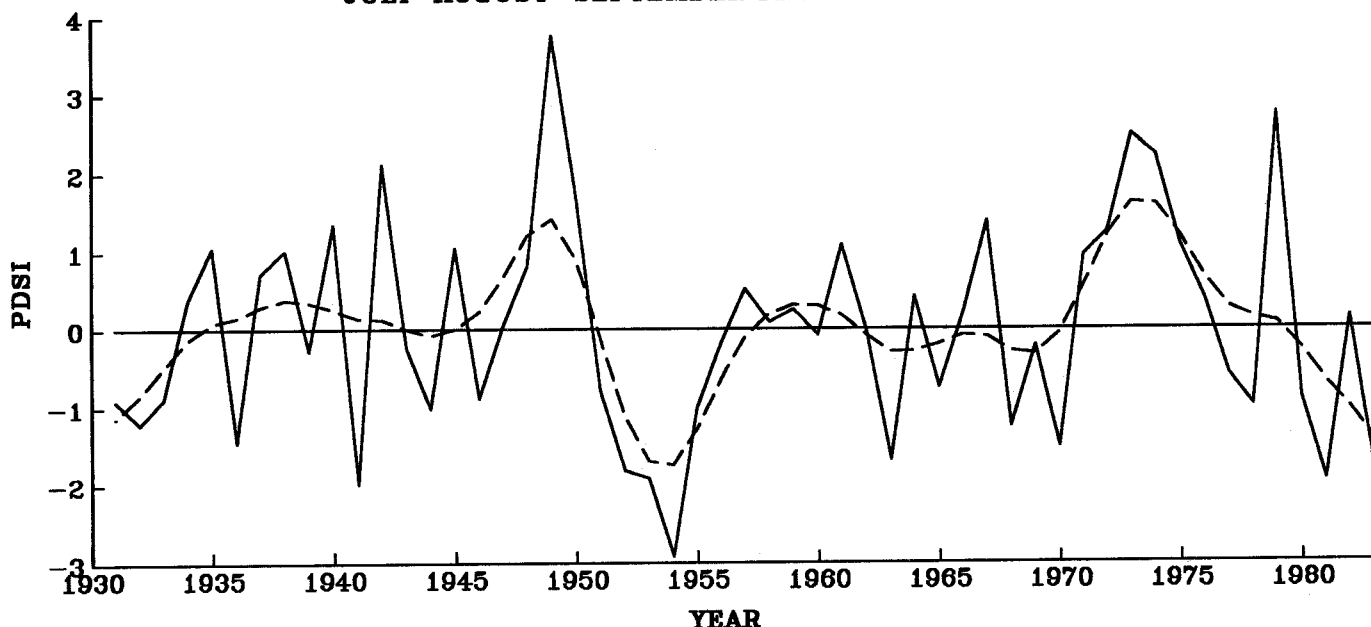


Figure 7.--July, August, and September average Palmer Drought Severity Indices (PDSI) series for the southern Appalachian Mountains. The dashed line highlights variance at frequencies less than 1/10 year.

with the scores. The resulting R^2 's for the below-5,400-, 5,400- to 6,000-, and above-6,000-foot strata were 0.252, 0.203, and 0.123, respectively. The actual and predicted scores from these models are shown in figure 9.

SYNTHESIS OF RESULTS

The results of this study indicated that red spruce in the southern Appalachian Mountains have exhibited, to varying degrees, some irregular behavior in their ring widths since the mid-1960's. At elevations above 6,000 feet, statistical evidence suggest a steplike decline in radial increment since about 1966. This decline has not been correlated with any specific climatic deviation in this study. However, the way in which the magnitude of the decline increased with elevation suggested that the cause of the decline was somewhat related to elevation. A more thorough search for natural and anthropogenic causes of this putative decline is warranted. In addition, new and improved collections of ring width data are highly desirable to refine the statistical analyses and validate or refute the intervention results presented here.

The decline of the southern red spruce at high elevations could lead to broad scale mortality, as found in northern Appalachian stands. However, the dendroclimatic modeling has revealed an apparent singular difference between the northern red spruce and southern red spruce conditions in the Appalachian Mountains since the 1960's. In the northern red spruce, the dendroclimatic signal completely disappeared after the trees entered the post-1960 period of declining ring widths (Cook 1987, McLaughlin and

others 1987, Cook and others 1987). However, based on the temperature modeling demonstrated in this study (fig. 6), the dendroclimatic signal appeared to continue through the post-1965 decline period. Thus the reported decline does not seem to represent a major loss of tree vitality as was indicated for the northern red spruce. At this stage of inquiry, the Appalachian Mountain northern and southern red spruce situations appear to be different.

The dendroclimatic analyses revealed that previous summer temperatures correlated significantly with red spruce ring width the following year. The lag-1 negative temperature correlations were remarkably consistent with more rigorously developed dendroclimatic models for numerous stands of red spruce in the northern Appalachians (McLaughlin and others, [in press], Cook and others [in press]). It is increasingly clear that the role of previous summer temperature as a determinant of red spruce growth and vigor is genetically based. More importantly, warm summer temperatures appear to be strongly correlated with past and present declines of red spruce in the northern Appalachians (Cook and others 1987). Should the apparent increase in sensitivity to prior-summer temperatures be correct for the below-5,400-foot spruce, low-elevation spruce in the southern Appalachians are likely to decline if warmer than average summer temperatures persist. A warmer world caused by CO_2 and other greenhouse gases would not positively affect the future of red spruce in North America.

The apparent increase in red spruce sensitivity at all elevations to drought since 1966 and with sensitivity to summer temperatures since 1977, suggests that the southern red spruce

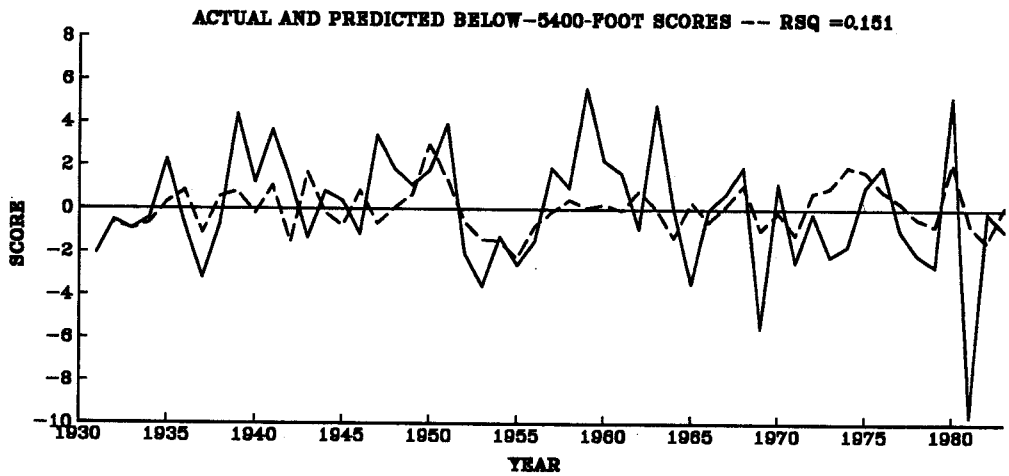
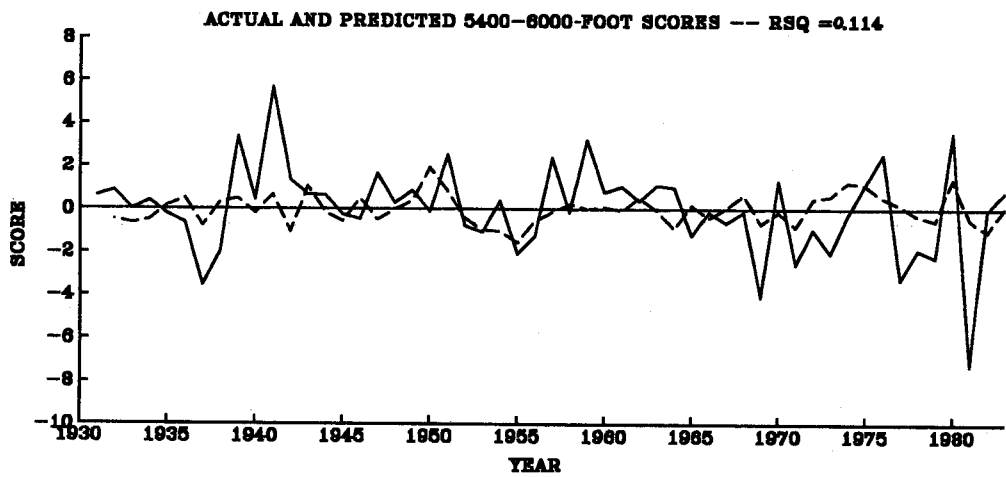
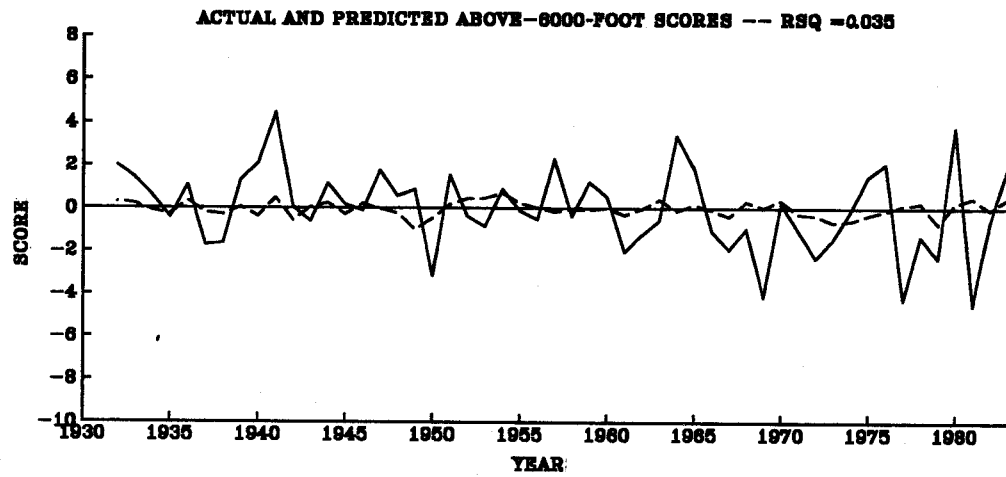


Figure 8.--Actual (solid) and predicted (dash) prewhitened tree ring scores. The summer PDSI series (fig. 7) was used as the predictor of tree rings. The R^2 of each model is indicated by the RSQ value.

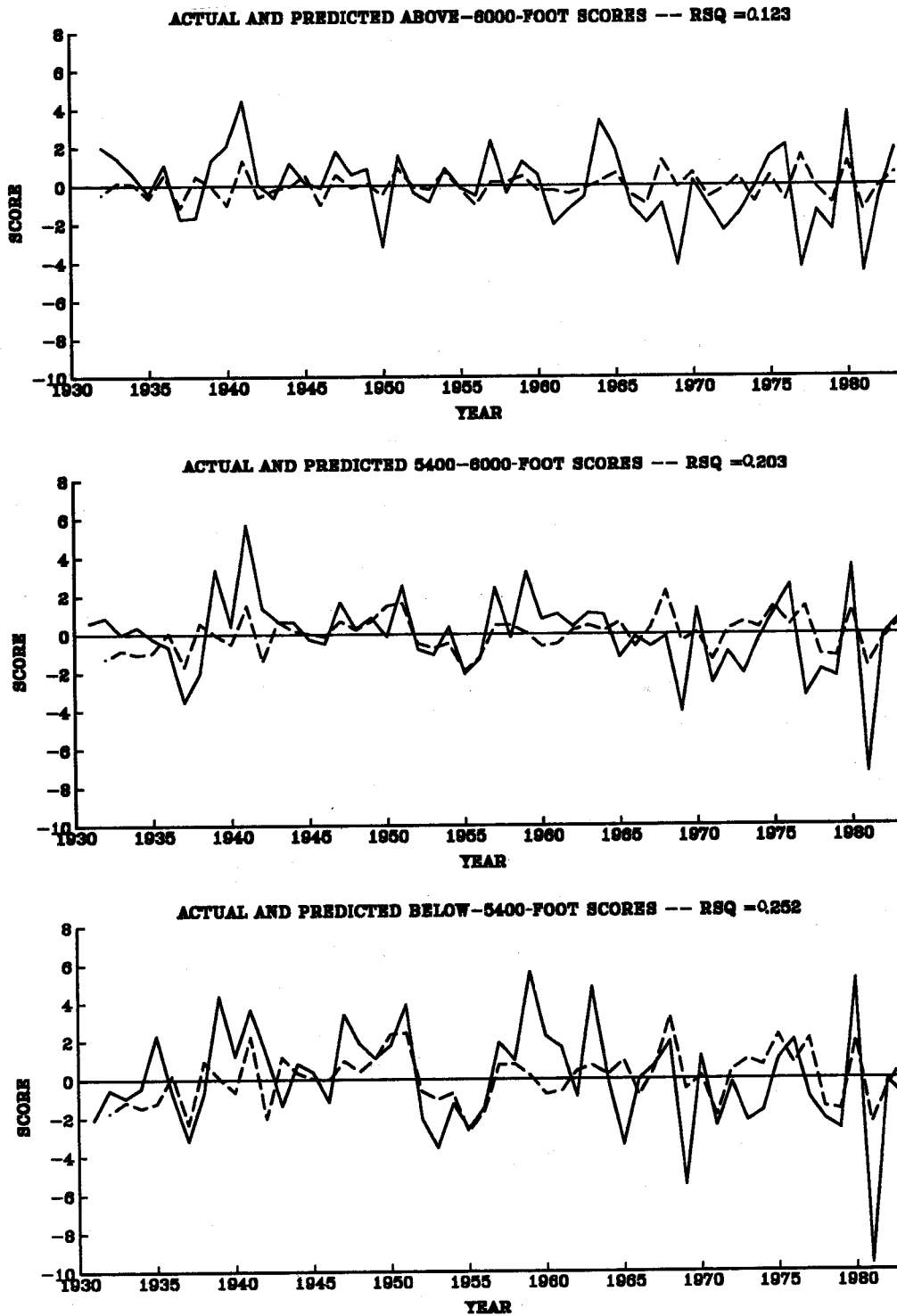


Figure 9.--Actual (solid) and predicted (dash) prewhitened tree ring scores. The predictors in the multiple regression analysis were summer temperature and summer drought. The R^2 of each model is indicated by the RSQ value.

are in a prolonged period of climatic stress. A similar pattern of increased climatic stress from about 1938-60 preceded the current broad scale decline of red spruce in the northern Appalachians (Cook and others 1987). Presently it is impossible to say that this circumstantial agreement in symptomology is part of the epidemiology of red spruce decline. However, it is cause for concern and warrants further study.

LITERATURE CITED

- Adams, H.S.; Stevenson, S.L.; Blasing, T.J.; Duvick, D.N. 1985. Growth-trend declines of spruce and fir in the mid-Appalachian Subalpine forest. *Environment and Experimental Botany*. 25(3): 315-325.
- Box, G.E.P.; Jenkins, G. 1970. Time series analysis: forecasting and control. San Francisco: Holden-Day. 553 p.
- Box, G.E.P.; Tiao, G.C. 1975. Intervention analysis with application to economic and environmental problems. *Journal of American Statistics Association*. 70(349): 70.
- Conkey, L.E. 1979. Dendroclimatology in the Northeastern United States. Tucson, AZ: University of Arizona. 78 p. M.S. thesis.
- Cooley, W.W.; Lohnes, P.R. 1971. Multivariate data analysis. New York: Wiley & Sons. 364 p.
- Cook, E.R. 1985. A time series analysis approach to tree-ring standardization. Tucson, AZ: University of Arizona. 171 p. Ph.D. dissertation.
- Cook, E.R. 1987. The use and limitations of dendrochronology in studying the effects of air pollution on forests. In: Proceedings of the NATO advanced research workshop: Effects of acid deposition on forest, wetlands, and agricultural ecosystem; 1985, May 12-17. Toronto, Canada. Springer-Verlag. 277-290.
- Cook, E.R.; Johnson, A.H.; Blasing, T.J. 1987. Forest decline: modeling the effect of climate. *Tree Physiology*. 3: 27-40.
- Eagar, C. 1984. Review of the biology and ecology of the balsam woolly aphid in the southern Appalachian spruce-fir forest. In: White, P.S., ed. The southern Appalachian spruce-fir ecosystem: Its biology and threats. Resource/Research Management Report. SER-71. U.S. Department of Interior. National Park Service - Southeast Region.
- Fritts, H.C. 1976. Tree rings and climate. New York: Academic Press. 567 p.
- Holmes, R.L. 1983. Computer assisted quality control in tree-ring dating and measurement. *Tree-Ring Bulletin*. 43: 69-78.
- Johnson, A.H.; Siccama, T.G. 1983. Acid deposition and forest decline. *Environmental Science and Technology*. 17(7): 294A-305A.
- McLaughlin, S.B. 1985. Effects of air pollution on forests: A critical review. *Journal of the Air Pollution Control Association*. 35(75): 511.
- McLaughlin, S.B.; Downing, D.J.; Blasing, T.J.; Cook, E.R.; Adams, H.S. 1987. An analysis of climate and competition as contributors to the decline of red spruce in the high elevation Appalachian forests of Eastern North America. *Oecologia*. 72: 487-501.
- Palmer, W.C. 1965. Meteorological drought. Weather Bureau Research Paper Number 45. U.S. Department of Commerce, Washington, DC. 58 p.
- White, P.S. 1984. The southern Appalachian spruce-fir ecosystem, and introduction. In White, P.S., ed., The southern Appalachian spruce-fir ecosystem: Its biology and threats. Resource/Research Management Report SER-71. U.S. Department of Interior, National Park Service - Southeast Region.

Utilizing Time Series Models and Spatial Analysis of Forecast Residuals for Tree Ring Analysis of Red Spruce

J. Keith Ord and Janice A. Derr

SUMMARY

The information from a field study on permanent plots established by the Tennessee Valley Authority in the Great Smoky Mountains was used to detect and evaluate recent changes in annual ring width of red spruce (*Picea rubens* Sarg.). Time series models were fit to mean annual ring widths of a maximum of 5 mature red spruce trees for each of 44 plots for the years 1900-84. The mean level of residuals from forecasts for the last 20 years of the series were generally negative, indicating a reduced ring width relative to predicted ring width. These forecast residuals showed substantial spatial dependence that could not be explained by geographical factors alone. When both geographical and biotic factors, primarily measures of stand quality, were taken into account, the residual variation in ring widths showed a weaker pattern of local spatial dependence.

INTRODUCTION

The National Park Service (NPS) and the Tennessee Valley Authority (TVA) conducted studies on experimental plots in the Great Smoky Mountains, producing a substantial data base of information that can be used to examine annual ring widths of red spruce (*Picea rubens* Sarg.). In this report we discuss one approach to analyzing ring widths. The objective of our study was to detect recent changes during a designated time series (1900-84) that may be attributable to environmental changes, such as the occurrence of acid deposition. Variations in ring widths relative to historical patterns are assessed. Also described is how to determine whether such patterns exist because of plot characteristics or additional spatial effects.

The main steps of the study may be summarized as follows:

1. Construct an average ring width time series for each of the study plots established by the TVA. Plots established by the NPS were not included.
2. Develop measures of recent increases or decreases in ring width for each plot relative to forecast values.
3. Relate the increases or decreases in ring width to geographical and biotic factors.
4. Determine whether there is any spatial pattern to the values of excess or deficiency and whether geographical and biotic factors are responsible for the pattern.

METHODOLOGY AND RESULTS

Step 1.--Construct an average ring width time series for each of the study plots established by the TVA.

The following are decisions made during the exploratory stage of the analysis:

Choice of Plots.--The analysis reported in this project concerns 48 experimental plots established by the TVA in the Great Smoky Mountains in North Carolina. The decision not to include the experimental plots established by the NPS in the same general region was motivated by time and resource constraints.

Choice of Measurement Scale.--Graphs of the time series for each of two cores taken from five trees usually produced very similar patterns. Since the overall plot was the focus for this study, the two core series were averaged for each tree. The selection of a designated time period as a series for the entire plot was more difficult, since individual trees may show considerable variations from year to year. The overall mean was chosen as the measure of average ring width for the plot. Further consideration of this issue is presented in the Discussion section.

Selection of Trees and Time Frame for Analysis.--Graphs for the time series of ring widths for each of the 5 trees per plot were then constructed for all 48 plots. Examples of four of these graphs are shown in figures 1 through 4. From an examination of the 48 graphs, the following decisions were made:

1. Only red spruce would be used in the data analysis to remove some heterogeneity from the time series of ring widths averaged across trees in a plot. Sample size was not seriously reduced because 214 of 234 trees in the study were red spruce, and only 4 plots had no red spruce.
2. Only red spruce trees with a pith date earlier than 1940 would be included in the study. Therefore 25 red spruce trees were eliminated, and some heterogeneity caused by an apparent initial rapid increase in ring width in the early years of growth was alleviated.
3. Ring widths from 1900 onward were analyzed. The heterogeneity caused by the staggered entrance of trees into the plot averages and by the apparent initial rapid increase in ring width was minimized.

J. Keith Ord is a professor in the Departments of Management Science and Statistics. Janice A. Derr is managing director of the Statistical Consulting Center, Pennsylvania State University, University Park, Pennsylvania.

TVA PLOTS

ARITHMETIC MEANS OF TWO SIDES EACH TREE
PLOT=6

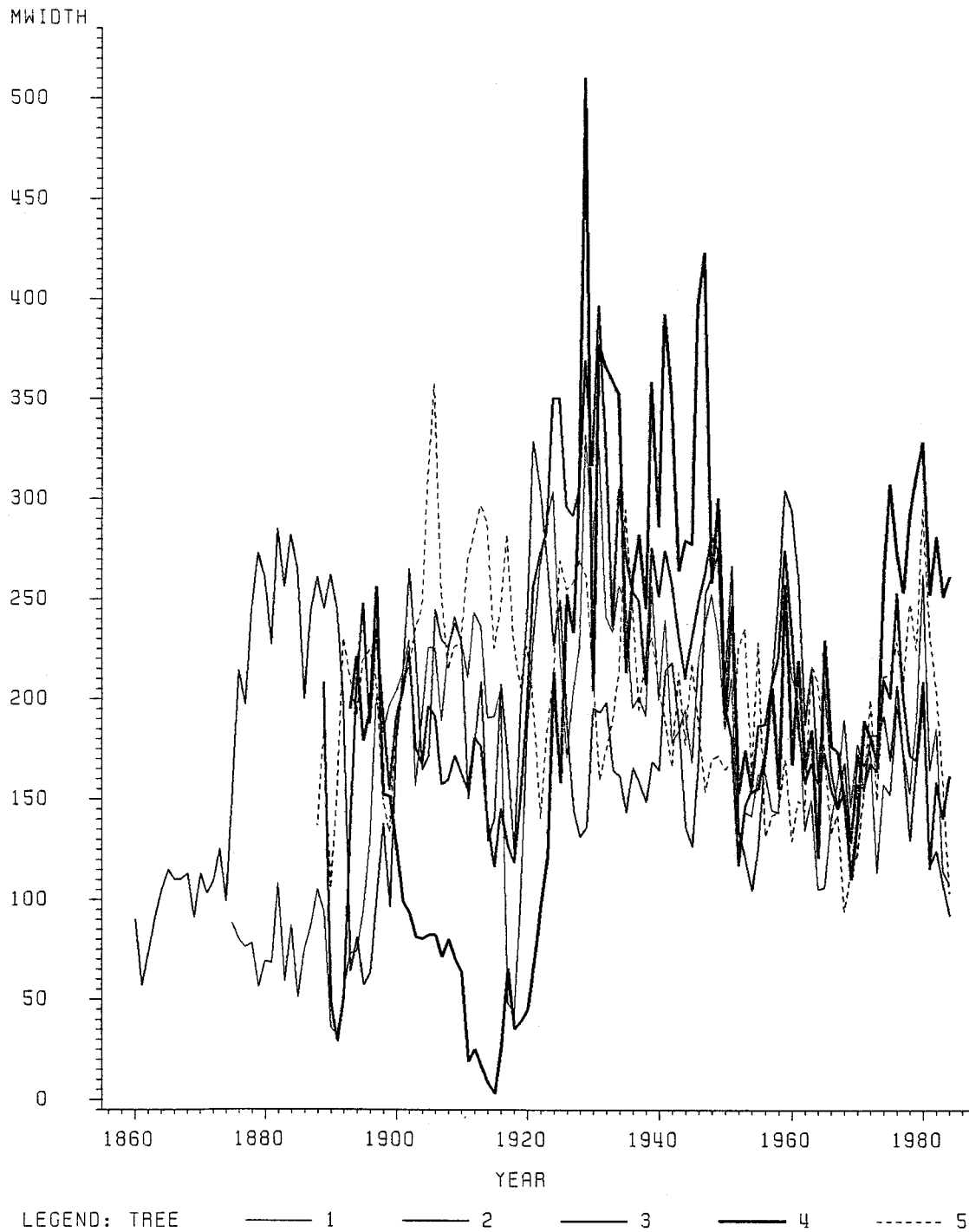


Figure 1.--Graph of ring widths of red spruce (*Picea rubens* Sarg.) on plot 6 of 48 selected experimental plots established by the Tennessee Valley Authority in the Great Smoky Mountains.

TVA PLOTS

ARITHMETIC MEANS OF TWO SIDES EACH TREE
PLOT=18

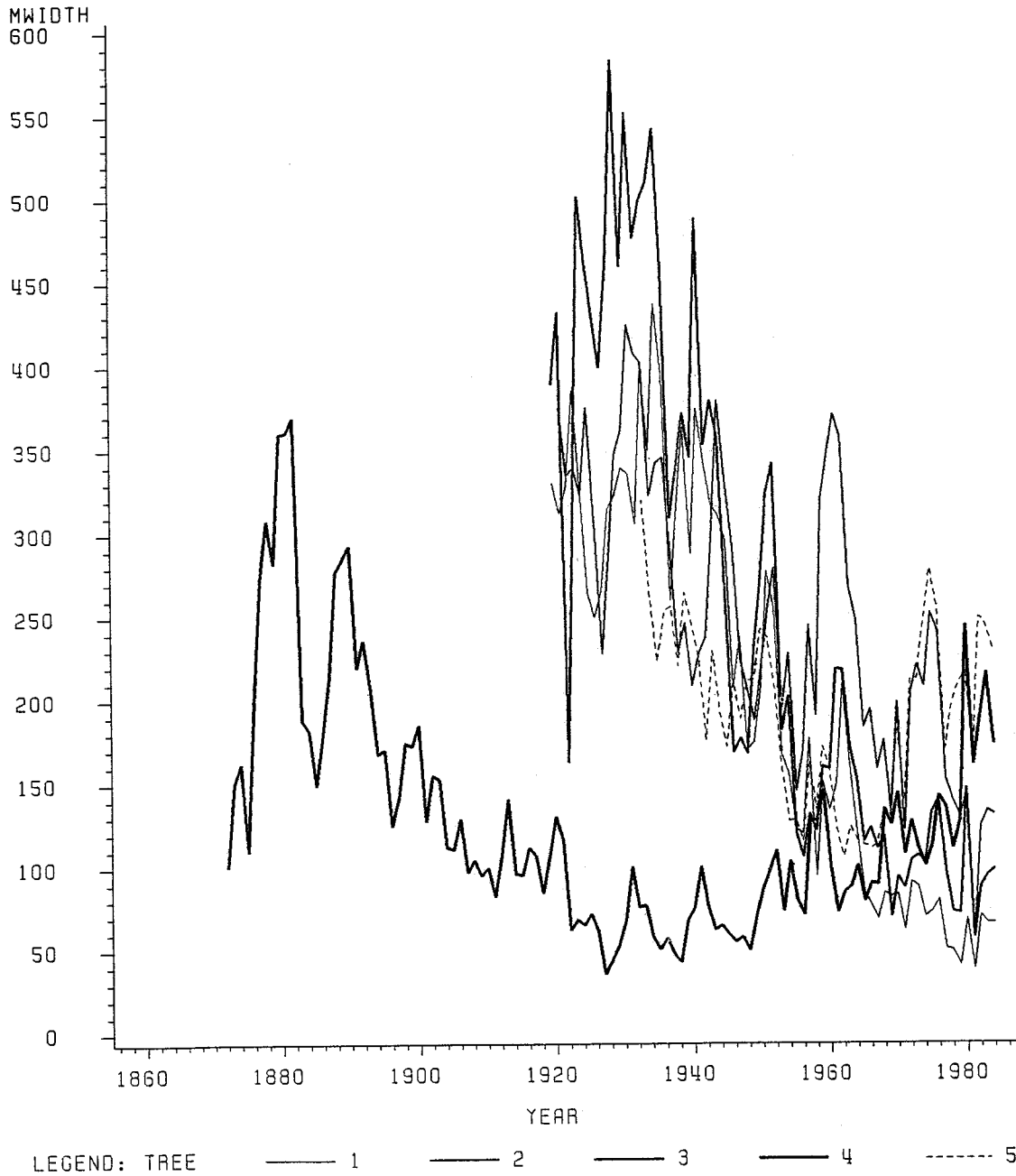


Figure 2.--Graph of ring widths of red spruce (*Picea rubens* Sarg.) on plot 18 of 48 selected experimental plots established by the Tennessee Valley Authority in the Great Smoky Mountains.

TVA PLOTS

ARITHMETIC MEANS OF TWO SIDES EACH TREE
PLOT=23

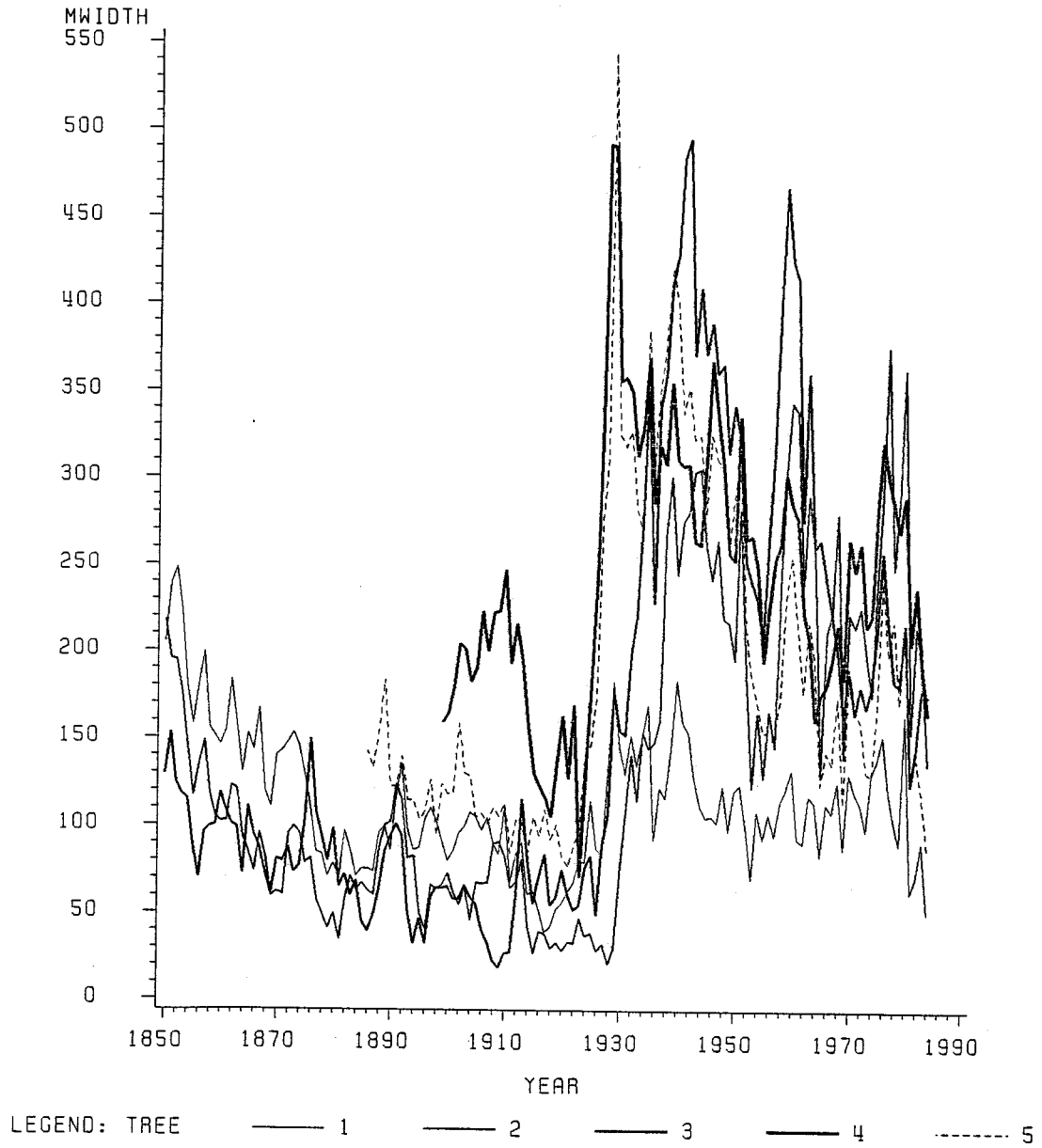


Figure 3.--Graph of ring widths of red spruce (*Picea rubens* Sarg.) on plot 23 of 48 selected experimental plots established by the Tennessee Valley Authority in the Great Smoky Mountains.

TVA PLOTS

ARITHMETIC MEANS OF TWO SIDES EACH TREE
PLOT=31

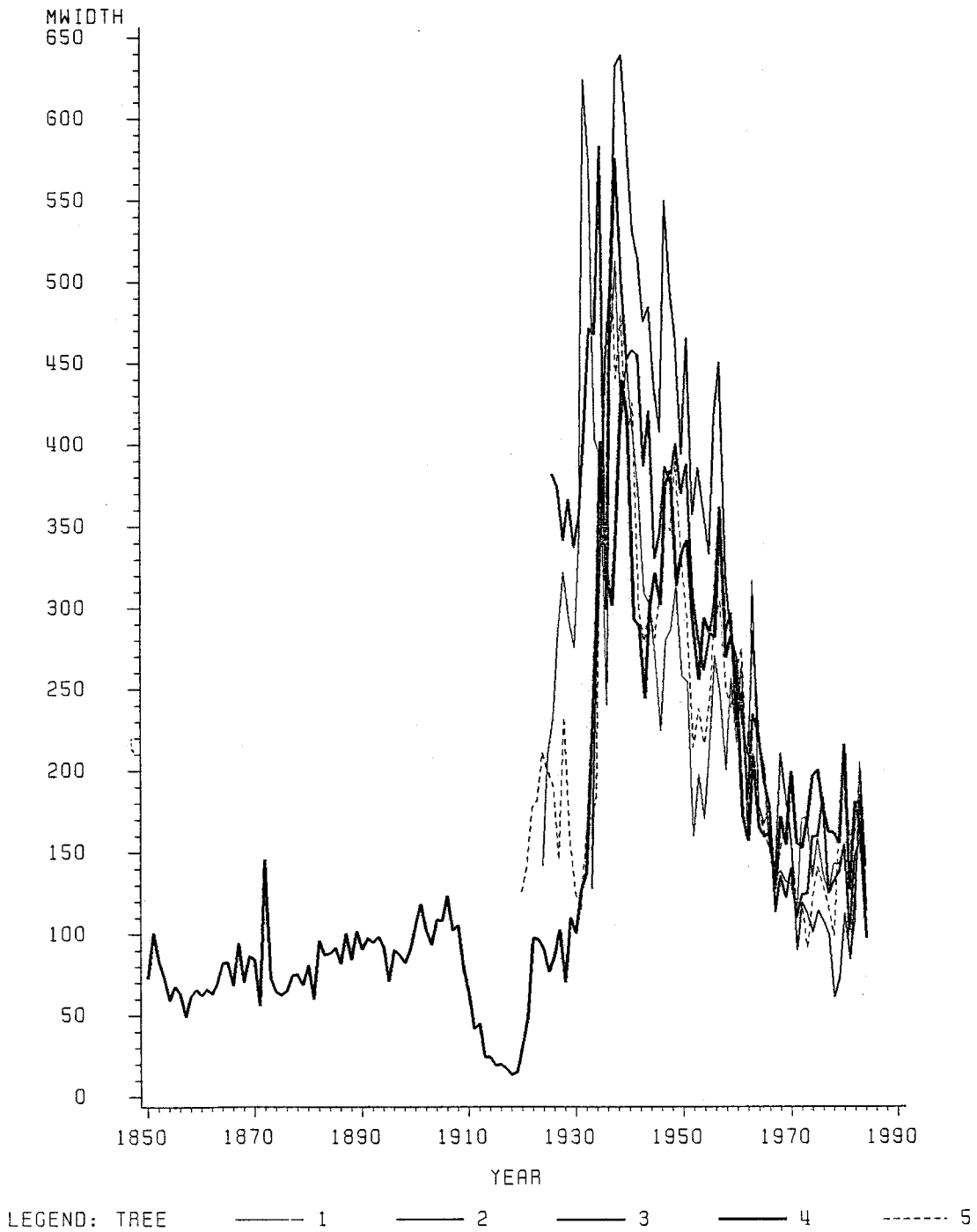


Figure 4.--Graph of ring width of red spruce (*Picea rubens* Sarg.) on plot 31 of 48 selected experimental plots established by the Tennessee Valley Authority in the Great Smoky Mountains.

Choice of Explanatory Variables.--The plot characteristics that were used in the study included both geographical and biotic factors as measured by survey teams. Average annual temperature and total annual precipitation for the three climatic regions in the study (North Carolina northern mountains, North Carolina southern mountains, and Virginia southern mountains) appeared to be fairly similar in the occurrence of peaks and dips. Therefore, because detailed models of precipitation are being developed by others in the project, climate variables were not included at this stage.

Upon completion of the exploratory data analysis, 1 time series of ring widths was constructed for each of the 44 remaining plots

(48 minus the 4 with no red spruce) from the TVA study. The time series began with the year 1900 and ended with 1984. The series included only those red spruce trees with pith dates earlier than 1940. Each time series entry was an average of the width of two cores from each tree, taken from a maximum of five red spruce trees. Table 1 summarizes characteristics of the data for each plot and refers to geographical factors, and table 2 refers to biotic factors.

Step 2.--Develop measures of recent increases or decreases in ring width for each plot relative to forecast values.

Time Series Analysis.--To determine the recent pattern of tree ring growth on each plot, an

Table 1.--Plot characteristics and geographical variables

Observation	Plot	ELEV	ASPECT	LAT	LONG
1	1	5200	21	36.6653	81.5375
2	2	5640	330	36.6597	81.5472
3	3	5200	210	36.6542	81.5333
4	4	6020	35	36.1055	82.1333
5*	5	6140	213	36.1000	82.1222
6	6	5700	90	35.3278	82.9612
7	7	5740	16	35.3500	82.9612
8	8	4480	205	36.3417	81.6500
9	9	6000	220	35.7375	82.3195
10	10	6060	225	35.7250	82.2917
11	11	5520	220	35.7292	82.2792
12	12	6200	245	35.7445	82.3250
13	13	6000	255	35.8305	82.2555
14	14	6360	137	35.7750	82.2583
15	15	5880	303	35.8167	82.2555
16	16	6280	300	35.7833	82.2583
17	17	4480	340	36.3500	81.6417
18	18	5470	190	36.6375	81.6055
19	19	5490	345	36.6403	81.6055
20	20	5300	55	36.6638	81.5403
21	21	5340	55	35.7208	82.2792
22*	22	5420	142	35.7458	82.2722
23	23	5140	125	35.7417	82.2750
24	24	5100	190	35.7458	82.2667
25	25	5280	305	35.7333	82.3250
26	26	5340	123	35.7250	82.3125
27	27	5300	301	35.7222	82.3083
28	28	4140	23	35.7250	82.2722
29	29	5700	30	36.1042	81.8125
30*	30	6015	345	36.0917	82.1500
31	31	4540	235	36.3388	81.6542
32	32	5840	0	35.4638	83.1375
33	33	5040	90	36.1112	81.7958
34	34	5110	290	36.1083	81.8250
35*	35	6000	305	35.8250	82.2555
36	36	5780	120	35.8458	82.2417
37	37	4880	193	35.8388	82.2388
38	46	4400	50	36.3458	81.6500
39	54	5120	35	35.4750	83.1167
40	55	5800	268	35.4750	83.0958
41	109	5650	220	35.7888	82.2667
42	113	6240	265	35.7292	82.2917
43	125	5000	350	36.1083	82.1333
44	132	4480	215	36.1292	82.2917
45	153	5060	305	35.2945	82.9375
46	158	4620	20	35.3625	82.8833
47	159	5240	60	35.3388	82.9612
48	207	4880	340	35.3583	82.8542

*Plots eliminated from study because no red spruce was present.

Table 2.--Plot characteristics and biotic variables

Observation	SBALIVE	SBADEAD	SBAX	LIVETREE	DEADTREE	TREEX
1	56.7	4.3	0.92951	6672	185	0.97302
2	38.6	5.9	0.86742	10329	247	0.97665
3	39.6	7.3	0.84435	7771	1186	0.86759
4	11.6	11.1	0.51101	642	1482	0.30226
5*	41.5	6.0	0.87368	3064	544	0.84922
6	30.2	3.3	0.90149	4695	704	0.86961
7	31.2	3.7	0.89398	1507	408	0.78695
8	43.1	0.5	0.98853	1742	148	0.92169
9	48.2	3.5	0.93230	9798	111	0.98880
10	37.5	6.3	0.85616	4547	111	0.97617
11	30.1	2.8	0.91489	1532	988	0.60794
12	41.7	26.6	0.61054	10687	185	0.98298
13	14.7	2.6	0.84971	1705	309	0.84657
14	26.6	7.2	0.78698	1915	741	0.72101
15	25.1	12.5	0.66755	4176	1161	0.78246
16	12.0	12.6	0.48780	7141	543	0.92933
17	39.0	2.4	0.94203	2508	222	0.91868
18	55.7	3.3	0.94407	1174	383	0.75401
19	34.2	1.5	0.95798	1507	74	0.95319
20	45.1	4.9	0.90200	2002	99	0.95288
21	45.9	1.3	0.97246	1149	173	0.86914
22*	52.8	2.6	0.95307	8698	124	0.98594
23	37.7	0.0	1.00000	531	0	1.00000
24	60.7	1.1	0.98220	3286	222	0.93672
25	43.5	19.6	0.68938	3632	136	0.96391
26	69.0	0.0	1.00000	7401	0	1.00000
27	52.5	8.8	0.85644	3410	432	0.88756
28	63.2	10.1	0.86221	840	210	0.80000
29	18.5	15.1	0.55060	4707	334	0.93374
30*	45.0	10.0	0.81818	9044	2557	0.77959
31	35.4	2.7	0.92913	1680	297	0.84977
32	10.5	32.4	0.25060	1075	1631	0.39727
33	18.9	2.9	0.86697	1025	86	0.92259
34	36.3	4.9	0.88107	1248	556	0.69180
35*	15.5	0.2	0.98726	1520	25	0.98382
36	38.7	13.7	0.73855	4213	272	0.93935
37	59.6	0.9	0.98512	914	12	0.98704
38	34.1	0.5	0.98555	1124	148	0.88365
39	5.9	0.8	0.88060	37	80	0.31624
40	39.5	2.4	0.94272	1606	219	0.88000
41	28.2	4.9	0.85196	2718	292	0.90299
42	15.3	0.0	1.00000	3497	0	1.00000
43	38.4	4.1	0.90353	8686	1819	0.82684
44	46.0	0.4	0.99138	1594	70	0.95793
45	46.7	0.9	0.98109	1557	173	0.90000
46	21.6	1.9	0.91915	1890	400	0.82533
47	10.5	7.8	0.57377	1408	2088	0.49275
48	28.2	19.1	0.59619	803	738	0.52109

*Plots eliminated from study because no red spruce was present.

autoregressive-integrated-moving average (ARIMA) time series model for each of the plots was first developed. Kendall and others (1983) and Vandaele (1983) provide details of ARIMA models and the underlying assumptions.

Time Series Modeling.--Various years of the series indicated marked trends of tree ring growth. To accommodate trends, the series were differenced where necessary. Other approaches to this problem are covered in the Discussion section. In this data set, it was never necessary to difference more than once. A summary of the fitted models is presented in table 3. From the table, it can be seen that

many of the series were described satisfactorily by an autoregressive scheme of order 2, occasionally with higher order moving average (MA) terms.

The MA terms improved the fit as measured by the diagnostics but did not materially affect the forecasts. The autoregression [AR(2)] coefficients were usually both positive with $\phi_1 + \phi_2$ in the range 0.6 to 0.9, indicating a carry-over from one growing season to the next, as would be expected. When $\phi_1 + \phi_2$ exceeded 0.9, nonstationarity in the series was evident, and differencing was performed. A low-order MA scheme usually gave an adequate description of

Table 3.--Summary of autoregressive-integrated-moving average models for each plot

Plot No.	Difference	Lag Structure ⁺		Comments
		AR	MA	
1	No	2	0	
2	No	2	0	
3	No	2	0	
4	No	2	0	
6	No	2	0	
7	No	2	(??)	
8	Yes	0	(1,4,10)	Short series
9	No	2	0	
10	No	2	0	
11	No	3	0	Short series
12	No	2	0	Short series
13	Yes	0	1	Short series
14	Yes	2	0	Short series
15	Yes	(3)	0	Short series
16	Yes	0	(4)	Short series
17	Yes	0	2	
18	No	2	(8)	
19	No	2	0	
20	Yes	0	2	
21	Yes	1	0	
23	Yes	0	1	
24	Yes	0	3	
25	No	2	0	
26	No	2	0	
27	No	2	0	
28	No	2	0	
29	Yes	0	(2,9)	
31	Yes	0	(1,2,6)	
32	No	2	(6)	
33	Yes	0	(1,2,6)	
34	No	2	0	
36	No	2	0	
37	No	2	(10?)	Structural change in series?
46	No	1	0	
54	No	2	0	
55	No	2	0	
109	Yes	0	2	First seven terms deleted
113	Yes	0	0	
125	Yes	0	2	Short series
132	Yes	0	1	
153	Yes	0	(1,4,5,6)	
158	Yes	0	(2,5)	
159	Yes	0	(1,4)	Short series
207	No	2	(3,7?)	

⁺ k indicates lags 1, 2, ..., k
(k) indicates lag k only
(j,k) indicates lags j,k only
(k?) indicates lag k a possibility
AR = autoregression coefficient
MA = moving average

the differenced series. It is well known that AR schemes with a root of the auxiliary equation near unity can often be well approximated by a low-order MA scheme with a single difference. Therefore the models are not very different in practice despite their distinct theoretical properties.

The only series that caused major problems was that for plot 109, where major increases in the first 7 years were followed by steady declines. After the data for the first 7 years were deleted, a satisfactory model was fitted. It can be assumed that the use of ring width rather than incremental basal area was the cause of these nonstationarity problems.

Measures of Recent Relative Change in Ring Width.--To assess recent relative increases or decreases in ring width, each series over the periods was forecasted:

1. 1965-1984, using 1964 as the forecast origin.
2. 1975-1984, using 1974 as the forecast origin.

The residuals, the difference between observed and predicted values, were then computed for each year in the period. The means and standard deviations of these residuals were computed for each plot (table 4). It should be noted that the models were fitted to the entire series, 1900-84, and forecasts were then generated from the forecast origin. A pure forecasting method would

have involved fitting to 1964 (or 1974) and then forecasting. However, the risk of structural changes in the series was such that the pure forecasts might misrepresent recent trends. Although our approach biases the residuals somewhat towards zero, the method seemed to provide a clearer picture of recent developments.

Because changes in ring width might be considered in either absolute or percentage terms, also considered were the indicators:

$$\text{proportional change} = \frac{\text{average of residuals}}{\text{average ring width}}$$

over the two forecast periods. These values are also listed in table 4 as PCT20 and PCT10.

Assessment of Mean Change.--One should note whether the residual ring widths are below the expected value of zero for the periods considered. The results of one-tailed t-tests on the data in table 4 were as follows:

Variable	Mean	t-value	Adjusted t-value
RES20	-17.47	-3.28	-1.89
PCT20	-0.108	-3.46	-2.34
RES10	4.43	0.93	0.50
PCT10	0.022	0.79	0.47

Table 4.--Summary statistics from time series analysis

Observation	Summary Statistics [±]						
	OVMEAN	RES20	R20SD	PCT20	RES10	R10SD	PCT10
1	189.5	18.3	34.4	0.9657	-14.3	43.3	-0.07546
2	158.5	-34.5	25.3	-0.21767	-4.8	21.5	-0.03028
3	187.3	-48.1	24.8	-0.25681	-1.0	9.9	-0.00534
4	147.1	-50.5	20.6	-0.34330	-15.6	22.1	-0.10605
5*							
6	198.6	-3.7	30.4	-0.01863	5.2	33.7	0.02613
7	147.9	-37.1	23.1	-0.25085	-35.1	26.9	-0.23732
8	375.3	44.8	63.5	0.11937	93.7	63.9	0.24967
9	140.0	-42.1	30.8	-0.30071	-22.1	16.0	-0.15786
10	138.7	-31.5	23.9	-0.22711	-28.8	29.9	-0.20764
11	321.9	-57.7	52.1	-0.17925	-30.2	43.0	-0.09382
12	163.6	-16.3	22.4	-0.09963	-5.4	26.9	-0.03301
13	152.0	17.4	34.7	0.11447	62.6	35.6	0.41184
14	259.1	25.8	31.4	0.09958	41.1	31.3	0.15863
15	132.4	-18.5	18.6	-0.13973	26.6	21.8	0.20091
16	134.9	84.4	75.5	0.62565	85.6	48.1	0.63454
17	189.9	3.4	30.6	0.01790	15.4	13.7	0.08110
18	182.3	-39.0	22.5	-0.21393	-17.6	29.1	-0.09654
19	81.6	-32.7	8.3	-0.40074	6.6	7.6	0.08088
20	232.5	-58.1	37.1	-0.24989	-9.2	37.3	-0.03957
21	239.0	-113.1	48.9	-0.47322	-39.7	43.5	-0.16611
22*							
23	182.4	-25.1	36.9	-0.13761	24.3	48.5	0.13322
24	192.5	-45.8	30.4	-0.23792	36.6	32.0	0.19013
25	126.5	-26.4	21.0	-0.20870	-16.1	24.8	-0.12727
26	172.6	-20.7	31.2	-0.11993	-23.5	40.5	-0.13615
27	131.2	-31.2	28.2	-0.23780	-24.0	32.3	-0.18293
28	125.5	-19.3	16.2	-0.15378	-10.3	19.5	-0.08270
29	82.7	8.4	22.2	0.10157	27.7	23.2	0.33495
30*							
31	203.9	-55.5	20.4	-0.27219	-5.8	22.1	-0.02845
32	165.2	-15.9	24.2	-0.09625	31.6	26.0	0.19128
33	184.3	-3.4	37.7	-0.01845	26.6	48.5	0.14433
34	173.8	21.3	30.8	0.12255	26.8	38.9	0.15420
35*							

Table 4.--Summary statistics from time series analysis--Continued

Observation	Summary Statistics [±]						
	OVMEAN	RES20	R2OSD	PCT20	RES10	R1OSD	PCT10
36	103.1	-19.4	16.5	-0.18817	-10.1	23.5	-0.0979
37	112.1	-12.4	15.8	-0.11062	-5.8	21.7	-0.05174
38	189.5	-14.5	41.8	-0.07652	-24.5	51.2	-0.12929
39	136.5	-27.4	20.9	-0.20073	-21.9	25.1	-0.16044
40	236.2	-12.5	31.0	-0.05292	-20.8	33.1	-0.08806
41	288.5	41.0	31.6	0.14211	33.4	21.3	0.11577
42	187.7	-22.1	32.3	-0.11774	-3.5	35.6	-0.01865
43	185.9	24.6	36.8	0.13233	50.7	39.6	0.27273
44	189.2	-4.9	33.4	-0.02590	23.6	39.9	0.12474
45	139.3	-88.8	34.8	-0.63747	-35.7	30.4	-0.25628
46	176.9	1.3	23.5	0.00735	-7.8	32.2	-0.04409
47	273.3	-45.2	37.5	-0.16539	-7.2	37.6	-0.02634
48	127.9	14.2	13.7	0.11102	17.5	14.8	0.13683

+ OVMEAN = overall mean of series.
 RES20 = residuals from forecasts for last 20 years.
 R2OSD = standard deviation of RES20 values.
 PCT20 = RES20/OVMEAN.
 RES10, R1OSD, PCT10 are defined similarly.

* Plots eliminated from study because no red spruce was present.

The adjusted t-values were computed following the approach described by Cliff and Ord (1981) modified to the one-sample case. The adjustment takes account of the positive spatial dependence among the data and may be written as:

$$t_{adj} = t(1 - I),$$

where I is defined in equation (1) under Step 4.

Evidently the 20-year residual ring widths have a mean that is significantly less than zero, while the null hypothesis of a zero mean is accepted for the 10-year values. Therefore a drop is indicated in average ring width in the 1960's that has subsequently stabilized at that lower level.

Step 3.--Relate recent increases and decreases in ring width to geographical and biotic factors.

In this step, the changes in ring width were related to the various plot characteristics to determine if there were any explanation for the changes.

Regression Analysis.--Each of the four residual ring width measures was modeled using stepwise regression with the following variables:

geographical: latitude (LAT), longitude (LONG), (latitude)² = LAT2, (longitude)² = LONG2, latitude * longitude = LATLONG, elevation (ELEV), and aspect (coded as sine and cosine, SASP and CASP).

biotic: number of live trees (LIVETREE), number of dead trees (DEADTREE), stand basal area of live trees (SBALIVE), stand basal area of dead trees (SBADEAD), and two derived indices:

$$TREEX = \frac{LIVETREE}{(LIVETREE + DEADTREE)}$$

$$SBAX = \frac{SBALIVE}{(SBALIVE + SBADEAD)}$$

where TREEX is proportion of live trees, and SBAX is the proportion of live basal area. The values of these variables are listed in table 1.

The quadratic factors of latitude and longitude were included to allow a low-order trend surface analysis (Cliff and others 1975). However, initial runs using only the geographical variables showed virtually no correlation between any of these variables and the residual ring width measures; therefore they have not been reported separately. A total of eight analyses are reported in tables 5 through 8. For each of the residual ring width measures, the analysis was performed using both unweighted and weighted least squares (LS). The weights used were the standard deviations given in table 4. In all cases, the significance level for a variable to leave or stay was set at 0.25. The residuals from the regression analyses are given in tables 9 and 10.

Interpretation of Regression Results.--Comparisons within and across tables 5 through 8 show the following:

1. The value of R² is in all cases somewhat higher for weighted LS than for unweighted. A high standard deviation in the time series residuals shows an erratic ring width pattern. Therefore the weighting is useful because greater emphasis is given to the plots with more stable ring width development. Otherwise the same variables were selected by the stepwise procedures for both estimation procedures, and the two sets of estimates were broadly consistent for each of the four dependent variables.
2. The proportional change indicators yield models with a higher degree of explanatory power than those based on absolute changes. Since average ring widths vary considerably between sites, use of the proportional change indicator seems preferable.

Table 5.--Regression analysis for the dependent variable 20-year mean residual ring width (RES20)

Unweighted least squares					
Source	df	Sum of squares	Mean square	F value	Prob>F
Model	4	10813.450	2703.362	2.466	0.0608
Error	39	42758.529	1096.373		
C total	43	53571.979			
Root MSE		33.111517	R-square	0.2018	
Dep mean		-17.465909	Adj R-sq	0.1200	
C.V.		-189.578			

Variable	df	Parameter estimate	Standard error	T for H0: Parameter=0	Prob > T
Intercept	1	70.597735	70.426505	1.002	0.3223
ELEV	1	-0.013709	0.010648	-1.287	0.2055
SBAX	1	-69.517093	40.250901	-1.727	0.0921
TREEX	1	91.734416	36.388501	2.521	0.0159
SBALIVE	1	-0.916871	0.442469	-2.072	0.0449

Weighted least squares					
Source	df	Sum of squares	Mean square	F value	Prob>F
Model	4	800896	200224	4.859	0.0028
Error	39	1607051	41206.433		
C total	43	2407947			
Root MSE		202.994	R-square	0.3326	
Dep mean		-13.665677	Adj R-SQ	0.2642	
C.V.		-1485.43			

Variable	df	Parameter estimate	Standard error	T for H0: Parameter=0	Prob > T
Intercept	1	99.187126	81.765087	1.213	0.2324
ELEV	1	-0.017920	0.011910	-1.505	0.1405
SBAX	1	-105.865	45.857356	-2.309	0.0264
TREEX	1	136.208	39.969084	3.408	0.0015
SBALIVE	1	-1.201380	0.502896	-2.389	0.0218

3. The regression analyses for geographical variables provided only very little explanatory power. When the biotic variables were also included, elevation became important, and the residual ring width became more negative as elevation increased. This suggests that the higher elevation plots did worse than average over the 10- and 20-year periods considered. The only other geographical variables that appeared in any models were LONG2 and SIN (aspect). The coefficient on LONG2 suggests a downward trend in the 10-year change variables from east to west. Since the plot locations extended approximately northeast to southwest, this may reflect the influence of climatic factors. The coefficient for SIN (aspect) indicates that the proportional change variable for the 10-year period is higher in plots with a southerly aspect. Again, this may reflect climatic effects.

4. The most important variable in almost all cases was the tree index, TREEX, which is probably an indicator of stand health, and strong, positive correlation is to be expected. The other major biotic variable was SBALIVE, but this appears with a negative sign in the regression. SBADEAD and the stand basal area index (SBA) also appear on occasion, again with negative signs in all cases. The interpretation of these effects is unclear, but these variables may relate to other biotic factors such as the age of the stand and the degree of competition.

Overall, the weighted regressions on the proportional change indicators appear to give a reasonable explanation of the variations in residual ring width.

Step 4.--Determine whether there is any spatial pattern to the values of excess or deficiency and

Table 6.--Regression analysis for 10-year mean residual ring width (RES10)

Unweighted least squares					
Source	df	Sum of squares	Mean square	F value	Prob>F
Model	2	6777.608	3388.804	3.939	0.0272
Error	41	35269.460	860.231		
C total	43	42047.067			
Root MSE		29.329690	R-square	0.1612	
Dep mean		4.427273	Adj R-sq	0.1203	
C.V.		662.4776			

Variable	df	Parameter estimate	Standard error	T for H0: Parameter=0	Prob > T
Intercept	1	814.995	404.974	2.012	0.0508
SBALIVE	1	-0.763081	0.303229	-2.517	0.0159
LONG2	1	-0.115851	0.059378	-1.951	0.0579

Weighted least squares					
Source	df	Sum of squares	Mean square	F value	Prob>F
Model	2	301627	150813	4.325	0.0198
Error	41	1429655	34869.627		
C total	43	1731281			
Root MSE		186.734	R-square	0.1742	
Dep mean		7.603876	Adj R-sq	0.1339	
C.V.		2455.775			

Variable	df	Parameter estimate	Standard error	T for H0: parameter=0	Prob > T
Intercept	1	1097.709	474.049	2.316	0.0257
SBALIVE	1	-0.852323	0.342500	-2.489	0.0170
LONG2	1	-0.156754	0.069541	-2.254	0.0296

whether this can be accounted for by geographical and biotic factors.

In this section, the spatial methods used are first described. Then the spatial analysis for the residual ring widths and for their residuals from the regression equations developed in step 3 is presented. The objective of the spatial analysis is to discover if there is any spatial pattern in the recent changes in ring width, both among the initial values and the residuals, from the regression equations.

Spatial Methods.--The first step in any spatial analysis is to determine whether or not there is any evidence of spatial pattern among the data, given the plot locations. If the n plots have observed values x_i ($i = 1, \dots, n$), we set $z_i = x_i - \bar{x}$ and use the spatial autocorrelation statistic:

$$I = \frac{n \sum_{i,j} w_{ij} z_i z_j}{S_0 \sum_i z_i^2} \quad (1)$$

where $S_0 = \sum_i \sum_j w_{ij}$ and the $\{w_{ij}\}$ are a set of non-negative weights to be specified, with $w_{ii} = 0$.

Under the null hypothesis (H_0) of no spatial autocorrelation (or independence), it may be shown that:

$$E(I) = -1/(n-1).$$

Cliff and Ord (1981) show the distribution of I under H_0 to be approximately normal, provided that n is not too small. For the configurations of weights used and the number of plots available ($n = 44$), the normal approximation is satisfactory. It should be noted that I is not defined quite like a regular correlation coefficient; in particular, the values tend to be closer to the origin than one would expect. For this reason, the magnitudes of the standard deviates

$$[I - E(I)]/\sqrt{V(I)}$$

are often more useful than the values of I themselves. From Cliff and Ord (1981), the variance of I under H_0 is:

$$V(I) = E(I^2) - [E(I)]^2,$$

Table 7.--Regression analysis for 20-year mean residual ring width divided by overall mean ring width (PCT20)

Unweighted least squares					
Source	df	Sum of squares	Mean square	f value	Prob>F
Model	5	0.466992	0.093398	2.592	0.0411
Error	38	1.369366	0.036036		
C total	43	1.836359			
Root MSE		0.189831	R-square	0.2543	
Dep mean		-0.107706	Adj R-sq	0.1562	
C. V.		-176.249			

Variable	df	Parameter estimate	Standard error	T for H0: parameter=0	Prob > T
Intercept	1	0.995842	0.583306	1.707	0.0959
ELEV	1	-.0000856071	.00006109282	-1.401	0.1692
SBAX	1	-1.074991	0.566563	-1.897	0.0654
SBADEAD	1	-0.013608	0.011104	-1.225	0.2279
TREEX	1	0.579832	0.215236	2.694	0.0105
SBALIVE	1	-0.00389848	0.002933337	-1.329	0.1918

Weighted least squares					
Source	df	Sum of squares	Mean square	F value	Prob>F
Model	5	35.672534	7.134507	6.069	0.0003
Error	38	44.671739	1.175572		
C total	43	80.344273			
Root MSE		1.084238	R-square	0.4440	
Dep mean		-0.073059	Adj R-sq	0.3708	
C. V.		-1484.05			

Variable	df	Parameter estimate	Standard error	T for H0: Parameter=0	Prob > T
Intercept	1	1.311741	0.583284	2.249	0.0304
ELEV	1	-.0000828751	.00006361611	-1.303	0.2005
SBAX	1	-1.582828	0.531610	-2.977	0.0050
SBADEAD	1	-0.022603	0.011481	-1.969	0.0563
TREEX	1	0.800385	0.214337	3.734	0.0006
SBALIVE	1	-0.00426758	0.003139655	-1.359	0.1821

where

$$E(I^2) = \frac{\{n[(n^2 - 3n + 3)S_1 - nS_2 + 3S_0^2] + b_2[(n^2 - n)S_1 - 2nS_2 + 6S_0^2]\}}{(n-1)(n-2)(n-3)S_0^2} \quad (2)$$

where n = number of plots,
 $S_0 = \sum_i \sum_j w_{ij}$,
 $S_1 = \sum_i \sum_j (w_{ij}^2 + w_{ij} w_{ji})$,
 $S_2 = \sum_i (w_{i.} + w_{.i})^2$, and
 $w_{i.} = \sum_j w_{ij}$ and $w_{.i} = \sum_j w_{ji}$.

Choice of Weights.--Given the irregular array of plot locations, the choice of weights for use in (1) is somewhat arbitrary. However, when the variables X are normally distributed, it is known (Cliff and Ord 1981) that I is the locally most powerful test for alternatives of the form:

$$H_1: \text{Var}(X) = \sigma^2 [I - \beta W]^{-1} \quad (3)$$

where β and σ^2 are parameters and W is symmetric. The null hypothesis then becomes $H_0: \beta = 0$, or $\text{Var}(X) = \sigma^2 I$. Since we are interested in detecting local spatial similarities, this suggests that $w_{ij} > 0$ when plots i and j are close, but $w_{ij} \approx 0$ when they are distant.

Table 8.--Regression analysis for 10-year mean residual ring width divided by overall mean ring width (PCT10)

Unweighted least squares					
Source	df	Sum of squares	Mean square	F value	Prob>F
Model	7	0.678485	0.096926	4.467	0.0012
Error	36	0.781208	0.021700		
C total	43	1.459693			
Root MSE		0.147310	R-square	0.4648	
Dep mean		0.021891	Adj R-sq	0.3607	
C. V.		672.9362			

Variable	df	Parameter estimate	Standard error	T for H0: Parameter=0	Prob > T
Intercept	1	3.999241	2.193178	1.823	0.0765
ELEV	1	-.0000812191	.00004886896	-1.662	0.1052
SASP	1	-0.053525	0.035049	-1.527	0.1355
LONG2	1	-0.000375621	0.0003257647	-1.153	0.2565
SBALIVE	1	-0.00354181	0.002301411	-1.539	0.1326
SBAX	1	-1.411441	0.455795	-3.097	0.0038
SBADEAD	1	-0.020464	0.009001847	-2.273	0.0291
TREEX	1	0.520329	0.181001	2.875	0.0067

Weighted least squares					
Source	df	Sum of squares	Mean square	F value	Prob>F
Model	7	27.779442	3.968492	5.605	0.0002
Error	36	25.489160	0.708032		
C total	43	53.268603			
Root MSE		0.841447	R-square	0.5215	
Dep mean		0.035922	Adj R-sq	0.4285	
C.V.		2342.437			

Variable	df	Parameter estimate	Standard error	T for H0: Parameter=0	Prob > T
Intercept	1	4.831085	2.305746	2.095	0.0432
ELEV	1	-0000758574	.00005072042	-1.496	0.1435
SASP	1	-0.069365	0.033810	-2.052	0.0475
LONG2	1	-0.000484338	0.0003417928	-1.417	0.1651
SBALIVE	1	-0.00324435	0.002267685	-1.431	0.1611
SBAX	1	-1.564668	0.436777	-3.582	0.0010
SBADEAD	1	-0.024429	0.009060183	-2.696	0.0106
TREEX	1	0.554004	0.181281	3.056	0.0042

Furthermore, given the rapid changes in local topography that are possible in the study area, it is reasonable to set $w_{ij} = 0$ when there are several plots between i and j . Given that (1) is being used primarily as an exploratory device, these guidelines may be incorporated into the set of weights by use of nearest neighbor linkages (Cliff and others 1975). The exact specification of weights is not critical. Thus two sets of weights are considered:

- $w_{ij} = 1$, if plots i and j are nearest neighbors, otherwise $= 0$.

- $w_{ij} = 1$, if plots i and j are first or second nearest neighbors, otherwise $= 0$.

These weights are not symmetric, but this does not cause any problems. In each case, a distance criterion was used to eliminate linkages across very long distances. The sets of neighbors are summarized in (B) of the Appendix. These weights were used in all subsequent analyses. A program listing for a simple FORTRAN program to compute I and the corresponding standard deviate is listed in the Appendix (A). For the first nearest neighbor, $S_0 = 42$, $S_1 = 68$, and $S_2 = 192$. For

Table 9.--Residuals from ordinary least squares regression for RES20, RES10, PCT20, PCT10, respectively

Observation	RRES20	RRES10	PCRES20	PCRES10
1	46.334	-15.807	0.26047	-0.04145
2	-21.678	-19.937	-0.13374	-0.12678
3	-31.993	-15.635	-0.14916	-0.08203
4	-20.136	-40.225	-0.25344	-0.21953
5*				
6	14.431	10.602	0.10100	0.12306
7	-10.443	-28.935	-0.07859	-0.13183
8	59.306	83.942	0.21011	0.17438
9	-12.145	-15.249	-0.11850	-0.11506
10	-14.668	-30.645	-0.11789	-0.24663
11	-17.193	-37.930	0.08391	0.00267
12	-11.397	-3.404	0.04620	0.01085
13	23.945	42.668	0.14752	0.25374
14	55.349	30.302	0.27781	0.23123
15	-10.846	14.604	-0.10033	0.05556
16	59.557	63.661	0.37119	0.14592
17	11.190	2.355	0.07027	-0.03010
18	12.921	-18.585	0.09821	0.04559
19	-17.522	-10.792	-0.29572	0.02309
20	-39.395	-19.506	-0.13238	-0.02975
21	-80.534	-35.373	-0.27386	-0.03539
22*				
23	-12.884	22.290	-0.05130	0.16258
24	-8.476	51.982	-0.03284	0.27436
25	-25.229	-12.730	-0.13405	-0.16915
26	22.956	-0.910	0.10552	0.02366
27	-2.885	-14.081	-0.04947	-0.13986
28	11.355	7.095	0.05162	0.04954
29	-14.474	2.247	-0.07823	0.00537
30*				
31	-44.763	-21.355	-0.19854	-0.14849
32	-15.831	25.363	-0.08487	0.08936
33	-11.938	1.136	-0.07265	-0.00901
34	51.827	15.167	0.31837	0.14705
35*				
36	-10.105	-11.982	-0.10263	-0.06974
37	16.486	8.212	0.04258	-0.01989
38	-6.060	-41.126	-0.00886	-0.16374
39	9.809	-32.049	0.03889	-0.00258
40	17.441	-5.710	0.13757	-0.01437
41	50.106	23.982	0.19884	0.01594
42	-15.341	-22.285	-0.02459	-0.07543
43	44.717	46.526	0.26187	0.26913
44	9.138	28.242	0.05684	0.07427
45	-61.570	-18.162	-0.47302	-0.20437
46	2.029	-10.456	0.02660	-0.08615
47	-31.393	-16.830	-0.18230	-0.17132
48	30.003	19.321	0.24156	0.15529

* Plots eliminated from study because no red spruce was present.

first and second neighbors, $S_0 = 80$, $S_1 = 138$, and $S_2 = 670$.

The results for the four initial residual ring width measures are summarized in table 11. The spatial autocorrelation generally appears to be higher, based on the second nearest neighbor weights. Given that neighboring plots may sometimes have different aspects of soil conditions, it can be assumed the set of weights based on the first and second order nearest neighbors gives a more reliable indication of spatial structure.

Spatial autocorrelation coefficients were also calculated for the residuals from the regression

analyses shown in tables 9 and 10. These values are presented in table 12. The standard deviates were computed using the same formulae as were used to obtain table 11. More exact expressions are given by Cliff and Ord (1981), but these are very tedious to use, and the differences in magnitude are generally slight.

Interpretation of Spatial Analyses.—The results in table 11 show clearly that pronounced spatial dependence exists, whichever measure of residual ring width is used. The first question that arises is whether such dependence can be ascribed to purely geographical effects. However, the geographical variables do not

Table 10.—Residuals from weighted least squares regression for RES20, RES10, PCT20, and PCT10, respectively

Observation	RRES20	RRES10	PCRES20	PCRES10
1	46.282	-21.521	0.24740	-0.06286
2	-27.445	-27.201	-0.17263	-0.16189
3	-35.316	-22.902	-0.16155	-0.10963
4	-14.947	-45.974	-0.28882	-0.23249
5*				
6	12.526	12.103	0.07637	0.13770
7	-8.492	-27.345	-0.08494	-0.12596
8	56.781	77.765	0.20111	0.14621
9	-11.847	-16.480	-0.14614	-0.14344
10	-19.367	-33.018	-0.16035	-0.27380
11	-7.760	-41.048	0.11976	-0.01109
12	-23.543	-5.178	0.06126	0.02172
13	18.035	38.016	0.08884	0.21764
14	57.645	26.732	0.25975	0.22866
15	-18.072	10.880	-0.14416	0.03250
16	37.223	58.788	0.19865	0.09214
17	5.943	-4.243	0.05390	-0.05542
18	23.991	-23.934	0.13074	0.02145
19	-20.837	-18.059	-0.32424	-0.00782
20	-42.430	-26.236	-0.15413	-0.04206
21	-76.887	-37.081	-0.27356	-0.03565
22*				
23	-17.231	19.823	-0.08004	0.16041
24	-4.281	51.511	-0.03817	0.25346
25	-37.022	-14.344	-0.13453	-0.16752
26	28.356	-0.332	0.08779	0.01210
27	-2.566	-15.003	-0.04214	-0.15656
28	13.939	6.884	0.10000	0.06398
29	-35.314	-5.038	-0.19339	-0.01416
30*				
31	-48.186	-28.191	-0.20507	-0.17886
32	-25.403	26.303	-0.09078	0.12401
33	-23.449	-6.225	-0.13246	-0.01701
34	56.338	9.554	0.34085	0.12116
35*				
36	-18.279	-14.585	-0.12892	-0.05920
37	17.310	7.456	0.02603	-0.04263
38	-9.898	-48.106	-0.01409	-0.16916
39	22.400	-31.660	0.09583	0.02397
40	19.639	-2.465	0.12665	-0.02988
41	44.136	20.611	0.15549	-0.00942
42	-21.431	-26.640	-0.06461	-0.10528
43	44.173	43.168	0.25985	0.25656
44	5.930	26.627	0.04146	0.05310
45	-59.933	-15.349	-0.47767	-0.21879
46	-4.259	-10.251	0.00789	-0.07634
47	-31.989	-17.088	-0.23592	-0.16713
48	28.479	19.917	0.28237	0.17932

* Plots eliminated from study because no red spruce was presented.

provide any degree of explanatory power, and the spatial pattern of the residuals is essentially the same. The next question is whether the biotic factors account for some or all of the spatial structure.

When tables 11 and 12 are compared, it may be seen that the level of spatial autocorrelation has diminished in all cases. For the variable PCT20, the autocorrelation has become negative, but this may be due to the uncorrected effects of autocorrelations among the explanatory variables. One may generally conclude that the regression analyses account for much, but not all, of the spatial pattern found in the residual ring width values. However, one should recall that the

major variables in these regressions related to stand health. While this analysis indicates that the ring width changes are related to current stand health, the reasons for that current health status remain undetermined.

DISCUSSION AND SUMMARY

The results of steps 1 through 4 suggest an overall decrease in ring width increment among red spruce in the Great Smoky Mountains from 1965 to 1975 or 1984, relative to time series forecasts for those time periods. The magnitude for these decreases appeared to be related to elevation, factors of stand quality, and the

Table 11.--Results of tests for spatial autocorrelation among original ring width residuals

<u>Variable</u> ⁺	<u>Coefficient</u> [*]		<u>Standard Deviate</u> [*]	
	NN1	NN2	NN1	NN2
RES20	0.256	0.425	1.48	3.21
RES10	0.388	0.466	2.15	3.47
PCT20	0.194	0.324	1.17	2.53
PCT10	0.314	0.403	1.78	3.05

⁺ RES20 and RES10 refer to the residuals from the time series models for ring widths averaged over the forecast periods, 20 and 10 years, respectively. PCT20 and PCT10 denote RES20 and RES10 divided by the overall mean ring width for the whole series.

^{*} NN1 and NN2 refer to the sets of weights for the spatial autocorrelation coefficient based upon first and upon first- and second-order nearest neighbors, respectively.

Table 12.--Results of tests for spatial autocorrelation among regression residuals^{1/}

Variable	<u>Coefficient</u>		<u>Standard Deviate</u>	
	NN1	NN2	NN1	NN2
Unweighted Regression				
RES20	0.018	0.054	0.22	0.55
PCT20	-0.187	-0.205	-0.85	-1.28
RES10	0.277	0.287	1.57	2.20
PCT10	0.093	0.203	0.60	1.59
Weighted Regression				
RES20	-0.082	-0.133	-0.30	-0.76
PCT20	-0.292	-0.393	-1.39	-2.59
RES10	0.266	0.268	1.51	2.06
PCT10	0.087	0.202	0.57	1.57

^{1/}See table 11 for definitions of variables, coefficients, and standard deviates. Regression residuals are listed in tables 8 and 9.

relative decreases of first and second order nearest neighboring plots. These findings should be compared to those generated by other approaches to gain an understanding of the impact of certain key decisions in the stages of the analysis.

Both Landau and others (1985) and Cook (1987) recommended that annual basal area growth increment is preferable to ring width as a measure of annual productivity. Use of this measure could have reduced the nonstationarity in several of the time series. One approach to time series that display marked trends is to transform the data (Cook 1987). Instead, we followed the usual ARIMA paradigm and differenced the series where there were marked trends; 20 of the 44 series actually required differencing. It would be useful to compare forecasts obtained from the untransformed, but possibly differenced, series to those obtained from transformed series. Additionally, the average of the ring width of the trees' cores that met our inclusion criteria was used. Landau and others (1985) recommended the use of trimmed means. Specific circumstances of other data sets may determine the advisability of one procedure over another as the best way to minimize heterogeneity.

The methods used in each of these steps are capable of further refinement, and several suggestions are included in the Recommendations section. Nevertheless, the basic paradigm represents a substantive approach to the evaluation of recent trends in the width of tree rings.

Results obtained from the steps taken in this study should be compared with results generated from other approaches. Future studies might include the use of basal area increment rather than ring width as a measure of annual productivity and may incorporate transfer function models of climatic factors as well as intervention analysis to filter out the effect of important forest perturbations.

RECOMMENDATIONS

1. Following Landau and others (1985), it is recommended that future studies should use incremental basal area rather than ring width.
2. The possibility of using trimmed means rather than arithmetic means should be considered. However, the issue of how well measurements on five healthy trees reflect overall stand health requires further examination.
3. It is important to look for changes in ring width or other indicators relative to what might be expected. The forecasting approach used in this report is one way of excluding such trends, but others should be examined. The study of proportional changes seems preferable to that of absolute changes.
4. In future time series analyses, automated procedures might be used (AUTOBOX, developed by David Reilly of Automatic Forecasting Systems, Inc.).
5. Where known problems of fires, aphids, or infestations occur on particular plots, intervention analysis should be used to filter out such effects.

6. The inclusion of biotic variables in the regression models serves to link the change indicators to stand health. However, it does not resolve how the stands came to be in that condition. The lack of any worthwhile correlations between the indicators and the locational variables suggests that other factors may be at work in determining stand health; furthermore, the high levels of spatial autocorrelation in the ring width change data indicated that such factors are spatially concentrated.
7. The extremely variable topography and locations of the sites suggest that purely spatial models (Cliff and Ord 1981) are unlikely to be of direct value in this study. However, the potential exists for worthwhile applications with more homogeneous clusters of sites.
8. Future analyses could include transfer function models involving climatic variables, once detailed models of these variables have been developed.

LITERATURE CITED

- Cliff, A. D.; Hagget, P.; Ork, J.K.; Basset, K.; Davies, R. 1975. Elements of spatial structure. Cambridge, England: Cambridge University Press. 258 p.
- Cliff, A. D.; Ord, J.K. 1981. Spatial processes: Models and applications. London: Pion Press. 266 p.
- Cook, E. R. 1987. The use and limitations of dendrochronology in studying effects of air pollution in forests. In: Proceedings, of the NATO advanced research workshop: Effects of acid deposition on forest, wetlands, and agricultural ecosystem; 1985, May 12-17. Toronto, Canada. Springer-Verlag. 277-290.
- Kendall, M. G.; Stuart, A.; Ord, J.K. 1983. The advanced theory of statistics. Volume 3, 4th Edition. New York: Macmillan.
- Landau, E.; Swindel, B.F.; Thompson, J.R.; Van Ryzin, R.J. 1985. FORAST review report. American Statistician. 39(4): 250-254.
- Vandaele, W. 1983. Applied time series and Box-Jenkins models. New York: Academic Press: 417 p.

APPENDIX

FORTRAN program for computing the spatial autocorrelation coefficient

(A) Program

```
DIMENSION Z(100), X(100), NPL0T(100), NN1(100),
NN2(100), *WT1(100), WT2(100), NCROSS(250)
READ, N
READ, S01, S11, S21, S02, S12, S22
SUMX=0.0
DO 10 I=1,N
READ, NP, N1, N2, NREF
NPL0T (I)=NP
NN1(I)=N1
NN2(I)=N2
```

```

NCROSS(NP)=NREF
10 CONTINUE
DO 15 I=1,N
READ, XA
SUMX=SUMX+XA
X(I)=XA
15 CONTINUE
SUMZZ=SUMZ4=0.0
SAC1=SAC2=0.0
XBAR=SUMX/N
DO 20 I=1, N
Z(I)=X(I)-XBAR
SUMZZ=SUMZZ+Z(I)**2
SUMZ4=SUMZ4+Z(I)**4
20 CONTINUE
B2=N*SUMZ4/(SUMZZ**2)
PRINT, 'KURTOSIS=', B2
DO 30 J=1,N
KA=NN1(J)
KB=NN2(J)
KC=NPLOT(J)
IF (KA.EQ.0) GO TO 30
JA=NCROSS(KA)
JC=NCROSS(KC)
SAC1=SAC1+Z(JC)*Z(JA)
IF (KB.EQ.0) GO TO 30
JB=NCROSS(KB)
SAC2=SAC2+Z(JC)*Z(JB)
30 CONTINUE
SAC2=SAC1+SAC2
SAC1=SAC1/SUMZZ
SAC2=SAC2/SUMZZ
SD1=N*((N*N-3*N+3)*S11-N*S21+3*S01*S01)
SD1=SD1-B2*((N*N-N)*S11-2*N*S21+6*S01*S01)
SD1=SD1/((N-1)*(N-2)*(N-3)*S01*S01)
SD1=SD1-1.0/(N-1)**2
SD1=SQRT(SD1)
SD2=N*((N*N-3*N+3)*S12-N*S22+3*S02*S02)
SD2=SD2-B2*((N*N-N)*S12-2*N*S22+6*S02*S02)
SD2=SD2/((N-1)*(N-2)*(N-3)*S02*S02)
SD2=SD2-1.0/(N-1)**2
SD2=SQRT(SD2)

```

```

PRINT, 'SD1=', SD1, 'SD2=', SD2
PRINT, ' SPATIAL A/C FOR FIRST NN IS ', SAC1
PRINT, ' SPATIAL A/C FOR SECOND NN IS ', SAC2
SAC1=(SAC1+1.0/(N-1))/SD1
SAC2=(SAC2+1.0/(N-1))/SD2
PRINT, 'STD. DEVIATE FOR FIRST NN IS ', SAC1
PRINT, 'STD. DEVIATE FOR SECOND NN IS ', SAC2
STOP
END

```

(B) Plot Number--first nearest neighbor--second nearest neighbor-- order of plot in listing of values (required inputs to vectors NPLOT, NN1, NN2, AND NCROSS)

		(continued)
32	54 55 29	15 13 37 14
54	32 55 35	158 0 0 42
55	54 32 36	13 37 36 12
7	159 207 6	37 36 13 33
159	6 7 43	36 37 13 32
6	159 7 5	132 0 0 40
207	7 159 44 125 4 0 39	
153	6 159 41 4 125 0 4	
12	9 25 11	34 29 33 31
9	25 12 8	29 33 34 27
25	9 12 23	33 29 34 30
26	27 25 24	31 46 8 28
27	26 10 25 46 17 8 34	
10	11 113 9	17 8 46 16
113	10 11 38 8 17 46 7	
11	10 113 10 19 18 0 18	
21	11 10 20	18 19 0 17
28	23 11 26	2 20 1 2
23	24 28 21	20 1 2 19
24	23 14 22	1 20 2 1
14	24 23 13	3 1 20 3
16	109 14 15	
109	16 14 37	

A Fractal Approach to Analysis of Tree Ring Increments

R. A. J. Taylor

SUMMARY

Information from plots established in the Great Smoky Mountains by the National Park Service and the Tennessee Valley Authority was used to determine annual tree ring widths from core samples of red spruce (*Picea Rubens* Sarg.). The red spruce core samples showed a significant dependence of variance on the mean size of tree rings at 67 of 68 plots. At 9 of 48 plots, the variance has increased more rapidly since 1943; of the others, 7 have shown a decrease since 1940 and 32 showed no change. The dependence of variance on mean of a measurement was interpreted in terms of "fractals," a term coined to denote fractional dimension. The change in fractional dimension over time indicated an evolution of factors that influenced the dependence of variance on mean; these factors may have been successional, climatic, or anthropogenic, all of which seemed to vary on about the same time scale. It was concluded that variance-mean analysis may be an inexpensive and promising area of inquiry in dendrochronology.

INTRODUCTION

Mortality of large forest areas in several parts of the world has caused fear that the concentration of anthropogenic compounds in the atmosphere may be increasing. Acids and other oxidizing agents of human origin, notably ozone, have been detected in the atmosphere and are probably capable of interfering with tree growth and survival. However, there are no data concerning the level of atmospheric pollution (Cook 1987, Kiester and others 1985). Therefore other possible influences and causes must be considered, such as the effect of climate on tree ring growth. Because climate and anthropogenic effects are easily confounded, this report will focus on the analysis of change and not on distinguishing between pollution and climate.

Annual tree rings in temperate regions provide a convenient record of a tree's growth history. Comparison of tree rings over a geographical area has frequently been used to determine climatic changes; it is assumed that patterns common to all trees of the same species, similar age, and in the same soils should respond alike to weather conditions that are basically unvarying (Creber 1977, Guiot and others 1982).

BACKGROUND

It is commonly assumed that the width, $W(t)$, of a tree ring laid down in year t is the linear sum of four systematic components and a random component:

$$W(t) = A(t) + B(t) + C(t) + D(t) + e(t)$$

where

$A(t)$ = age factor(s) unique to each tree,

$B(t)$ = disturbances unique to each tree,

$C(t)$ = climatic effects common to all trees at a site,

$D(t)$ = disturbances common to all trees at a site, and

$e(t)$ = random component.

It may be helpful to review some of the assumptions frequently made about $W(t)$. The successive increments are assumed to be identically distributed. For the benefit of certain analyses, the increments are further assumed to be statistically independent, with the marginal distribution, $e(t)$, Gaussian with zero mean, and constant variance. Such a time series is called a stationary Gaussian random walk or Brownian motion. While no one working in dendrochronology seriously expects the Brownian assumption to be valid, the nature of statistics often demands that it be assumed.

The concepts of randomness are context dependent, and the word may be used in a confusing manner. There are two broad, alternative definitions of randomness: "predictable behavior, efficiently described by a statistical probability distribution" and "haphazard behavior, governed by no known rules" (Mandelbrot 1967). In addition, events in which the mean and variance are equal (Poisson distributed) are often said to be random. Predictable behavior is synonymous with stochastic and differs from deterministic because its expected or average outcome is predictable, while the specific outcome of a trial lies within certain bounds defined by the variance.

As stated above, statistical independence of successive increments is a well-known simplification. The assumption of stationarity, however, has a special implication that is rarely questioned: the sample moments vary little from sample to sample, provided the samples are large enough. In our analysis, this assumption is relaxed, and the assumption is made that the variance is infinite or at least so large that it may be treated as infinite. Thus the assumption of Gaussian marginal distribution is abandoned in favor of the Cauchy, permitting the Central Limit Theorem to be invoked without assuming constant variance (Mandelbrot 1969). Therefore the need to amend the other assumptions of independence and stationarity is alleviated (Berger and Mandelbrot 1963).

The assumption of infinite variance is equivalent to assuming randomness that is predictable but haphazard; the long-term trend is evident, but the short-term signal is unpredictable. Theory expounded by Mandelbrot

(1960, 1963, 1969) related haphazard time series with power laws and distributions with infinite variance.

THEORETICAL METHODS

Consider the series $x(t)$, $t = 1, 2, \dots, n$, of observations taken at equal intervals of time or space. Any particular series $[x(t)]$ is assumed to be the realization of a process $W(t)$ that will be defined later; t is used as an indicator variable at equal intervals of time or space. Defining the following variables:

$$\begin{aligned} V(k) &= E[x(t) - x(t+k)]^2 = 2[V(x) - C(x;k)], \\ V(x) &= E[x(t) - M(x)]^2, \\ M(x) &= E[x(t)], \\ C(x;k) &= E\{[x(t) - M(x)][x(t+k) - M(x)]\}. \end{aligned}$$

$V(x)$ is the variance of the series with $M(x)$ the mean. Theory based on the usual interpretation of the Central Limit Theorem permits one to assume that these parameters estimate population values. However, in this analysis the assumption is not necessarily valid: the parameters simply represent the sample values and are therefore not asymptotic to the population values. $C(x;k)$ is the spatial/temporal covariance across the data and is related to the standard treatments of time/space series data, including tree ring analyses (Guiot and others 1982). Information is given in $C(x;k)$ on the regular variations in the data at periods equal to k . The variogram is $V(k)$ and provides information on the nonregular variation at lag k .

Consider $V(k)$ as k varies: dividing $V(k) = 2\{V(x) - C(x;k)\}$ through by $V(x)$ gives $V(k) = 2V(x)\{1 - R(k)\}$, where $R(k)$ is the serial correlation coefficient that takes values $-1 \leq R(k) \leq 1$; therefore $V(k) = 2rV(x)\{1 - r\}$, $0 \leq r \leq 1$, and $0 \leq V(k) \leq 2V(x)$. Thus:

$$\begin{aligned} V(k) &= 0 \text{ when serial correlation at lag } k \text{ is } 1, \\ V(k) &= 2V(x) \text{ when no serial correlation at lag } k, \text{ and} \\ V(k) &= 4V(x) \text{ when serial correlation at lag } k \text{ is } -1. \end{aligned}$$

At any specific value of k , say k^* , $V(k)$ will give information on all variations not having a cycle at k .

To obtain information on all variations, $V(x)$ is commonly used, but we cannot say what variation we have at $t = i$, only that it is over the interval $t = i, i+1, i+2, \dots$, and so forth. Ideally, the variance would be partitioned in the manner of $V(k)$ but without limitation. If k goes to zero, all scales of variation are included and simultaneously $V(k)$ disappears. To estimate $V(0)$, compute $V(k)$ for $k > 0$ and extrapolate back to zero. To obtain the rate of approach of $V(k)$ to the origin, plot $\log V(k)$ against $\log(k)$ and determine the gradient, $d \log V(k) / d \log(k) = \beta$ as $k \rightarrow 0$.

Another approach to estimate the gradient of $V(0)$ is to replicate the generating process $W(t)$: $W_1(t), W_2(t), \dots$; $V(0)$ can then be estimated at any or all t . The estimates $V_i(0)$ are all at the origin, so the gradient must be extracted from them. Plotting the means and variances of several series against time shows that the actual

values vary according to no particular pattern; however, it must be noted that the magnitude of $V_t(0)$ seems to increase with time (figs. 1-8). Since $V_t(0)$ is partly dependent on $M_t(0)$, standardizing $V_t(0)$ with $M_t(0)$ may show a trend. Figures 1 through 8 also show the coefficient of variation $\{\sqrt{V_t(0)} / M_t(0)\}$ increasing with time.

Figure 9 plots $\log V(t)$ against $\log M(t)$ and shows how the variance increases with respect to mean. The gradient $d \log V / d \log M = b$ is an estimate of β . This is easily demonstrated by the following argument. Define a reference mean M_0 and a comparison mean $M_s = sM_0$ ($s > 1$). Now $V_0 = aM_0^b$ and $V_s = aM_s^b = a(sM_0)^b = s^b(aM_0^b) = s^bV_0$. Evidently the variance is scale independent, and its gradient b is an intrinsic component, as expected from $d \log V(k) / d \log(k)$.

Taking logs: $\log V_s = \log V_0 + b \log(s)$, remember that V_0 is a variance corresponding to an arbitrarily chosen mean M_0 . V_0 is thus also arbitrary; M_0 can be chosen such that V_0 is 1. Thus $\log V_s = b \log(s)$, which is very nearly $\log V(k) = \beta \log(k)$. Although k and s are not quite synonymous, if multiples are chosen as values of s , then $\log V = b \log(i) + C$ describes the locus of variance at spatial/temporal intervals $i = 1, 2, \dots$, and is, except for C , identical to $\log V(k) = \beta \log K$. Therefore $\beta = b$.

The same result can be obtained from an empirical argument. Let there be a series of samples taken along a transect AB. Divide AB into NK intervals such that there are N groups of K intervals. Neither the K groups nor the N groups need to be contiguous, but for simplicity it is assumed that they are. The number of entities in each of the NK intervals is counted. In the present case, the size of the tree ring increment is measured: x_{ij} where x is the size and $i = 1, 2, \dots, N$ and $j = 1, 2, \dots, K$. Now compute the mean M_i and variance V_i for each of the $i = 1, 2, \dots, N$ groups from

$$M_i = \sum x_{ij} / K \quad V_i = \sum (x_{ij} - M_i)^2 / (K-1).$$

Let the central interval of each group become the center of mass for that group. The center of mass has at least two parameters describing the distribution of observations within the group: M_i and V_i .

If $\log V$ is plotted against $\log M$, empirically they are related by the power law, $V = aM^b$, where a and b are empirically estimable parameters (Taylor 1961, Perry 1981). Consider the arbitrary series x_j^* ($j = 1, 2, \dots, K$) that has mean and variance M^* and V^* ; now compute the serial covariance $C^*(k)$ having lag k , from

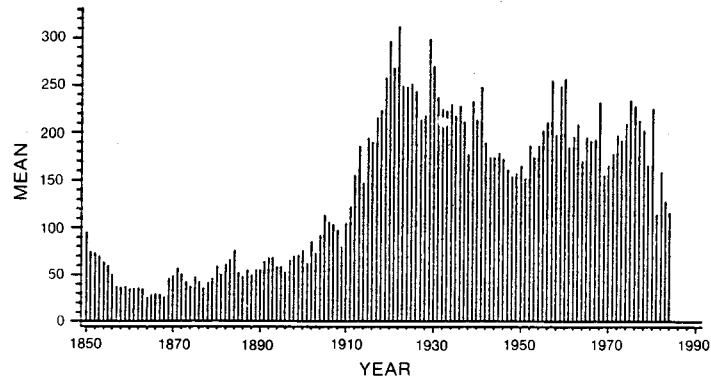
$$C^*(k) = E\{x_j^* - M^*\}[x_{j+k}^* - M^*].$$

From V^* and $C^*(k)$ the variance of increments is computed:

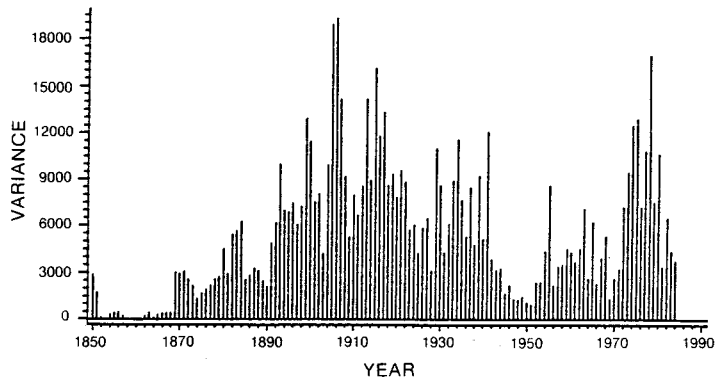
$$V^*(k) = E(x_j^* - x_{j+k}^*)^2 = 2[V^* - C^*(k)].$$

Half $V^*(k)$ is referred to as the variogram, and its computation is the first step in the interpolation process known as kriging (Journal and Huijbregts 1978). The covariance term is $C^*(k)$ and is related to the systematic part of the ring increments, particularly growth at small k . At larger k , long-period variations such as climatic cycles predominate. Filtering techniques (Guiot and others 1982) concentrate on the structure of $C^*(k)$ over varying periods of time. The total variance of the series V^* contains both the systematic and nonsystematic variance.

MEAN ANNUAL TREE—RING WIDTH — SITE 1 (1850 — 1984)



VARIANCE OF TREE—RING WIDTH



COEFFICIENT OF VARIATION OF TREE—RING WIDTH

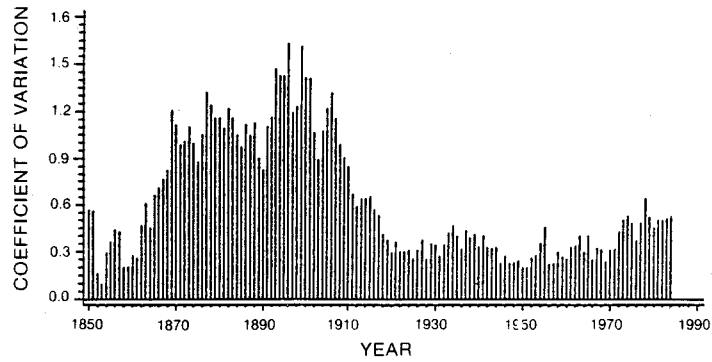
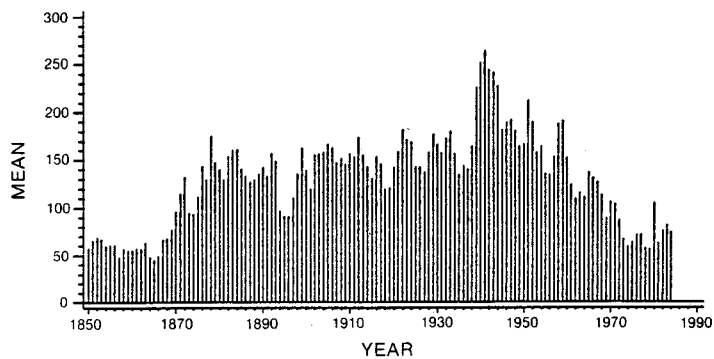
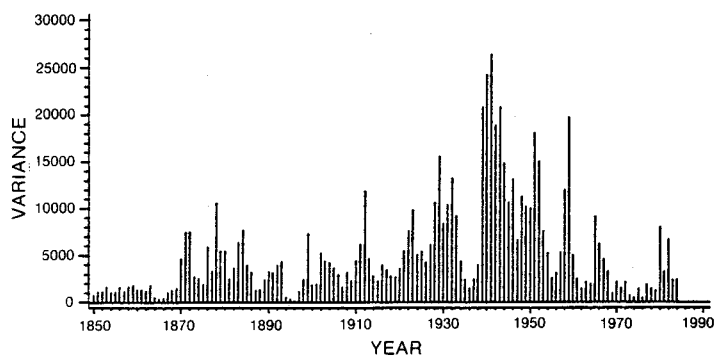


Figure 1.--Time series of mean, variance, and coefficient of variation of tree-ring increments from 1850 to 1984 at Tennessee Valley Authority site 1.

MEAN ANNUAL TREE—RING WIDTH — SITE 9 (1850 — 1984)



VARIANCE OF TREE—RING WIDTH



COEFFICIENT OF VARIATION OF TREE—RING WIDTH

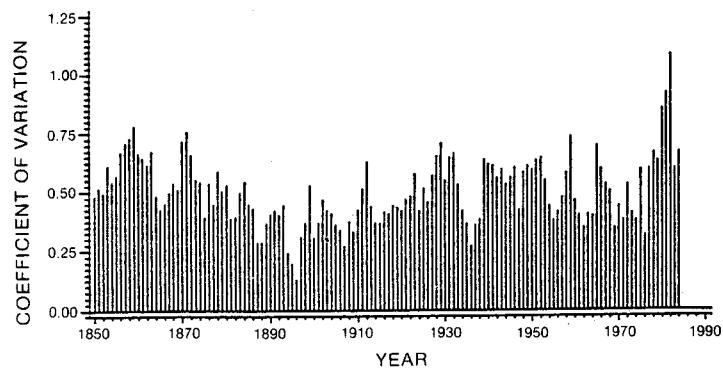
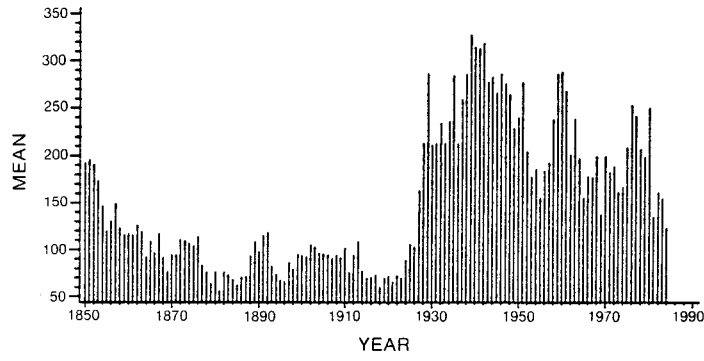
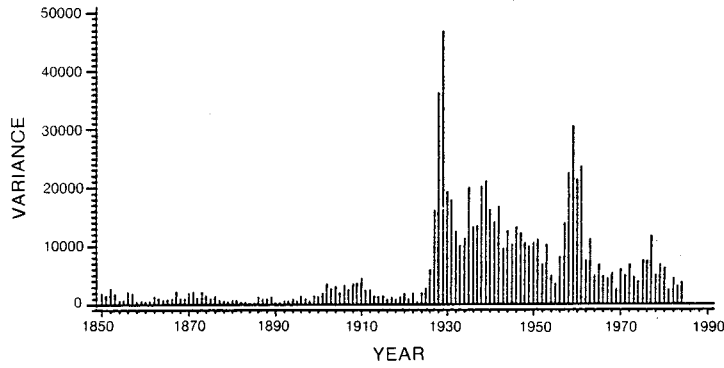


Figure 2.--Time series of mean, variance, and coefficient of variation of tree-ring increments from 1850 to 1984 at Tennessee Valley Authority site 9.

MEAN ANNUAL TREE-RING WIDTH — SITE 23 (1850 — 1984)



VARIANCE OF TREE-RING WIDTH



COEFFICIENT OF VARIATION OF TREE-RING WIDTH

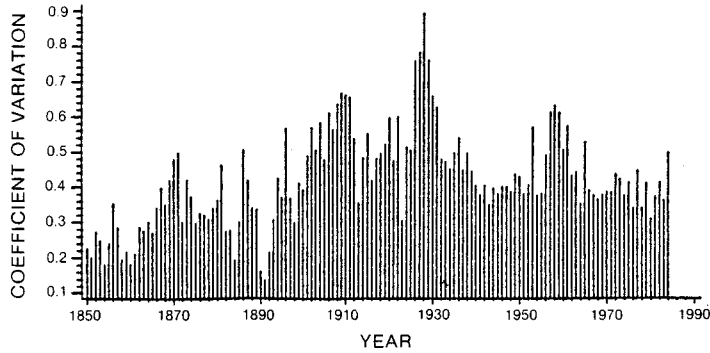
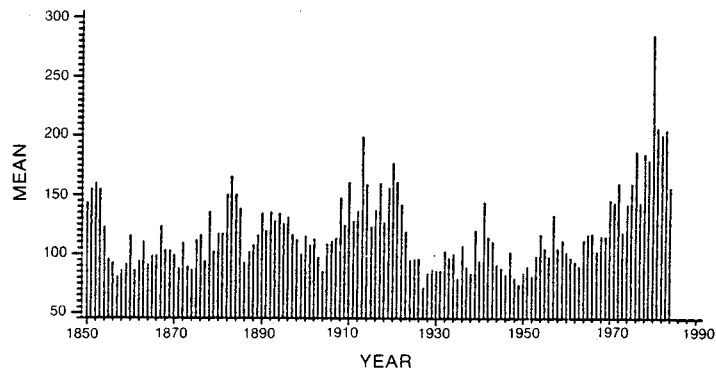
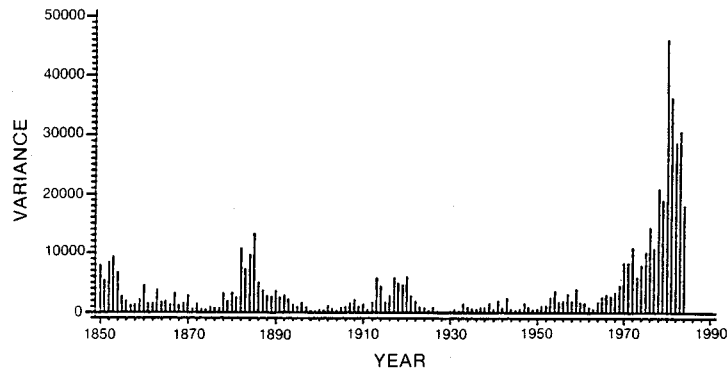


Figure 3.--Time series of mean, variance, and coefficient of variation of tree-ring increments from 1850 to 1984 at Tennessee Valley Authority site 23.

MEAN ANNUAL TREE-RING WIDTH — SITE 36 (1850 — 1984)



VARIANCE OF TREE-RING WIDTH



COEFFICIENT OF VARIATION OF TREE-RING WIDTH

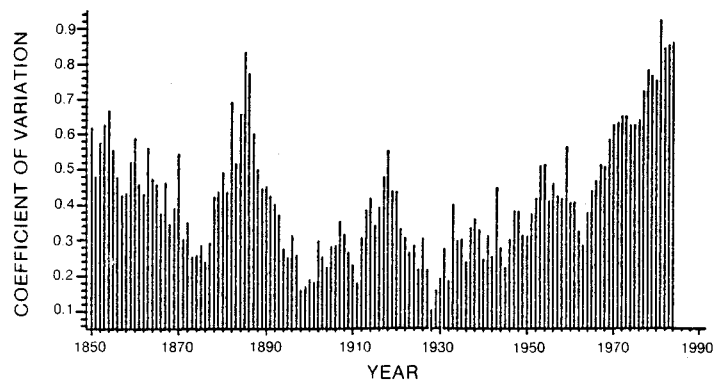
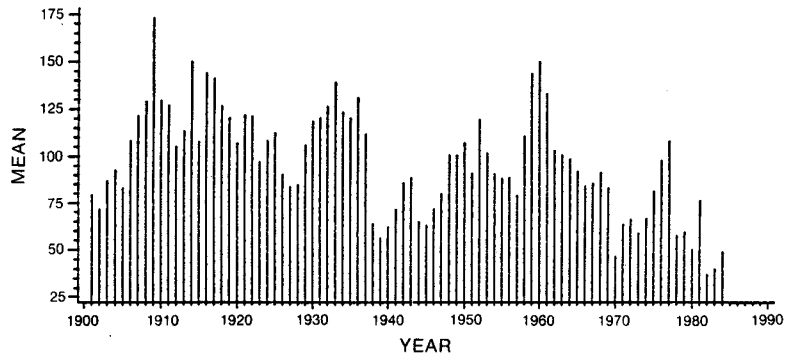
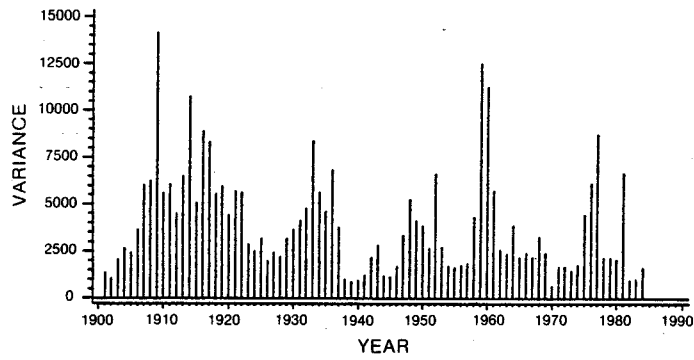


Figure 4.--Time series of mean, variance, and coefficient of variation of tree-ring increments from 1850 to 1984 at Tennessee Valley Authority site 36.

MEAN ANNUAL TREE-RING WIDTH — SITE 307 (1901 — 1984)



VARIANCE OF TREE-RING WIDTH



COEFFICIENT OF VARIATION OF TREE-RING WIDTH

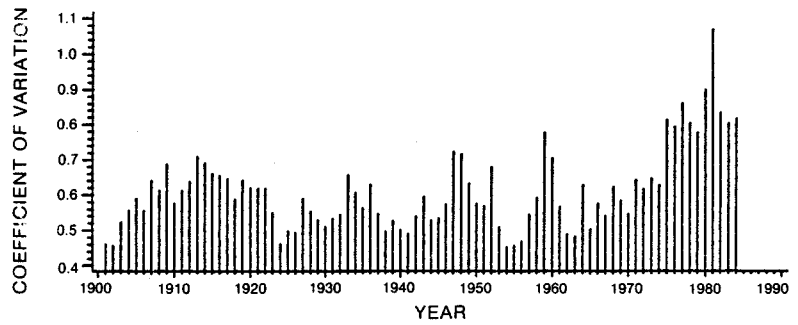


Figure 5.--Time series of mean, variance, and coefficient of variation of tree-ring increments from 1850 to 1984 at National Park Service site 307.

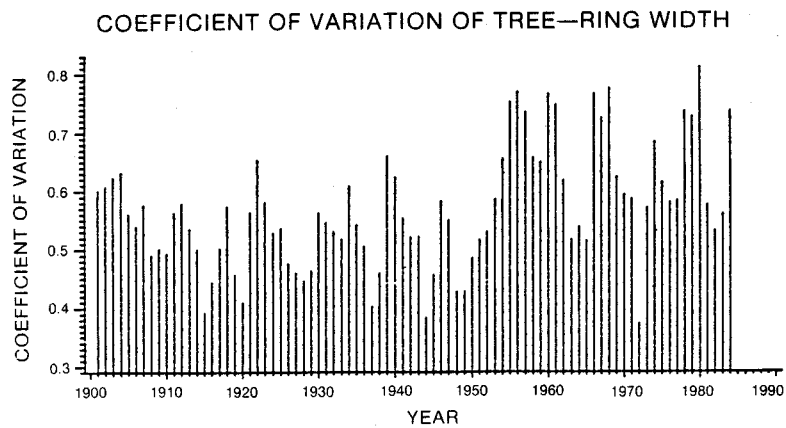
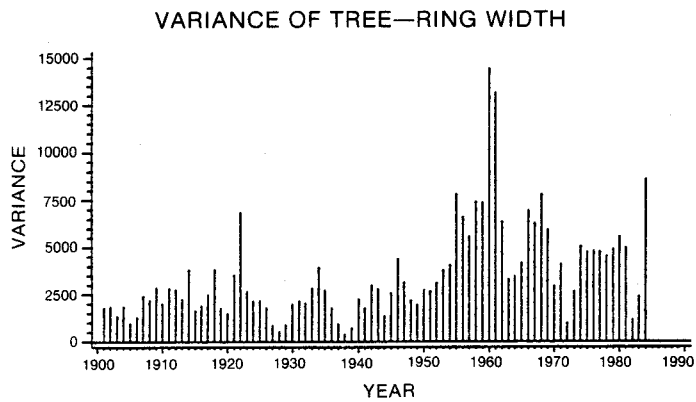
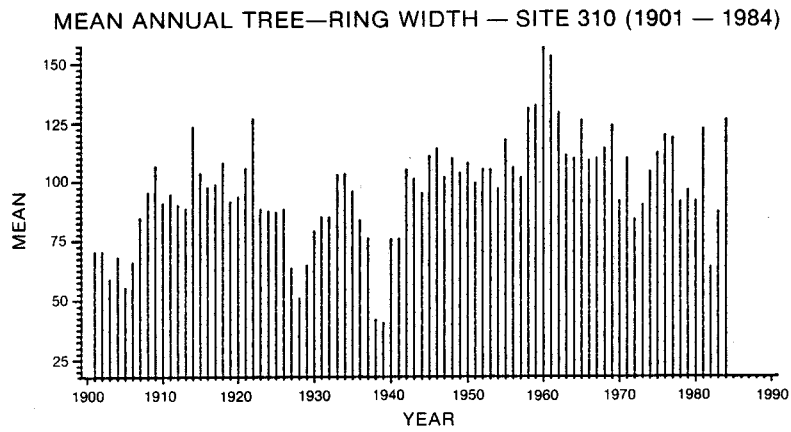


Figure 6.--Time series of mean, variance, and coefficient of variation of tree-ring increments from 1850 to 1984 at National Park Service site 310.

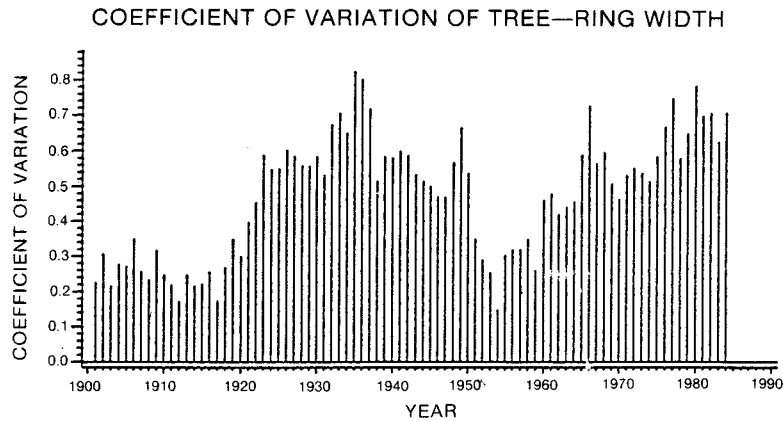
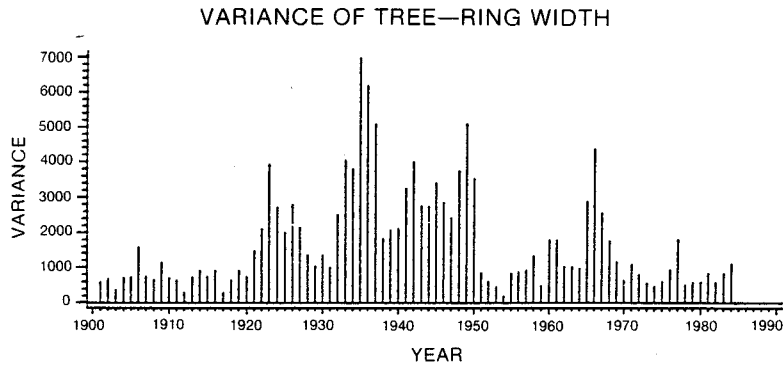
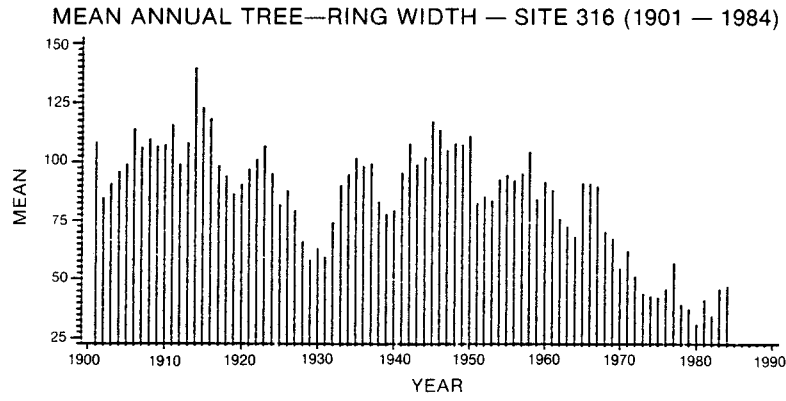


Figure 7.--Time series of mean, variance, and coefficient of variation of tree-ring increments from 1850 to 1984 at National Park Service site 316.

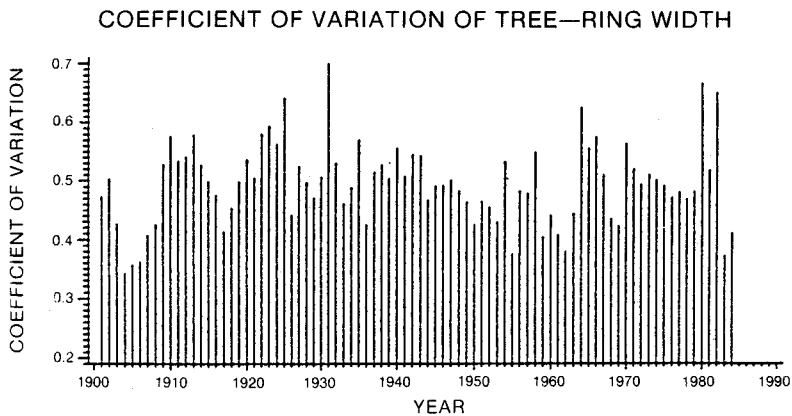
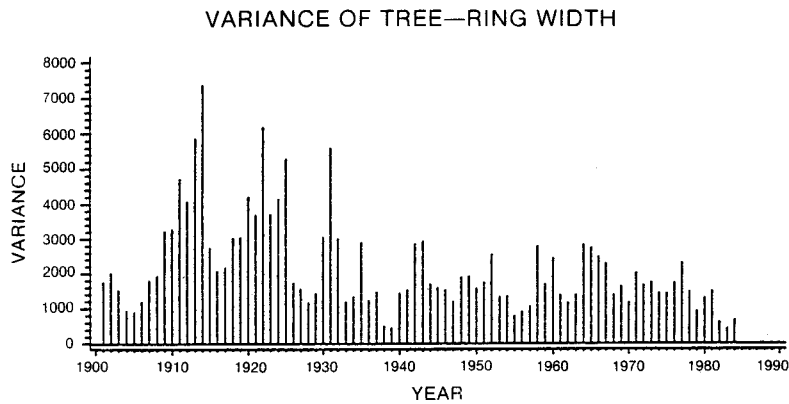
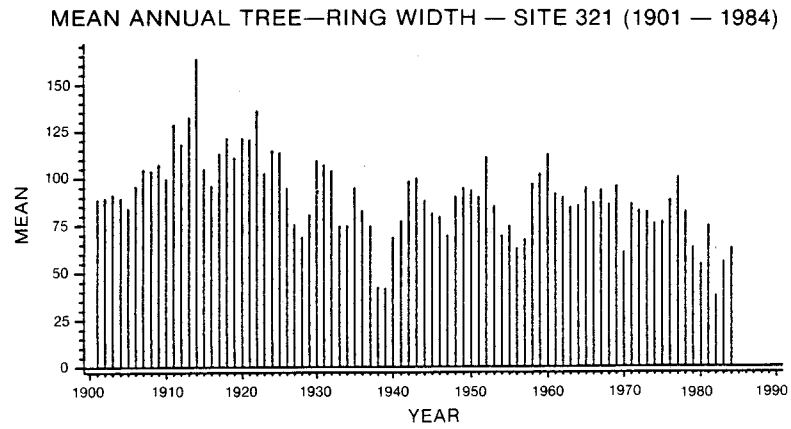


Figure 8.--Time series of mean, variance, and coefficient of variation of tree-ring increments from 1850 to 1984 at National Park Service site 321.

This study focuses primarily on the systematic variance common to all trees at a site. Therefore the variance across all cores at a site in each year was calculated to form the series V_t . The common systematic components at a site formed a baseline from which all other components of variance were referenced. To find the common systematic component, variance was plotted against mean to standardize variance. The mean was assumed to be linearly related to the baseline.

Also to be noted is the change in the common component, represented by the change in V_t relative to M_t . Changes between the relationship of V_t and M_t indicate changes in the normal behavior of the process $W(t)$. Changes result from evolution in the process variance. If a long-term change is anticipated, then evolution in the system process can be demonstrated by determining differences in the rates of change of variance before and after the reference point.

PROCEDURE

Of the plots established by the National Park Service (NPS) and the Tennessee Valley Authority (TVA), only those with five or more red spruce trees in the sample were selected for analysis. With 2 cores (series) per tree, means and variances for each year from the beginning of the series were computed from 10 ring width estimates. Series ranged in length from 40 to 135 years. These data yielded 20 bivariate series with length of approximately 84 years (NPS data), and 48 series with lengths varying from 40 to 135 years (TVA data). The logarithm of variance was then regressed on log mean with each point representing 1 year.

RESULTS

Figures 1 through 8 show the mean (M), variance (V), and coefficient of variation (CV) against time at TVA sites 1, 9, 23, and 36 and NPS sites 307, 310, 316, and 321. Both the mean and variance were highly variable, and the plots of CV against time gave the strong impression that the variance was increasing with time. Furthermore, the detailed behavior differed greatly from site to site. Figures 9 through 16 show variance-mean regression plots for the same 8 sites, and table 1 shows the results of regressions of 68 sites. Sixty-seven regressions were significant at probabilities of less than 0.05. Only site 113 showed no dependence of variance on mean.

To investigate the possibility that conditions in the post-World War II era were different from prewar conditions, the data of sites with runs longer than 80 years were split at 1943 and the variance-mean regressions repeated to test the hypothesis that the acceleration of variance with mean has changed. Table 2 shows that of the 28 TVA data sets suitable for analysis, 8 showed increases in dependence, 18 showed no change, and none showed a decrease in dependence. There were two sites with a nonsignificant regression. Interestingly, the NPS data showed the reverse pattern: only one site showed a significant increase in variance-mean dependence since 1943,

nine sites showed no difference and seven showed a significant decrease since 1943, three sites had a nonsignificant regression.

Preliminary analyses with multivariate methods (principal components analysis, PCA) failed to identify any differences in regression gradient attributable to differences in the two data sets. Variables included in the PCA were annual rainfall, mean annual maximum and minimum temperatures, xeric/mesic status, altitude, and stand basal area.

DISCUSSION

Tree rings reflect the net effect of age, health, soil, and biotic conditions on tree growth.

Age and health are unique aspects of each individual tree, but the environmental conditions experienced by all trees in close proximity are considered similar or common external factors. However, competition is one aspect of a tree's external environment that is considered unique.

Therefore three influences of growth can be established:

1. Age/growth---unique internal factors,
2. Competition---unique external factors, and
3. Environment---common external factors.

When samples are composed of mature and/or old trees, the age-dependent variance will be relatively small and may even be missing in the younger trees. When very young and very old trees are included in the sample, age/growth is likely to have an impact only in the early part of a series and variances are higher than normal.

Competition between trees in the sample may help one to understand the dependence of variance on mean. For a given value of the mean, a high variance indicates a wider range of individual responses. As the mean increases, the dependence of variance on the mean suggests that only some elements of a sample are increasing, while others may be decreasing or increasing very little. If increases in tree ring width were all equal at a site, the variance would be increasing proportionately and $b = 1$. The mean value of b was 1.77, suggesting that at the majority of sites, when conditions were conducive to growth increases, only some trees responded. A change in b over time was interpreted as a change in the relative competitiveness of the trees at a site due to a change in the external conditions.

CONCLUSIONS

Because the relationship between variance and mean is still uncertain, no definite conclusions can be made about the influences on tree growth. Because the nature of fractional dimension is still poorly understood, the theoretical treatment is not rigorous. Only since the publication of Mandelbrot's book (1982) has there been an increased awareness and interest in fractals among scientists other than topologists.

The ideas developed in this analysis were preliminary, but the reduction of the masses of tree core data to a single parameter, b , was a new contribution to statistical methods in dendrochronology. However, the results of splitting the data into two sections were

SITE 1

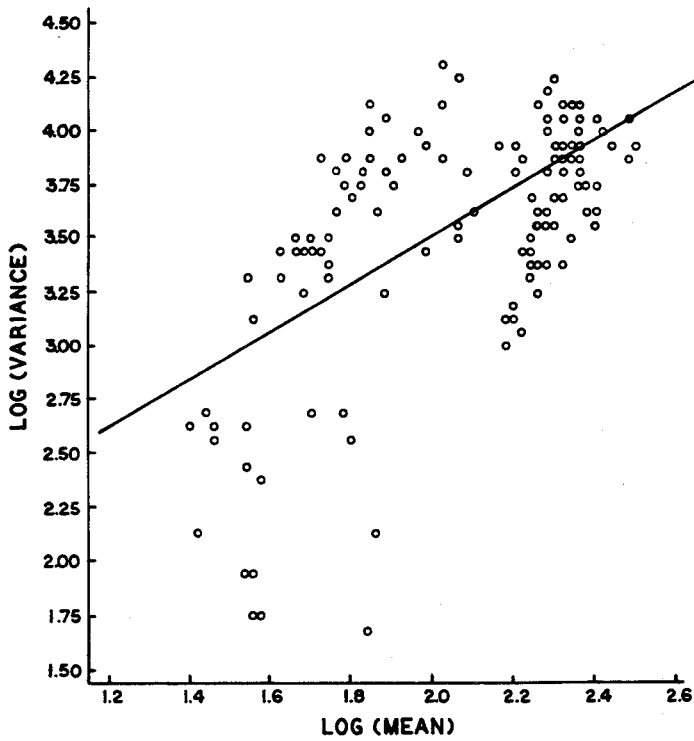


Figure 9.--Variance-mean plot (log scale) of Tennessee Valley Authority site 1. All regressions are significant at $p < 0.01$. This plot shows some nonlinearity.

SITE 9

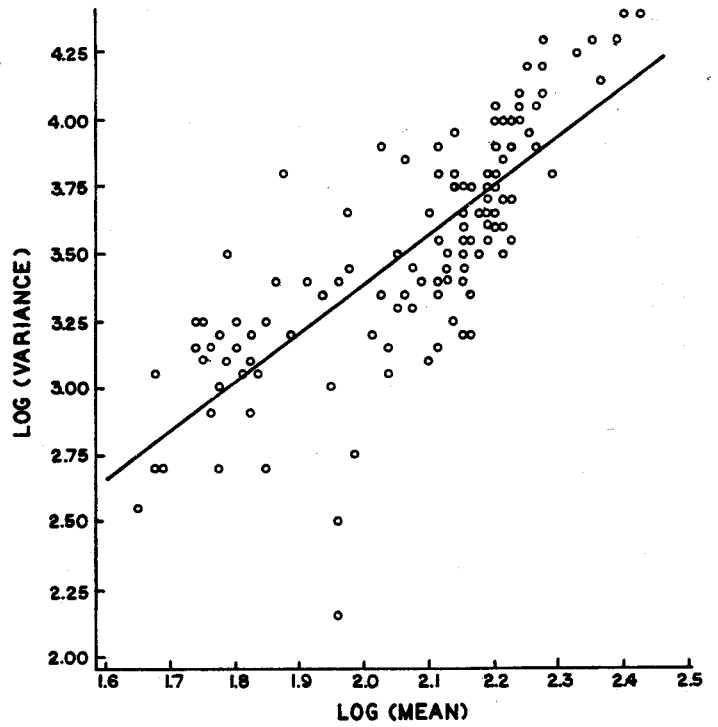


Figure 10.--Variance-mean plot (log scale) of Tennessee Valley Authority site 9. All regressions are significant at $p < 0.01$. This plot shows very good regression.

SITE 23

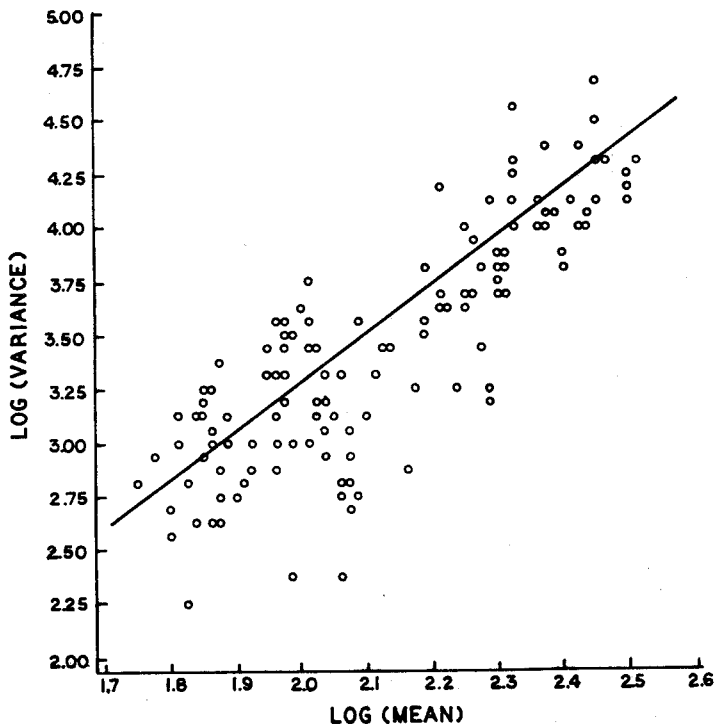


Figure 11.--Variance-mean plot (log scale) of Tennessee Valley Authority site 23. All regressions are significant at $p < 0.01$. This plot shows very good regression.

SITE 36

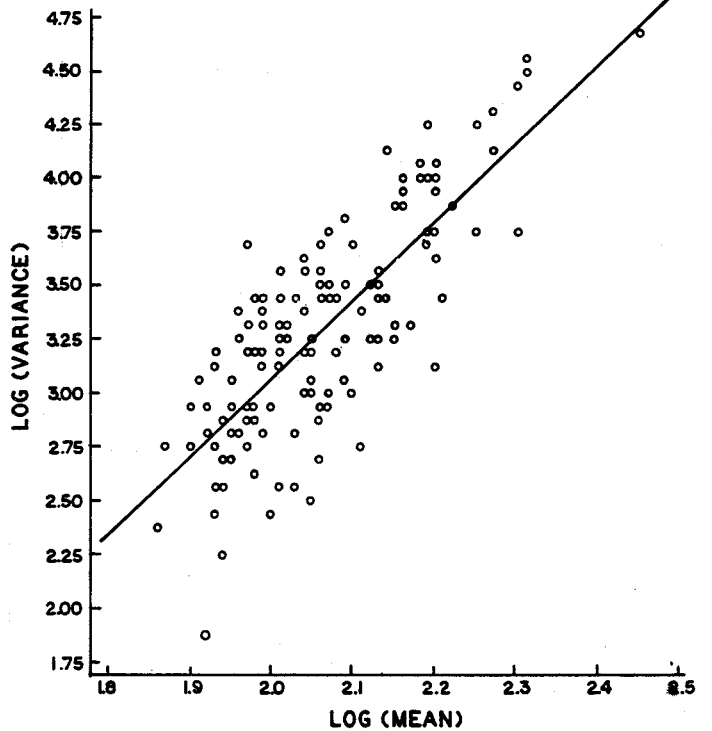


Figure 12.--Variance-mean plot (log scale) of Tennessee Valley Authority site 36. All regressions are significant at $p < 0.01$. This plot shows very good regression.

SITE 307

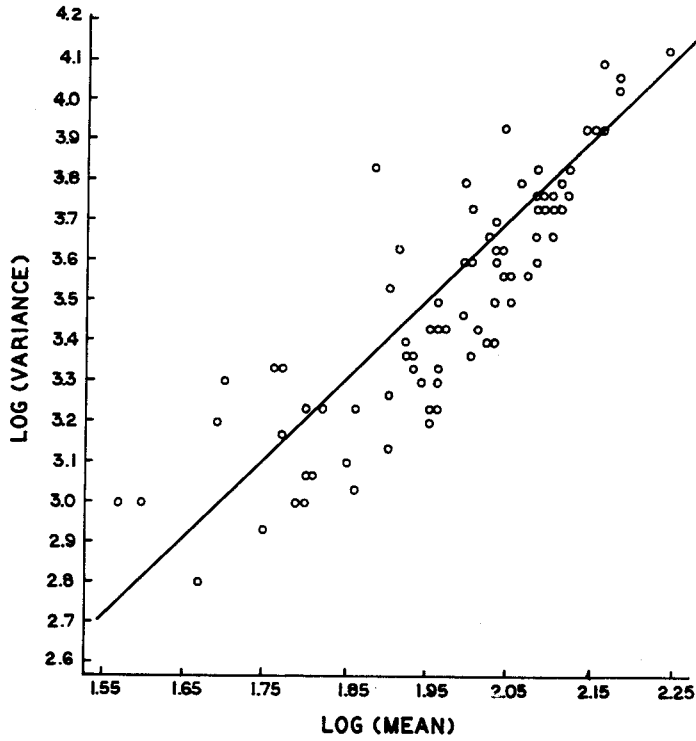


Figure 13.--Variance-mean plots (log scale) of National Park Service site 307. All regressions are significant at $p < 0.01$. This plot shows very good regression.

SITE 310

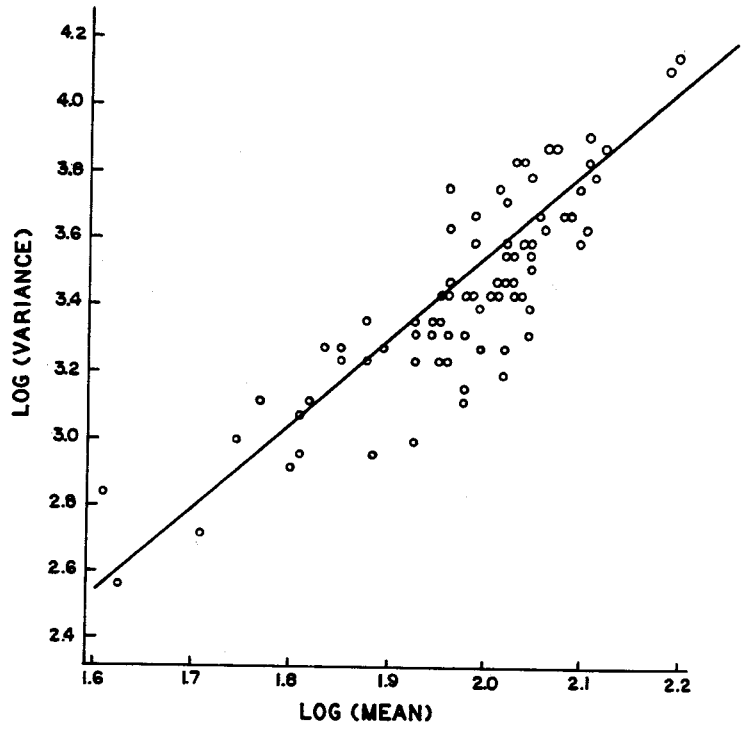


Figure 14.--Variance-mean plots (log scale) of National Park Service site 310. All regressions are significant at $p < 0.01$. This plot shows very good regression.

SITE 316

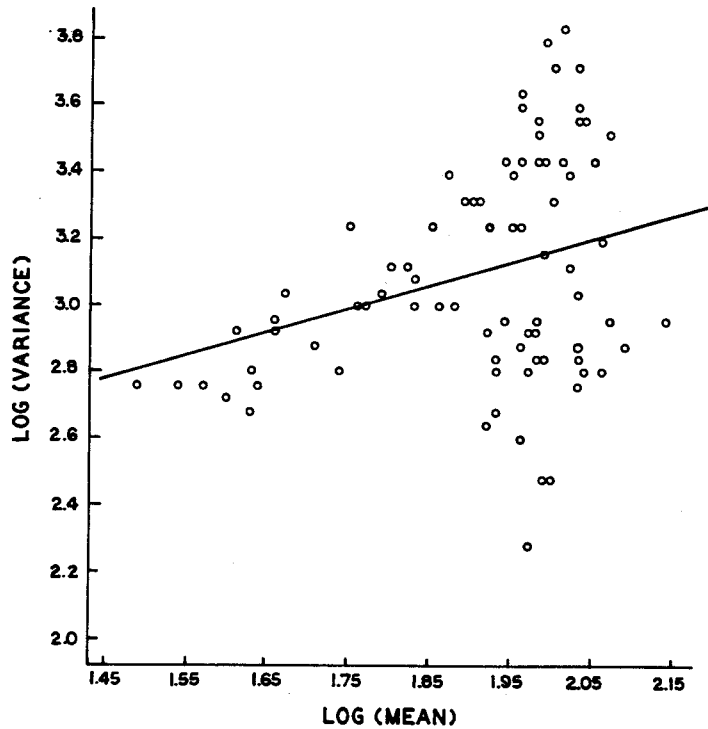


Figure 15.--Variance-mean plots (log-scale) of National Park Service site 316. All regressions are significant at $p < 0.01$. This plot shows some nonlinearity.

SITE 321

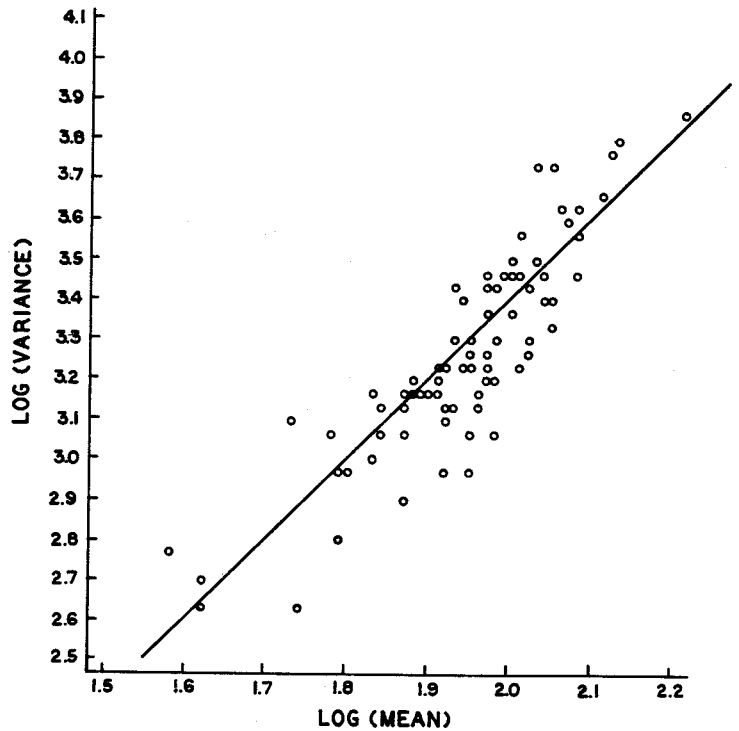


Figure 16.--Variance-mean plots (log scale) of National Park Service site 321. All regressions are significant at $p < 0.01$. This plot shows very good regression.

inconclusive. A reduction in variance in recent years at each TVA site may be indicated by the TVA data, while the NPS sites have become more variable. If this is so, the difference between the two data sets must be determined. The results of the PCA were also inconclusive, but the set of site characteristics used in the analysis was very small.

The fractal approach to the analysis of tree ring widths is a promising area for further research. However, this method may not help to identify anthropogenic influences on tree growth; change may be determined, but the cause of that change may still require carefully controlled, long-term, large-scale forest experiments.

Table 1.--Regression analyses of the log (variance) against log (mean) of tree ring increments⁺

Site No.	N	Log(a)	b	Standard error of b	Adjusted R ²	F-ratio	Significance
Tennessee Valley Authority Plots							
1	135	1.38	1.05	0.126	0.34	68.8	
2	71	-0.72	1.84	0.346	0.28	28.2	
3	88	1.50	0.96	0.159	0.29	36.1	
4	92	-1.98	2.55	0.194	0.65	172.0	
5	35	-1.04	1.90	0.587	0.22	10.4	**
6	96	1.83	0.77	0.319	0.05	5.9	*
7	108	0.41	1.55	0.145	0.51	114.0	
8	57	-1.02	2.05	0.223	0.60	85.1	
9	135	-0.32	1.85	0.122	0.63	230.0	
10	135	1.18	1.06	0.204	0.16	26.8	
11	45	1.56	0.94	0.246	0.23	14.5	***
12	125	0.10	1.64	0.176	0.41	86.6	
13	45	-3.22	3.08	0.549	0.41	31.4	
14	43	0.92	1.28	0.239	0.40	28.6	
15	57	2.02	0.74	0.206	0.18	12.9	***
16	64	0.90	1.19	0.147	0.51	66.1	
17	80	0.21	1.57	0.144	0.60	118.0	
18	65	-2.05	2.63	0.151	0.83	304.0	
19	128	-0.50	1.81	0.107	0.69	283.0	
20	115	0.16	1.52	0.131	0.54	135.0	
21	26	-2.81	2.71	0.971	0.21	7.8	**
22	100	1.91	0.80	0.148	0.22	29.1	
23	135	-1.06	2.13	0.118	0.71	323.0	
24	106	-1.94	2.52	0.124	0.80	414.0	
25	135	0.51	1.42	0.161	0.36	77.3	
26	115	1.23	1.06	0.163	0.27	42.2	
27	135	0.77	1.31	0.206	0.23	40.1	
28	132	0.65	1.28	0.266	0.14	23.1	
29	95	-0.34	1.93	0.199	0.50	94.2	
30	25	-3.47	3.10	0.809	0.36	14.7	***
31	61	-0.02	1.56	0.195	0.51	64.0	
32	54	3.00	0.36	0.172	0.06	4.5	*
33	47	0.40	1.57	0.263	0.43	35.6	
34	125	1.92	0.71	0.081	0.38	77.7	
35	34	1.98	0.83	0.401	0.09	4.3	*
36	135	-4.28	3.68	0.249	0.62	218.0	
37	134	1.29	0.96	0.100	0.41	93.2	
46	135	-0.22	1.86	0.091	0.75	413.0	
54	135	-2.46	2.74	0.290	0.40	89.6	
55	85	-0.97	2.17	0.228	0.52	90.4	
109	53	-0.87	1.91	0.218	0.59	76.3	
113	46	2.73	0.49	0.394	0.01	1.5	N/S
Tennessee Valley Authority Plots							
125	40	1.10	0.96	0.272	0.23	12.5	***
132	90	0.73	1.30	0.137	0.50	90.3	
153	100	0.25	1.58	0.113	0.66	195.0	
158	87	1.13	1.14	0.074	0.73	236.0	
159	50	-6.99	4.37	0.751	0.40	33.8	
207	48	-2.47	2.62	0.311	0.60	70.7	

Table 1.--Regression analyses of the log (variance) against log (mean) of tree ring increments--Continued.

Site No.	N	Log(a)	b	Standard error of b	Adjusted R ²	F-ratio	Significance
National Parks Service Plots							
301	84	-1.50	2.60	0.187	0.70	193.0	
302	84	-0.88	2.05	0.205	0.54	100.0	
303	84	-1.57	2.58	0.201	0.66	164.0	
304	84	2.04	0.75	0.237	0.10	10.1	**
305	84	0.04	1.63	0.111	0.72	214.0	
307	84	-0.20	1.88	0.121	0.74	242.0	
308	84	-1.75	2.62	0.352	0.40	55.4	
309	84	-2.46	2.88	0.332	0.47	75.1	
310	84	-1.25	2.38	0.150	0.75	253.0	
311	84	0.05	1.66	0.164	0.55	103.0	
312	84	0.72	1.36	0.154	0.48	78.4	
313	83	0.16	1.54	0.501	0.09	9.5	**
314	83	1.12	1.11	0.284	0.15	15.4	***
315	84	-1.90	2.54	0.207	0.64	152.0	
316	84	1.63	0.73	0.244	0.10	0.9	**
317	84	-0.13	1.72	0.169	0.55	104.0	
318	84	-1.23	2.36	0.250	0.52	89.1	
319	84	-1.82	2.51	0.217	0.61	133.0	
320	84	-0.60	2.11	0.142	0.73	221.0	
321	84	-0.62	2.00	0.123	0.76	263.0	

+ All regressions are significant at P < 0.0001, except where indicated:
 N/S = not significant, * = P < 0.05, ** = P < 0.01, *** = P < 0.001.

Table 2.--Regression analyses of the log(variance) against log(mean) of tree ring increments before and after 1943⁺

Site No.	Pre/post	N	Log(a)	b	Standard error of (b)	Adjusted R ²	F-ratio	Signif.
Tennessee Valley Authority Plots								
1	0	93	1.04	1.26	0.158	0.40	63.2	
	1	42	-0.43	1.77	0.546	0.19	10.6	**
3	0	46	2.32	0.60	0.274	0.08	4.8	*
	1	42	0.38	1.47	0.187	0.60	62.1	
4	0	50	-0.65	1.97	0.341	0.40	33.4	
	1	42	-2.28	2.73	0.190	0.83	206.0	
6	0	54	3.48	0.12	0.300	0	0.2	N/S
	1	42	0	1.51	0.535	0.14	8.0	**
7	0	66	-0.65	2.05	0.220	0.68	86.5	
	1	42	-0.65	2.05	0.220	0.68	86.5	
9	0	93	-0.23	1.79	0.147	0.61	147.0	
	1	42	-0.54	2.00	0.202	0.70	97.6	
10	0	93	0.36	1.44	0.213	0.33	45.7	
	1	42	4.35	0	0	0	1.0	N/S
12	0	83	0.44	1.49	0.184	0.44	66.2	
	1	42	-0.82	2.04	0.508	0.27	16.1	***
17	0	38	-0.91	2.02	0.560	0.24	13.0	***
	1	42	-1.03	2.18	0.226	0.69	93.0	
19	0	86	0.08	1.54	0.160	0.52	92.0	
	1	42	-0.90	2.02	0.225	0.48	38.7	
20	0	73	0.14	1.54	0.171	0.52	79.6	
	1	42	0.78	1.26	0.252	0.37	25.0	
22	0	58	1.69	0.87	0.302	0.11	8.4	**
	1	42	0.87	1.28	0.247	0.39	27.1	
23	0	93	-0.96	2.07	0.178	0.59	134.0	
	1	42	-0.91	2.07	0.292	0.66	80.4	

Table 2.--Regression analyses of the log(variance) against log(mean) of tree ring increments before and after 1943⁺--Continued

Site No.	Pre/post	N	Log(a)	b	Standard error of (b)	Adjust R ²	F-ratio	Signif.
24	0	64	-1.81	2.46	0.158	0.79	242.0	
	1	42	-2.25	2.66	0.330	0.61	64.6	
25	0	93	0.48	1.42	0.215	0.32	41.6	
	1	42	0.79	1.30	0.204	0.49	40.7	
26	0	73	1.76	0.84	0.188	0.20	19.5	
	1	42	0.84	1.23	0.375	0.19	10.8	**
27	0	93	1.05	1.16	0.350	0.10	11.1	**
	1	42	-0.23	1.83	0.258	0.55	50.2	
28	0	90	1.59	0.84	0.382	0.04	4.9	*
	1	42	-2.68	2.91	0.443	0.51	43.1	
29	0	53	-0.41	1.85	0.109	0.64	95.3	
	1	42	-2.21	3.04	0.147	0.91	425.0	
34	0	83	1.24	1.10	0.096	0.62	132.0	
	1	42	-0.67	1.77	0.499	0.22	12.6	***
36	0	93	-3.31	3.17	0.370	0.44	73.4	
	1	42	-4.67	3.95	0.181	0.92	477.0	
37	0	92	-1.68	0.79	0.139	0.25	32.1	

Tennessee Valley Authority Plots

	1	42	-1.19	2.22	0.253	0.65	76.5	
46	0	93	-0.09	1.79	0.110	0.74	267.0	
	1	42	-1.64	2.48	0.339	0.56	53.3	
54	0	93	-0.66	1.94	0.471	0.15	16.9	
	1	42	-2.66	2.80	0.511	0.42	30.1	
55	0	43	-2.37	2.71	0.270	0.70	101.0	
	1	42	-4.09	3.57	0.572	0.48	38.9	
132	0	48	1.08	1.25	0.216	0.36	27.4	
	1	42	-0.57	1.85	0.454	0.28	16.7	***
153	0	59	2.28	0.49	0.231	0.06	4.4	*
	1	42	1.32	1.14	0.286	0.27	15.9	***
158	0	45	1.48	0.93	0.108	0.62	74.0	
	1	42	-2.95	2.89	0.370	0.59	60.9	

National Park Service Plots

301	0	42	-1.50	2.57	0.421	0.47	37.2	
	1	42	-1.96	2.86	0.152	0.90	353.0	
302	0	42	-2.77	2.86	0.404	0.54	50.1	
	1	42	-1.46	2.40	0.193	0.79	153.0	
303	0	42	-1.40	2.44	0.236	0.72	108.0	
	1	42	-1.50	2.59	0.211	0.78	150.0	
304	0	42	-0.92	2.11	0.439	0.35	23.1	
	1	42	2.58	0.51	0.261	0.07	3.9	*
305	0	42	-0.78	2.04	0.239	0.64	73.0	
	1	42	0.29	1.49	0.159	0.68	87.2	
307	0	42	-1.73	2.61	0.109	0.93	571.0	
	1	42	0.27	1.65	0.194	0.63	72.3	
308	0	42	-1.79	2.58	0.441	0.45	31.2	
	1	42	-2.49	3.06	0.504	0.47	36.9	
309	0	42	-3.51	3.34	0.558	0.46	35.8	
	1	42	-1.19	3.31	0.272	0.63	72.1	
310	0	42	-0.41	1.92	0.158	0.78	148.0	
	1	42	-2.02	2.77	0.372	0.57	55.5	
311	0	42	-2.43	2.70	0.224	0.78	145.0	
	1	42	-0.18	1.83	0.166	0.75	122.0	
312	0	42	2.40	0.59	0.261	0.09	5.1	*
	1	42	1.63	0.84	0.237	0.22	12.5	**
313	0	41	-3.64	3.16	0.448	0.53	49.7	
	1	42	5.19	0.63	0.585	0	1.2	N/S
314	0	41	0.30	1.46	0.333	0.31	19.1	

Table 2.--Regression analyses of the log(variance) against log(mean) of tree ring increments before and after 1943⁺--Continued

Site No.	Pre/post	N	Log(a)	b	Standard error of (b)	Adjust R ²	F-ratio	Signif.
National Parks Service Plots								
	1	42	2.35	0.57	0.357	0.04	2.6	N/S
315	0	42	-4.42	3.34	0.341	0.72	108.0	
	1	42	-1.14	2.22	0.207	0.74	115.0	
316	0	42	4.28	0.51	0.673	0	0.6	N/S
	1	42	0.95	1.14	0.249	0.33	21.1	
317	0	42	-0.18	1.73	0.225	0.59	59.5	
	1	42	-0.39	1.87	0.281	0.52	44.6	
318	0	42	-0.60	1.98	0.330	0.46	35.8	
	1	42	-0.09	1.90	0.209	0.67	33.1	
319	0	42	-2.14	2.69	0.265	0.71	103.0	
	1	42	-2.99	2.99	0.380	0.60	62.1	
320	0	42	-1.62	2.61	0.181	0.83	208.0	
	1	42	0.86	1.40	0.183	0.59	59.1	
321	0	42	-0.95	2.17	0.173	0.79	158.0	
	1	42	0.12	1.60	0.191	0.63	70.1	

⁺All regressions are significant at P < 0.0001, except where indicated:
N/S = not significant, * = P < 0.05, ** = P < 0.01, *** = P < 0.001

LITERATURE CITATIONS

- Berger, J.M.; Mandelbrot, B.B. 1963. A new model for error clustering in telephone circuits. IBM Journal of Research and Development. 7:224-236.
- Cook, E.R. 1987. The use and limitations of dendrochronology in studying the effects of air pollution on forests. In: Proceedings of the NATO advanced research workshop: Effects of acid deposition on forest, wetlands, and agricultural ecosystem; 1985, May 12-17. Toronto Canada. Springer-Verlag. 277-290.
- Creber, G.T. 1977. Tree rings: a natural data-storage system. Biological Reviews. 52: 349-383.
- Guiot, V.; Berger, A.L.; Munaut, A.V. 1982. Response functions. In: Hughes, M. K.; Kelly, P. M. [and others.], eds. Climate From Tree Rings. Cambridge: Cambridge University Press: 38-50.
- Journal, A.G.; Huijbregts, C.J. 1978. Mining Geostatistics. London: Academic Press. 600 p.
- Kiester, A.R.; Van Duesen, P.C.; Dell, T.R. 1985. Status of the concepts and methodologies used in the study of the effects of atmospheric pollution on forests. Internal Report of the National Vegetation Survey of NAPAP. New Orleans, LA: U.S. Department of Agriculture, Forest Service, Southern Forest Experiment Station. [unpublished].
- Mandelbrot, B.B. 1960. The Pareto-Levy law and the distribution of income. International Economic Review. 1: 79-106.
- Mandelbrot, B.B. 1963. The variation of certain speculative prices. Journal of Business. 36: 394-419.
- Mandelbrot, B.B. 1967. The variation of some other speculative prices. Journal of Business. 40:393-413.
- Mandelbrot, B.B. 1969. Long-run linearity, locally Gaussian process, H-spectra and infinite variances. International Economic Review. 10: 82-111.
- Mandelbrot, B.B. 1982. The Fractal Geometry of Nature. San Francisco: Freeman Publishing. 461 p.
- Perry, J.N. 1981. Taylor's power law for dependence of variance and mean in animal abundance. Journal of the Royal Statistical Society. 30:(C) 254-263.
- Taylor, L.R. 1961. Aggregation, variance and the mean. Nature. 189: 732-735.

Red Spruce Tree Ring Analysis Using a Kalman Filter

Paul C. Van Deusen

SUMMARY

A Kalman filter was applied to red spruce (*Picea rubens* Sarg.) tree ring data collected from the Great Smoky Mountains by the Tennessee Valley Authority and the National Park Service. A new standardization method was developed that can be justified with a model-based assumption. The variance of the standardized growth chronology appears to have increased in recent years. The sensitivity of red spruce to climate began to increase in the late 1960's and leveled off in the early 1980's. It is possible that increasing climatic sensitivity and variance are related to balsam woolly adelgid activity in these stands.

INTRODUCTION

Tree ring data provide one of the few historical records for scientists to assess the impact of atmospheric deposition influences on forests (ADIF). However, to adequately assess this impact, historical information on weather and pollution levels are also needed. Although past weather records are available from weather stations, deposition levels can only be inferred from proxy variables such as coal consumption of nearby power plants. My analysis will be limited to examining the trends in the tree ring series and attempting to explain these trends with average monthly temperature and total precipitation records. The Kalman filter is shown to be a useful tool for this type of analysis.

DATA

The National Park Service (NPS) and the Tennessee Valley Authority (TVA) had collected data from plots located in the Great Smoky Mountains. Spatial relationships, current diameter, and species were recorded for each tree on each plot. A few dominant trees were selected at each NPS plot from which two increment cores were taken, but pith date was not recorded; tree rings were dated back to 1900. Dominant trees on TVA plots were not cored, but pith date was recorded; unfortunately tree ring widths were only available back to 1850. Information from approximately 200 red spruce trees were available in both data sets. A data set from a site on Clingman's Dome (North Carolina) consisting of 38 cores on 19 trees was also utilized in this study. Ed Cook of the Lamont-Doherty Tree Ring Laboratory collected and cross-dated this data set. The TVA and NPS tree ring data were processed at Oak Ridge National Laboratories.

Generally, only data that would be commonly available in a dendrochronological study were used; these data included ring width, elevation,

pith date, and regional weather data. National Weather Service Climatic Division data from stations in the northern mountains of North Carolina were summarized to provide total rainfall and average temperature by month beginning in 1931.

STANDARDIZATION

A basic goal of many tree ring studies is to produce a common chronology from a group of trees to be representative of a site. It is probable that this chronology will demonstrate a common signal to which all trees in the area have responded. In order to amplify the common signal, an attempt is made to eliminate individual tree signals that are unrelated to the common signal. The age-related biological growth signal can be removed by a number of procedures categorically referred to as standardization. Graybill (1982) presents methods where a growth model is individually fit to each tree ring series.

Graybill (1982) presents a hypothetical breakdown of the raw ring width for a single tree at time t , $R(t)$, as follows:

$$R(t) = C_t + B_t + D1_t + D2_t + e_t, \quad (1)$$

where C_t is the macroclimatic signal common to all trees;

B_t is the biological growth trend - a function of tree age;

$D1_t$ is a disturbance signal that is unique to the individual;

$D2_t$ is a disturbance signal common to most or all individuals--possibly caused by fire, insects, or pollution; and e_t accounts for random disturbance.

In order to maximize the macrosignals (C and $D2$), it is necessary to recognize and remove the microsignals (B and $D1$) as much as possible (Cook 1987). An index is formed as follows:

$$\text{Index}(t) = R(t)/Y(t), \quad (2)$$

where $Y(t)$ is the model-based prediction of $R(t)$. This produces a new index series with an expectation of 1, a more homogeneous variance, and a smaller first order autocorrelation than the original series (Fritts 1976). Graybill (1982) presents negative exponentials and orthogonal polynomials as potential prediction models.

Cook (1987) discusses the use of splines to replace Graybill's models. There is a possibility that the disturbance signal ($D1$) as well as the B -signal may be removed with the spline approach, and more user interaction and expert opinion are required. Warren (1980)

presents an alternate model-based approach that could also be used to remove the D1 signal, but it also requires much user interaction.

A NEW STANDARDIZATION PROCEDURE

A method was sought for this study that required little subjectivity and could be used to automatically process many hundreds of cores. The method begins with a standard sigmoidal model for diameter at some age, D(A):

$$D(A) = b(1 - e^{-kA}), \quad (3)$$

where b is the asymptote parameter, and k is the shape parameter. Differentiating model (3) with respect to age gives a diameter growth model:

$$\begin{aligned} \frac{d D(A)}{dA} &= be^{-kA} \\ &= 2 R(A). \end{aligned} \quad (4)$$

Model (4) is appropriate for radial increment data and is similar to standard dendrochronological methods.

Assuming model (4), two steps are required to remove the age-related trend from the data. First take the natural log of model (4), giving:

$$\log[R(A)] = \text{constant} - kA. \quad (5)$$

Then take the first differences of model (5), giving:

$$\begin{aligned} \log[R(A)] - \log[R(A-1)] &= -k \\ &= \Delta \log[R(t)]. \end{aligned} \quad (6)$$

Thus a simple transformation removes the age-related trend from the tree ring series. Result (6) can be justified intuitively by viewing it as a relative growth rate. Taking the log of R(t) puts it on a relative scale, and the first difference is just a numerical first derivative that can be viewed as a growth rate. This transformation can be quickly performed without sophisticated software or user interaction, an important advantage for large data sets.

Plotting the data before and after transformation indicated that the new series was stationary and that the age-related trend had been removed as expected (fig. 1). Figures 1 and 2 show how the transformation creates similar series from a young tree and an old tree that looked quite different before transformation. Notice that 1937, 1969, and 1981 are all low on the transformed series.

The analysis can then proceed on the transformed data by assuming that the new series is composed of the following signals:

$$\Delta \log[R(t)] = C_t + D1_t + D2_t + e_t, \quad (7)$$

where C_t , $D1_t$, $D2_t$, and e_t are defined as in model (1).

The age-related signal is now removed. Two macrosignal terms that are of interest remain (C and $D2$), as well as two uninteresting microsignal terms ($D1$ and e) that will be treated as noise.

KALMAN FILTER

A system for updating and predicting is presented by Kalman (1960) based on a linear dynamic model. These models are generalizations that can generate any of the class of ARMA models (Box and Jenkins 1976), standard multiple regression models, and regression models with time varying parameters (Harvey 1981). Applied to dendrochronology, the Kalman filter provides a means of simultaneously reducing a number of series to a single chronology and generating climate-based predictions. Furthermore, the climate parameters can be allowed to vary over time to provide a test of the uniformitarian principle that conditions in the past are similar to the present. The uniformitarian principle is the fundamental justification for the use of dendrochronology to infer past conditions.

The Kalman filter can be derived from Bayesian theory (Harrison and Stevens 1976; Meinhold and Singpurwalla 1983) or with least squares methods presented by Duncan and Horn (1972). The equations needed to implement the Kalman filter are presented below, and the reader is referred to the citations for the theoretical development.

The basic difference between the Kalman filter and usual regression models is that the parameters are allowed to vary over time. The relationship between the vector of observed standardized ring widths at time t (Y_t) and the parameters (α_t) is called the observation or measurement equation:

$$Y_t = F_t \alpha_t + v_t,$$

where the matrix F_t is fixed and of order $n_t \times p$, α_t is a $p \times 1$ vector of underlying state parameters, and v_t is an $n_t \times 1$ vector of residuals with zero expectation and variance matrix V_t .

The state variable, α_t , evolves over time according to a first order Markov process as defined by the transition or system equation:

$$\alpha_t = G_t \alpha_{t-1} + w_t,$$

where G_t is a fixed $p \times p$ matrix, and w_t is a $p \times 1$ vector of residuals with zero expectation and variance matrix W_t .

The error terms v_t and w_t are assumed to be independent white noise series. The quantities that must be known include the matrices (F_t and G_t) that premultiply the state variables (α_t and α_{t-1}). The matrices F_t and G_t correspond to independent variables in regression theory, or, when dealing with rocket trajectories, they come from well-defined physical laws. The more complex problem comes from the need to know the variance matrices (W_t and V_t), because in many statistical applications this will require some user subjectivity.

The equations needed to estimate the state variables can be divided into three parts: prediction equations, updating equations, and smoothing equations. Let a_{t-1} denote the optimal estimator of α_{t-1} based on all information up to and including Y_{t-1} . The covariance matrix of $a_{t-1} - \alpha_{t-1}$ will be P_{t-1} . The prediction equations for α_t and the associated covariance matrix given a_{t-1} and P_{t-1} are:

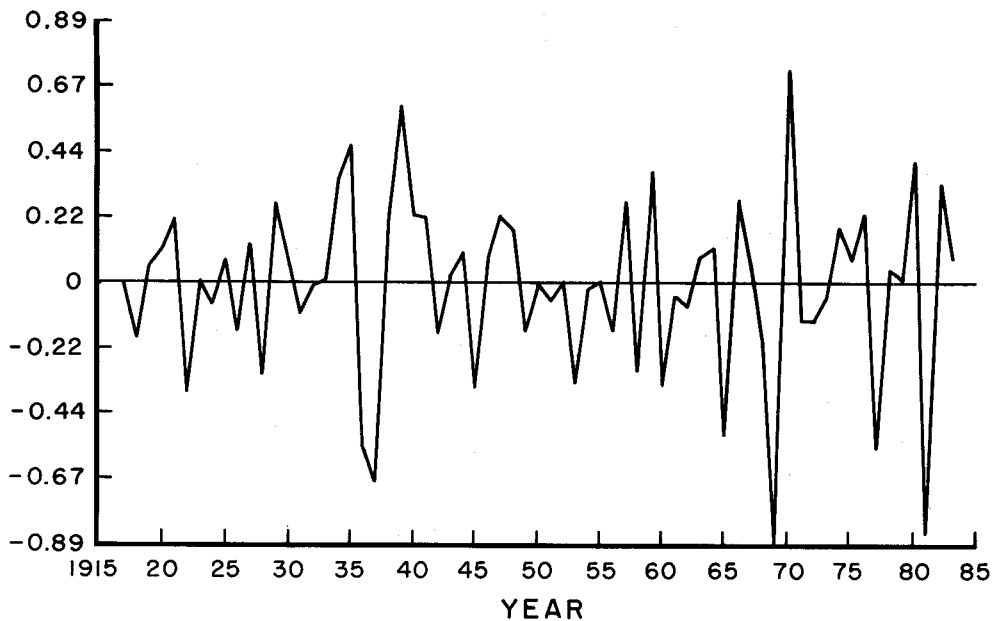
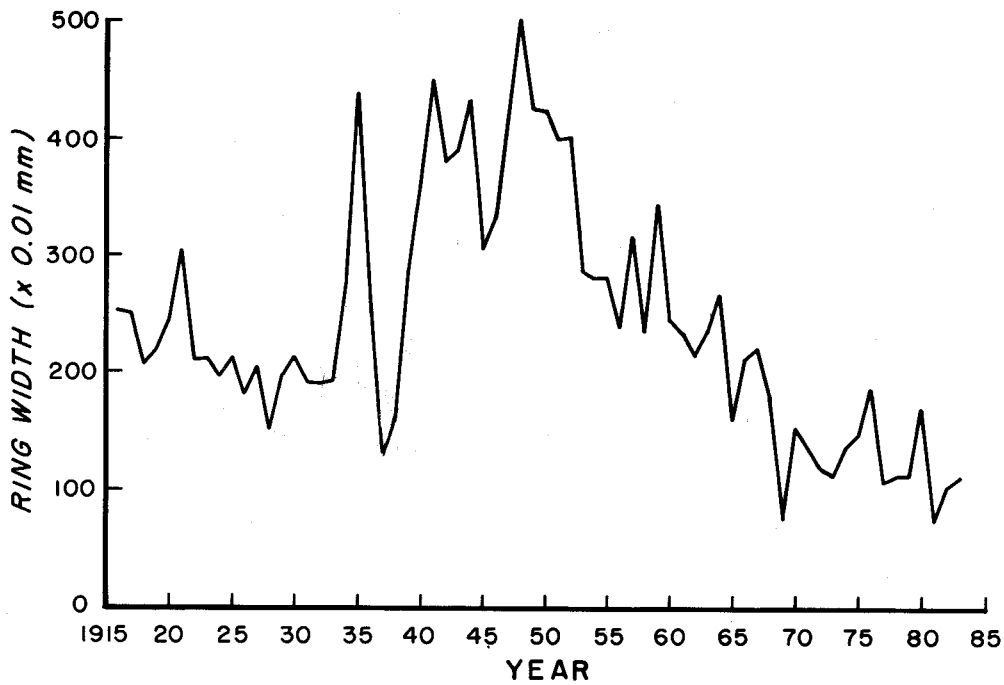


Figure 1.--Ring widths of a relatively young red spruce in raw (upper graph) and standardized (lower graph) form for a young tree. First differences of the natural log were used to produce the lower standardized series.

$$a_{t/t-1} = G_t a_{t-1}, \text{ and} \quad (3a)$$

$$P_{t/t-1} = G_t P_{t-1} G_t' + W_t. \quad (3b)$$

When Y_t becomes available, the updating equations for the estimate of α_t and the associated covariance matrix are:

$$a_t = a_{t/t-1} + P_{t/t-1} F_t' Z_t^{-1} E_t, \text{ and} \quad (4a)$$

$$P_t = P_{t/t-1} - P_{t/t-1} F_t' Z_t^{-1} F_t P_{t/t-1}, \quad (4b)$$

where

$$E_t = Y_t - F_t a_{t/t-1},$$

$$Z_t = F_t P_{t/t-1} F_t' + V_t, \text{ and, for computational savings,}$$

$$Z_t^{-1} = V_t^{-1} - V_t^{-1} F_t [F_t' V_t^{-1} F_t + P_{t/t-1}^{-1}]^{-1} F_t' V_t^{-1}.$$

The estimate of α_t in (4a) is the sum of its

estimate at time $t-1$ and a weighted average of the prediction errors (E_t).

At any time, a_t is an optimal estimate, given all previous information, but only the estimate at time T (the final period) contains all of the information available. Given all information, the optimal solution for any time t is referred to as signal extraction or smoothing. Smoothing begins with the solutions at time T and recursively goes backwards to time 1. This yields the optimal smoothed estimates of the state variables with associated covariance matrices as follows:

$$a_{t/T} = a_t + P_t^* (a_{t+1/T} - G_{t+1} a_t), \text{ and} \quad (5a)$$

$$P_{t/T} = P_t + P_t^* (P_{t+1/T} - P_{t+1/t}) P_t^*, \quad (5b)$$

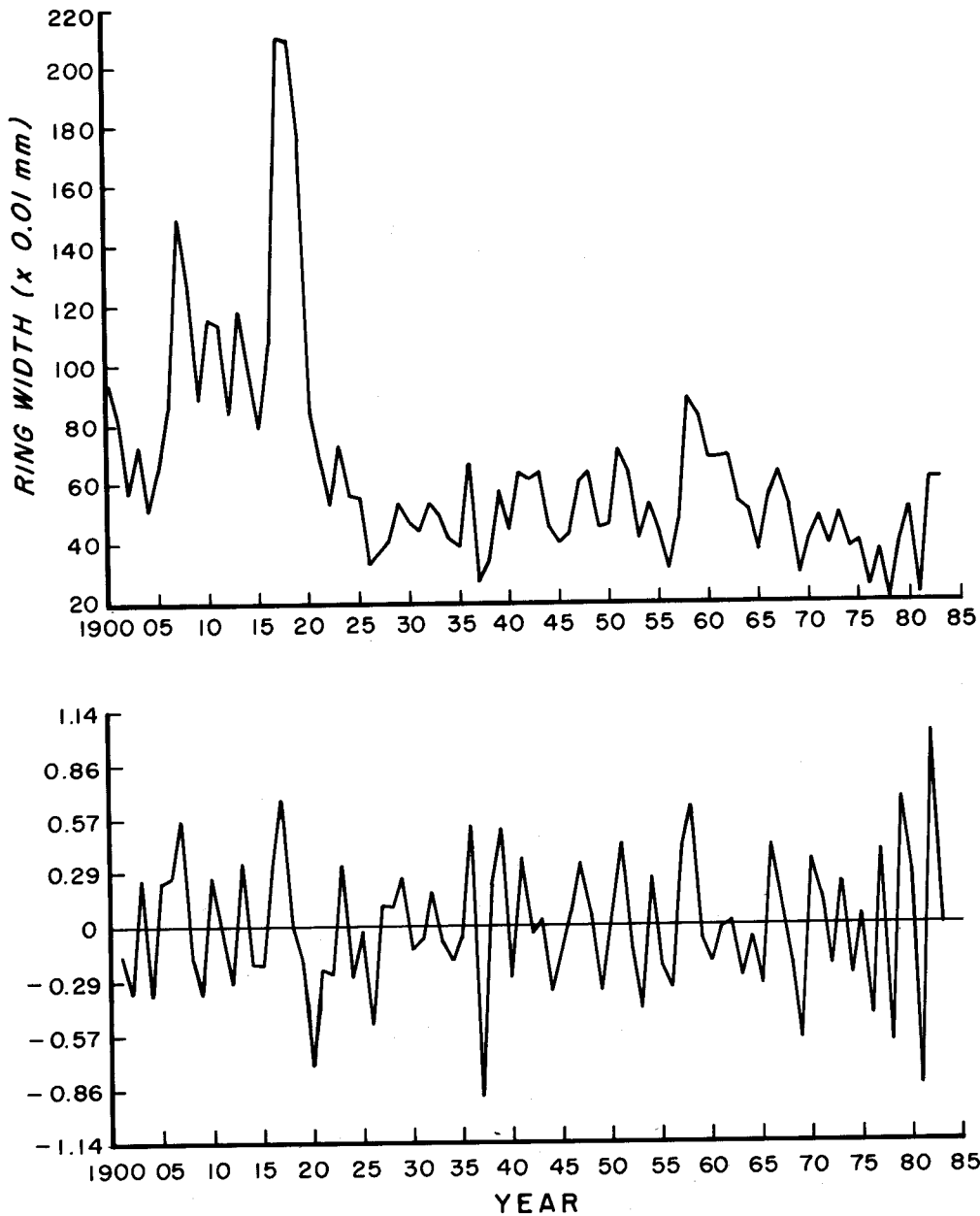


Figure 2.--Ring widths of an older red spruce in raw (upper graph) and standardized (lower graph) form for an old tree. First differences of the natural log were used to produce the lower standardized series.

where

- $a_T/T = a_T$ for the starting value on the state variables,
- $P_T/T = P_T$ for the covariance starting values and
- $P_t^* = P_t G_{t+1}' P_{t+1}/t^{-1}$

APPLYING THE KALMAN FILTER IN DENDROCHRONOLOGY

The Kalman filter provides a complete system for prediction, updating, and smoothing that should appeal to the dendrochronologist. In particular, the usual procedure of climate prediction from a single chronology formed from many standardized tree ring series could be refined. Two applications of the Kalman filter will be presented. The first shows how a

chronology can be formed simultaneously with its climate predictor, and the second is an application to dendroclimatology. For an additional application, readers should see Jones (1980) where various models are fit to drought data reconstructed from tree rings.

Application 1

The Kalman filter was applied to the red spruce data collected by the NPS and TVA. The objective was to simultaneously form a single chronology and its climate-based prediction. The data were first standardized by taking the first difference of the logarithms. The following Kalman filter was then applied:

$$\text{Observation equation } Y_t = F_t \begin{bmatrix} \alpha_{1t} \\ \alpha_{2t} \end{bmatrix} + v_t \quad (6a)$$

$$\text{Transition equation } \alpha_{1t} = C_t \alpha_{2,t-1} + w_{1t} \quad (6b)$$

$$\alpha_{2t} = \alpha_{2,t-1} + w_{2t} \quad (6c)$$

where

Y_t is the $n_t \times 1$ vector of observed tree ring data at time t ,

F_t is a matrix with two columns of length n_t with the first column being 1's and the second 0's,

v_t , w_{1t} , and w_{2t} are random errors,

C_t is the climate variable,

α_{1t} is the value of the chronology at time t , and

α_{2t} is the climate effect at time t .

The covariance matrix V_t was defined to be $\sigma^2_t I_t$ where σ^2_t was estimated from vector Y_t as $\Sigma(Y_{1t} - \bar{Y}_t) / [n_t - 1]$, and I_t was an identity matrix of order n_t . In other words, the trees were treated a priori as independent. The covariance matrix W_t was defined as

$$W_t = \sigma^2_t \begin{bmatrix} n_t^{-1} & 0 \\ 0 & .01n_t^{-1} \end{bmatrix}$$

Thus the state variables were assumed to be a priori independent. The elements on the diagonal were chosen to allow the state variables to vary enough to respond to a trend, but not enough to absorb random fluctuations. Since α_{1t} might approximate the average of the vector Y_t , n_t^{-1} was chosen for the upper diagonal, and the factor 0.01 was used in the lower diagonal to prevent α_{2t} from fluctuating in response to random disturbances. The results were robust to changes in the W and V matrices, which lends credence to these values.

Data from NPS plots dates back to 1900. The above algorithm was applied to the data from 1901 through 1983, because taking first differences eliminates the first observation. The climate data were available from 1931 through 1983, so the filter was modified during the "preclimate" period (1901-30) by setting w_{2t} and C_t to zero.

Results of Application 1

Climate lagged by 1 year was found to best predict the chronology or time trend in the data. The climate variable used was a linear combination of all the monthly rainfall and temperature data for a year, as described in table 1.

Figure 3 presents the chronologies for the three data sets. The NPS and Clingman's Dome chronologies were very similar, particularly over the past 10 years. Variation in the standardized series had a tendency to increase in the more recent years. This increase was most evident in the TVA chronology, but there was no suggestion for the cause of increases.

The time trend predictions based on lagged climate and the climate effect variable α_{2t} with 95 percent confidence intervals are plotted in figures 4, 5, and 6. Lagged climate predicted the chronologies accurately beginning in the

Table 1. The climate variable used was a linear combination of monthly rainfall and temperature averages. The weight below is the value multiplied by the corresponding monthly average to create this combined climate variable. The principle components method was used to create this linear combination. September temperature and October rainfall have the largest weights.

Variable	Month	Weight
Temperature	J	0.056
	F	-0.176
	M	-0.124
	A	-0.257
	M	-0.106
	J	-0.112
	J	-0.270
	A	-0.264
	S	-0.409
	O	0.013
	N	0.204
	D	0.040
Rainfall	J	-0.056
	F	0.164
	M	0.083
	A	-0.039
	M	0.161
	J	0.199
	J	0.061
	A	0.026
	S	0.027
	O	-0.517
	N	0.166
	D	0.179

1960's, but did poorly before this. The corresponding plot of the parameter (the climate effect) that multiplies climate also showed an increase over time. This indicated that the trees were becoming more responsive to climate in the 1960's than they were previously. The reason for the increased sensitivity to climate cannot be determined from this study. One might speculate that this was caused by thinning in the stands as a result of insect damage to the fir component. Whether this is related to pollution has not been determined.

Application 2

The Kalman filter can be applied to simultaneous prediction of past climate and the single common chronology. This traditionally involves averaging the individual series together as a first step to form the single chronology. The climate prediction is then a separate step that takes place without the complete information contained in the original series.

A Kalman filter can be formulated to handle these steps simultaneously. This incorporates the full information contained in the data while automatically providing a prediction system for past climate with associated prediction intervals. Although the simple solution given

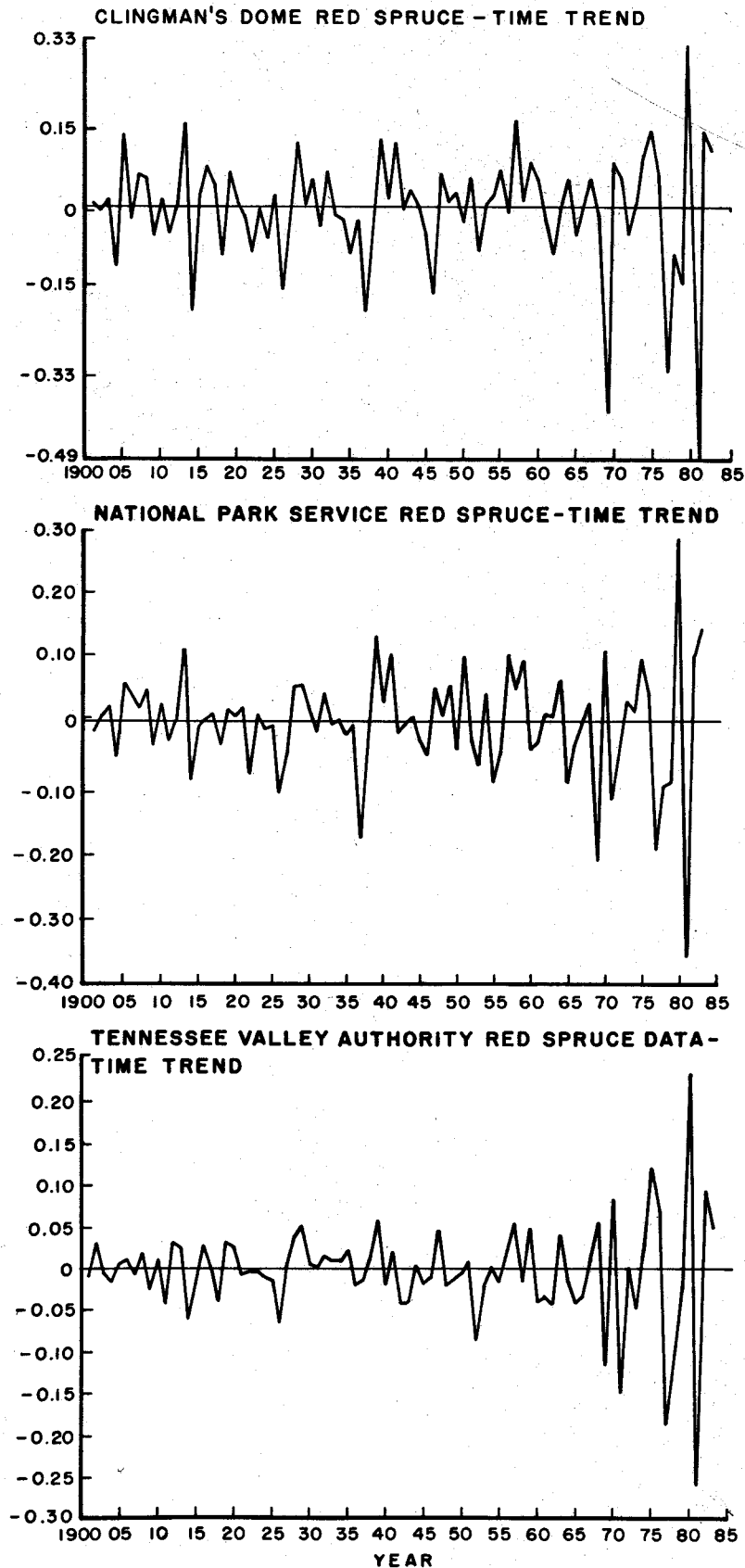


Figure 3.--Standardized chronologies from the Clingman's Dome, National Park Service, and Tennessee Valley Authority data sets. First differences of the log transform were used to standardize each tree ring series. A Kalman filter was used to produce the chronology as described in equations (6a), (6b), and (6c).

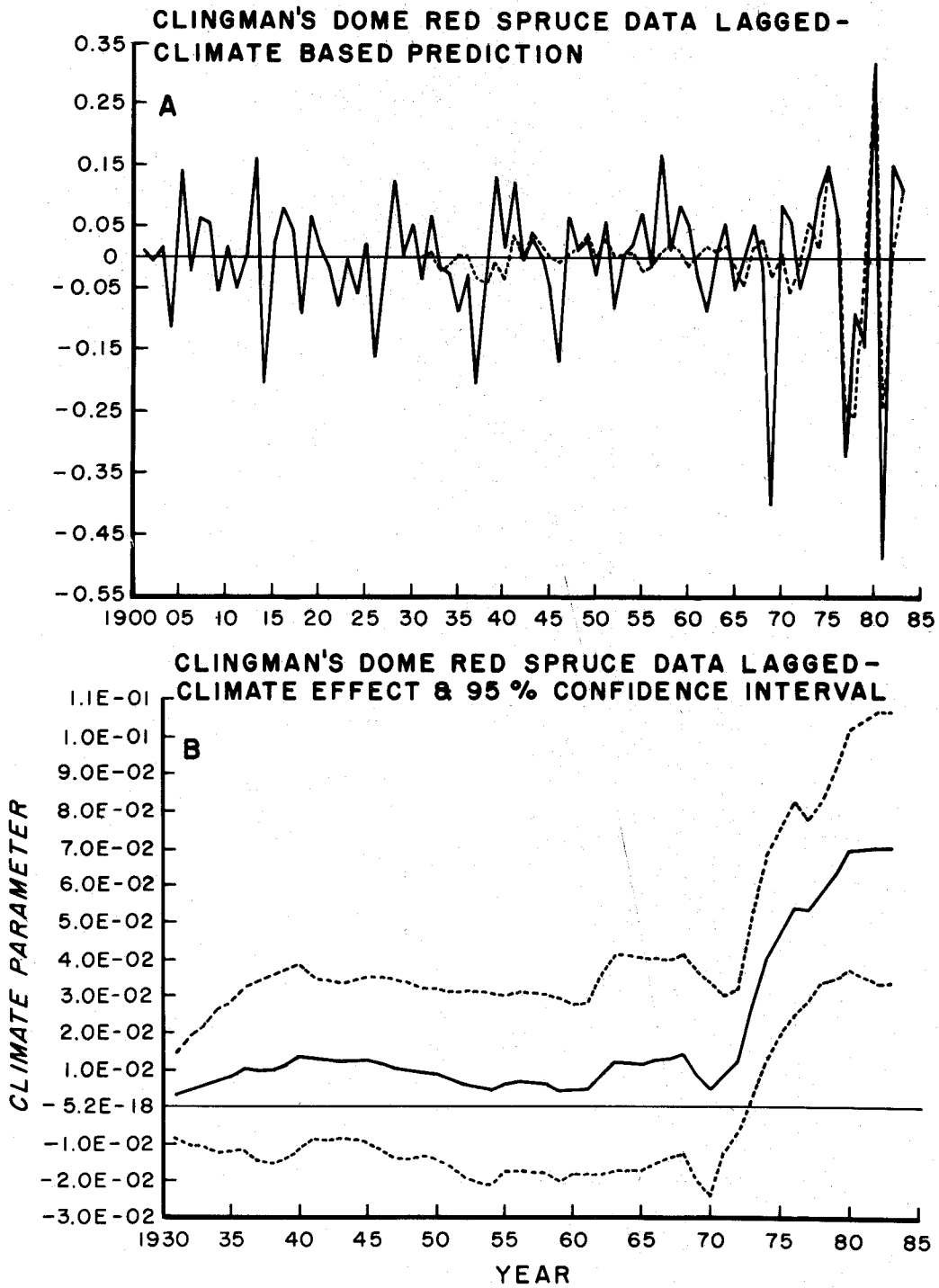


Figure 4.--Time trend predictions: A, Clingman's dome chronology (solid line) and its climate based prediction (dashed line) using the Kalman filter described by equations (6a), (6b), and (6c); B, the trend in the climate parameter given in equation (6a). The climate variable is a principle component (linear combination) of monthly average rainfall and temperature variables.

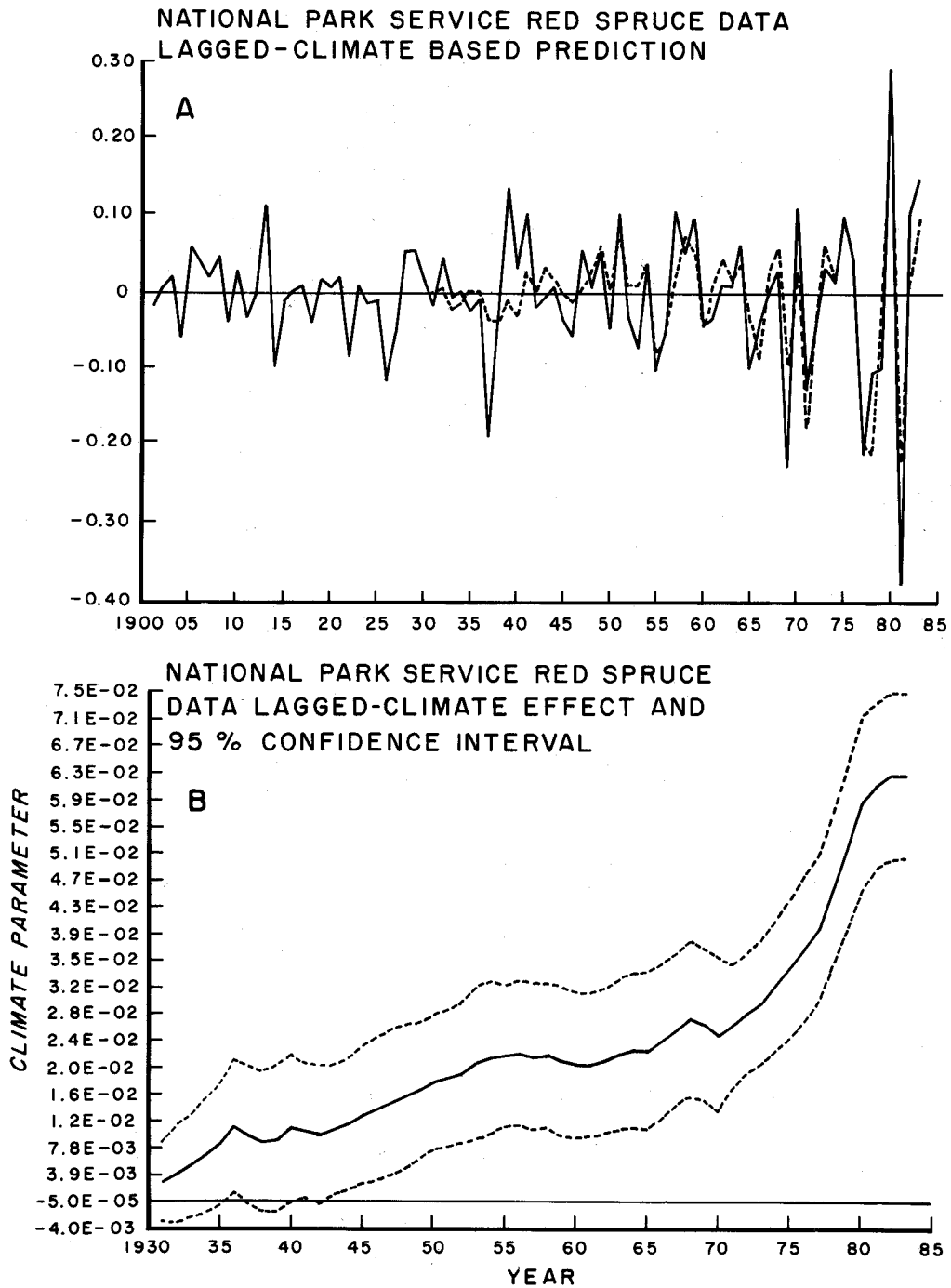


Figure 5.--Time trend predictions: A, National Park Service chronology (solid line) and its climate based prediction (dashed line) using the Kalman filter described by equations (6a), (6b), and (6c); B, the trend in the climate parameter with 95 percent confidence intervals, given in equation (6a). The climate variable is a principle component (linear combination) of monthly average rainfall and temperature variables.

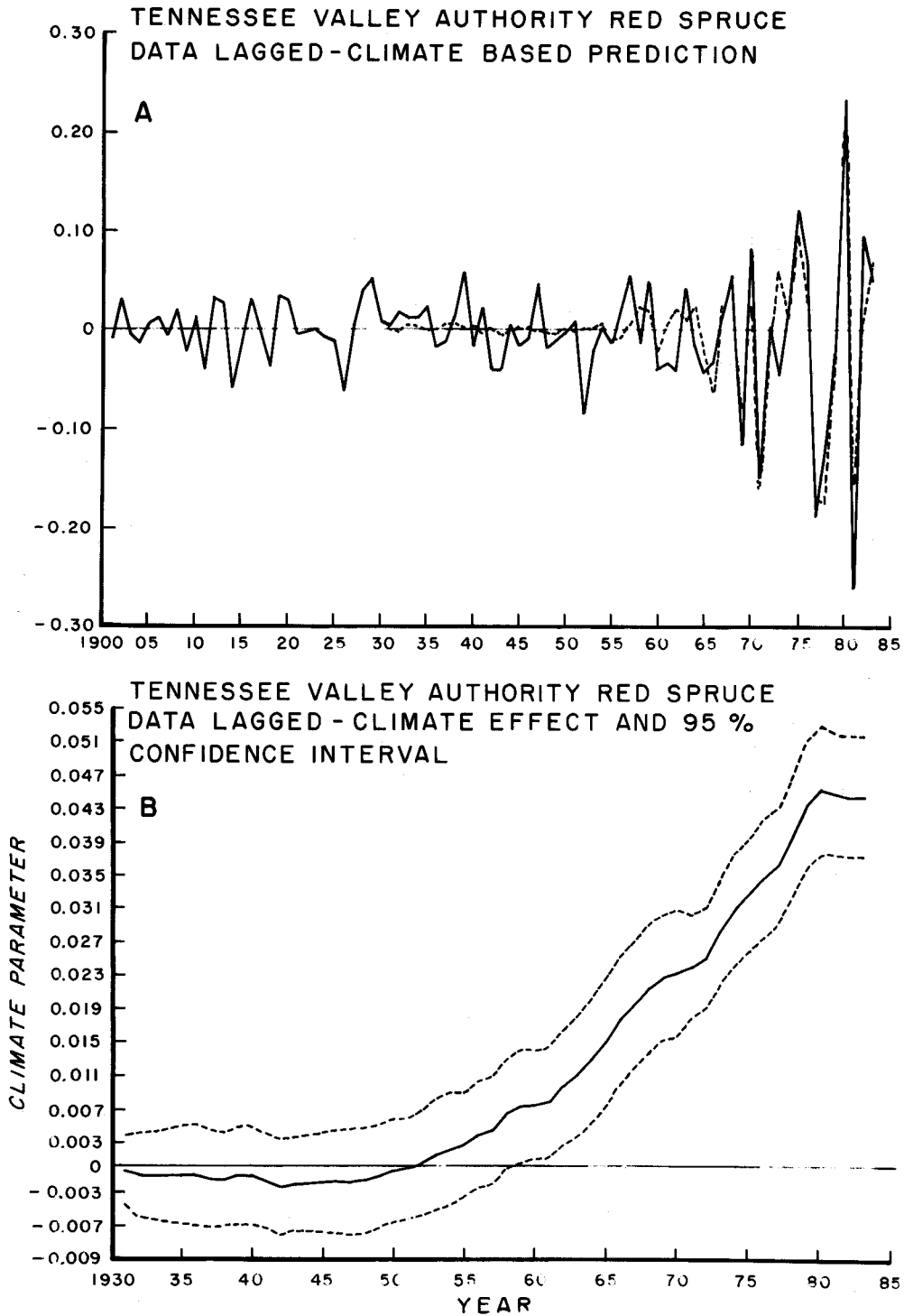


Figure 6.--Time trend predictions: A, Tennessee Valley Authority chronology (solid line) and its climate based prediction (dashed line) using the Kalman filter described by equations (6a), (6b), and (6c); B, the trend in the climate parameter given in equation 6a. The climate variable is a principle component (linear combination) of monthly average rainfall and temperature variables.

below does not achieve the potential of the method, it was chosen to emphasize some important points. Consider the following formulation:

$$\text{Observation equations } \begin{bmatrix} Y_t \\ C_t \end{bmatrix} = \begin{bmatrix} j_t & 0_t \\ 0 & \bar{Y}_{t+1} \end{bmatrix} \begin{bmatrix} \alpha_{1t} \\ \alpha_{2t} \end{bmatrix} + \begin{bmatrix} v_{1t} \\ v_{2t} \end{bmatrix} \quad (7a)$$

$$(7b)$$

$$\text{Transition equations } \begin{bmatrix} \alpha_{1t} \\ \alpha_{2t} \end{bmatrix} = \begin{bmatrix} 0 & 0 \\ 0 & 1 \end{bmatrix} \begin{bmatrix} \alpha_{1,t-1} \\ \alpha_{2,t-1} \end{bmatrix} + \begin{bmatrix} w_{1t} \\ w_{2t} \end{bmatrix} \quad (7c)$$

$$(7d)$$

where

Y_t is the $n_t \times 1$ vector of standardized ring widths at time t ,

C_t is a $q \times 1$ vector of observed climate variables,

j_t is a vector of 1's of length n_t ,

0_t is a vector of 0's of length n_t ,

\bar{Y}_t is the mean of the vector Y_t ,

α_{1t} is the value of the chronology at time t ,

α_{2t} is the climate parameter at time t , and $v_{1t}, v_{2t}, w_{1t}, w_{2t}$ are random errors.

Equations (7a) through (7d) define a system that handles the dendroclimatological problems of forming a single chronology for a site providing a means of predicting past climate, and testing the uniformitarian principle.

Some details on implementing the above system must be noted. The iterative process is started at time T rather than time 1, since past climate predictions are needed. Suppose that the climate variables are available from time T to time t^* , where $1 < t^* < T$. During this interval of known climate (INT_c) the parameter α_2 is estimated. Beyond INT_c , equation (7b) is eliminated and the Kalman filter is allowed to generate new values of α_2 back to time 1 (the earliest time for which tree data are available) and simultaneously produce the chronology and climate predictions as $\alpha_{2t}\bar{Y}_{t+1}$. Furthermore, the trend can be examined in the α_2 parameter over INT_c to see if the uniformitarian principle is valid, although the Kalman filter will tend to move α_2 along the established trend making the uniformitarian assumption less important.

Results of Application 2

Starting values must be supplied to the system in (7a) through (7d) for the parameter vector and the variance matrices V_t and W_t ; V_t was assumed diagonal with variances estimated from the vectors Y_t as in example 1. The last diagonal element in V_t is the variance of v_{2t} and was estimated from the variance in the known climate data. The matrix W_t was also assumed diagonal and chosen similarly to example 1.

A principle component of climate variables was used for C_t . A starting value of zero was used for the chronology parameter α_1 , and α_2 was started at 10. Unfortunately, climate was

predicted poorly (fig. 7). The values before 1931 were predictions generated by the model. Figure 7 shows the climate parameter α_2 trending over time with a 95 percent confidence interval. The parameter was tending toward zero as the confidence interval expanded, which is not surprising given the poor predictions. Although the model presented in equations (7a) through (7d) may not be ideal, this demonstrates how one could use the Kalman filter for predicting past climate.

CONCLUSION

The focus of this paper was to apply the Kalman filter to the study of tree rings. The Kalman filter provides a natural way of handling many of the problems that dendrochronologists encounter.

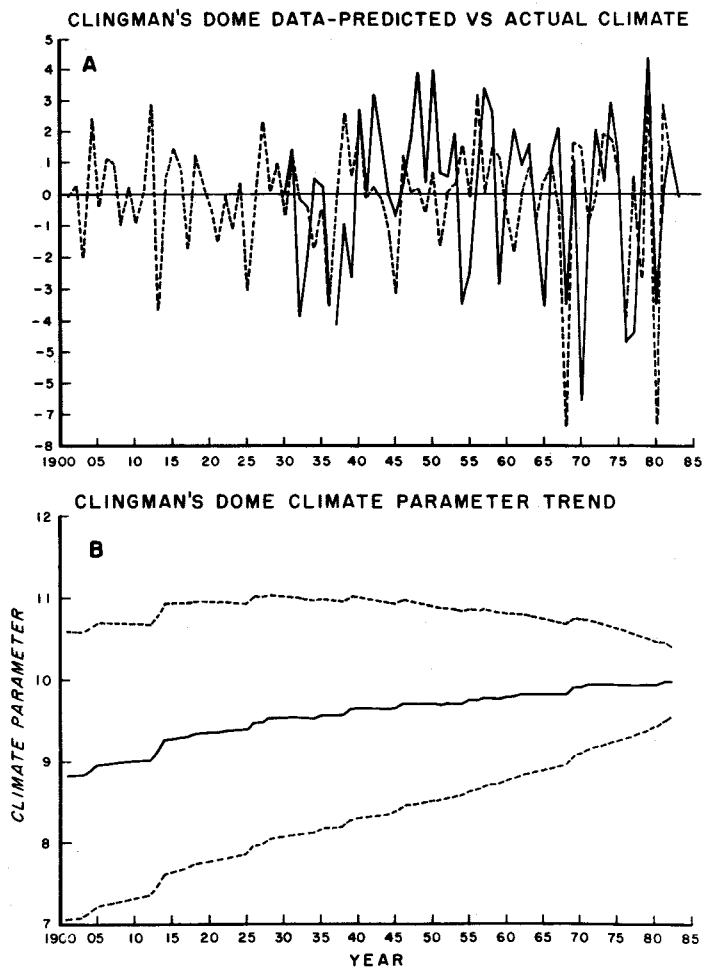


Figure 7.--Climate prediction: A, prediction (dashed line) of past climate obtained from tree ring data using the Kalman filter described by equations (7a) through (7d). The solid line is known climate, which is available back to 1931; B, the climate parameter trend and 95 percent confidence interval. This plot indicates that the uniformitarian principle does not hold here, since the parameter is tending toward zero.

The first application involved prediction of an average chronology with climate incorporated in the process. The parameter associated with the climate was allowed to vary over time. The climate parameter followed a sigmoid curve that implied an increasing sensitivity to climate with time. One might speculate that insect-caused thinning of the fir component accounts for this phenomenon.

The second application gave some insight as to how the method can be applied to more typical dendrochronological needs, i.e., predicting the past value of climate from tree rings. It was previously indicated in application 1 that the data set employed was insensitive to climate in the past and thus predictions were poor. Although the filter was not extremely sophisticated, it showed how one might proceed with such a problem. Future mean tree ring values were used to predict current climate while simultaneously developing the mean chronology. The trend in the climate parameter could also be inspected as an indication of the validity of the uniformitarian principle.

LITERATURE CITED

- Adams, H. S.; Stephenson, S.L.; Blasing T.J.; Duvick, D.N. 1985. Growth-trend declines of spruce and fir in mid-appalachian subalpine forests. *Environmental and Experimental Botany*. 25(4):315-325.
- Box, G. E. P.; Jenkins, G.M. 1976. *Time series analysis: Forecasting and control*. Holden-Day, Inc. 575 p.
- Cook, E. R. 1987. The use and limitations of dendrochronology in studying the effects of air pollution on forests. In: *Proceedings of the NATO advanced research workshop: Effects of acid deposition on forest, wetlands, and agricultural ecosystem*; 1985, May 12-17. Toronto, Canada. Springer-Verlag. 277-290.
- Duncan, D. B.; Horn, S.D. 1972. Linear dynamic recursive estimation from the viewpoint of regression analysis. *Journal of American Statistical Association*. 67(340): 815-821.
- Fritts, H.C. 1976. *Tree rings and climate*. London: Academic Press. 567 p.
- Graybill, D. A. 1982. Chronology development and analysis. In: *Climate from tree rings.*, M. K. Hughes, P. M. Kelly, J. R. Pilcher and V. C. Lamarche Jr., eds. Cambridge University Press, Cambridge: 21-28.
- Harrison, P. J. and C. F. Stevens. 1976. Bayesian Forecasting (with discussion). *J Royal Stat Soc B* 38: 205-247.
- Harvey, A. C. 1981. *Time series models*. Oxford: Philip Allan Publishers Limited. 229 p.
- Hornbeck, J. W. and R. B. Smith. 1985. Documentation of red spruce growth decline. *Canadian Journal of Forest Research*. 15: 1199-1201.
- Jones, R. H. 1980. Maximum likelihood fitting of ARMA models to time series with missing observations. *Technometrics* 23: 389-395.
- Kalman, R.E. 1960. A new approach to linear filtering and prediction problems. *Trans. ASME. J. Basic Engr.* 82: 34-45.
- Kiester, A. R., Van Deusen, P.C.; Dell, T.R. 1985. Status of the concepts and methodologies used in the study of the effects of atmospheric deposition on forests. Internal report for the National Vegetation Survey of NAPAP, Southern Forest Experiment Station. 701 Loyola Ave. New Orleans, La 70113.
- Meinhold, R. J.; Singpurwalla, N, D. 1983. Understanding the Kalman Filter, *American Statistician* 37: 123-127.
- Warren, W. G. 1980. On removing the growth trend from dendrochronological data. *Tree-Ring Bulletin* 40: 35-44.

Van Deusen, Paul C., editor. 1988. Analyses of Great Smoky Mountain Red Spruce Tree Ring Data. Gen. Tech. Rep. SO-69. New Orleans, LA: U.S. Department of Agriculture, Forest Service, Southern Forest Experiment Station. 67 p.

Four different analyses of red spruce tree ring data from the Great Smoky Mountains are presented along with a description of the spruce/fir ecosystem. The analyses use several techniques including spatial analysis, fractals, spline detrending, and the Kalman filter.